University of Cagliari

University of Sassari

PhD IN CHEMICAL SCIENCES AND TECHNOLOGIES

CYCLE XXXII

Biomasses for the obtainment of new functional polymer materials

Scientific disciplinary sectors

CHIM/04 - CHIM/05

Presented by Mariella Rassu

PhD school coordinator Prof. Stefano Enzo

Tutor Prof. Alberto Mariani

Final exam, academic year 2018 – 2019

Thesis defended during the session of February 2020

-Index-

-Index- 1

-Introduction- 5

-Abbreviations- 6

-CHAPTER I- 9

State of Art 9

1.1 Cyclodextrin 9

1.1.1 Introduction 9

1.1.2 Structure and properties 9

1.1.3 Physic-chemical properties 10

1.1.4 Inclusion complex 12

1.2 Cyclodextrins and polymers 13

1.2.1 Cyclodextrins and polyrotaxanes 16

1.2.2 Cyclodextrins and hydrogels 18

1.3 Cyclodextrins and biopolymers 23

1.3.1 Poly(lactic acid) 23

1.3.1.1 Properties and applications 27

1.3.2 Cork 29

1.3.2.1 Structure and composition 31

1.3.2.2 Functionalization of cork 34

1.4 Methyl cellulose 36

1.4.1 Cellulose 36

1.4.2 Structure and properties 36

1.4.5 Cellulose-derivates: hydrogels 41

1.4.6 Cellulose and cellulose-derivates interpenetrating polymer networks (IPNs) 42

1.5 Frontal polymerization 46

-MAIN PURPOSES- 67

-CHAPTER II- 69

Experimental Part 69

2.1 Synthesis of β-Cyclodextrin-based supramolecular poly(N-isopropylacrylamide) hydrogels 69

2.1.1 Starting materials 69

2.1.2. Hydrogels synthesis 69

2.1.3 Differential scanning calorimetry 70

2.1.4 Swelling measurements 71

2.2 Synthesis of Sliding Crosslinked Thermoresponsive materials made of Poly(N-Isopropylacrylamide) and Acrylamide-γ-Cyclodextrin. 71

2.2.1 Starting materials 71

2.2.2 Synthesis of Acrylamide-γ-Cyclodextrin 71

2.2.3 Synthesis of PNIPAAm Hydrogels Containing AγCD 72

2.2.4 Synthesis of pNIPAAm Hydrogels Containing γCD or MBAm 72

2.2.5 Differential Scanning Calorimetry 73

2.2.6 Swelling Measurements 74

2.2.7 Compression Tests 74

2.3 Synthesis of oxypropylated cork and preparation of PLA films 74

2.3.1 Starting materials 74

2.3.2 Oxypropylation reaction 75

2.3.3 Synthesis of PLA films 76

2.3.4 Solubility tests 76

2.3.5 Differential Scanning Calorimetry 77

2.3.6 Thermogravimetric analysis 77

2.3.7 Dynamic mechanical analysis 77

2.3.8 FT-IR spectroscopy 77

2.3.9 Scanning electron microscope 77

2.4 Synthesis of β-cyclodextrin-based oligomers of lactic acid and preparation of PLA films with OLA-β-CD as plasticizer 78

2.4.1 Starting materials 78

2.4.2 Synthesis of β-cyclodextrin-based oligomers of lactic acid 78
2.4.3 FT-IR spectroscopy 79
2.4.4 Scanning electron microscope 79
2.4.5 Differential Scanning Calorimetry 79
2.4.6 Mass spectroscopy 79
2.4.7 Preparation of films 80
2.4.8 Differential Scanning Calorimetry 80
2.4.9 Dynamic mechanical analysis 80
2.5 Semi-Interpenetrating Polymer Networks Based on Crosslinked Poly(N-Isopropyl Acrylamide) and methylcellulose prepared by Frontal Polymerization 81
2.5.1 Starting Materials 81
2.5.2 Synthesis of Trihexyltetradecylphosphonium Persulfate (TETDPPS) 81
2.5.3 Synthesis of PNIPAAm–MC Semi-Interpenetrating Polymer Networks 81
2.5.4 FTIR-ATR Measurements 82
2.5.5 Dynamic-Mechanical Analysis 83
2.5.6 Differential Scanning Calorimetry 83
2.5.7 Swelling Measurements 83
2.6 Semi-interpenetrating Polymer Networks of Methyl Cellulose and Polyacrylamide Prepared by Frontal Polymerization 84
2.6.1 Starting materials 84
2.6.2 Monomer Mixtures Preparation 84
2.6.3 Frontal Polymerizations 85
2.6.4 Differential Scanning Calorimetry 86
2.6.5 Dynamic Mechanical Analysis 86
2.6.6 Tensile Tests 87
2.6.7 Swelling Measurements 87
-CHAPTER III- 89
Results and discussion 89
3.1 Synthesis of β-Cyclodextrin-based supramolecular poly(N-isopropylacrylamide) hydrogels 89

3.2 Synthesis of Sliding Crosslinked Thermoresponsive materials made of Poly(N-Isopropylacrylamide) and Acrylamide-γ-Cyclodextrin..... 94

3.3 Synthesis and characterization of oxypropylated cork and preparation and characterization of PLA films 99

3.3.1 Oxypropylated cork with CDs 99

3.3.2 Preparation and characterization of PLA films with CD-based oxypropylated cork 106

3.4 Synthesis of β-cyclodextrin-based oligomers of lactic acid and preparation of PLA films with β-CD-OLA as plasticizers..... 108

3.4.1 Synthesis and characterization of β-cyclodextrin-based oligomers of lactic acid 108

3.4.2 Preparation and characterization of PLA films with β-CD-OLA 112

3.5 Semi-Interpenetrating Polymer Networks Based on Crosslinked Poly(N-Isopropyl Acrylamide) and methylcellulose prepared by Frontal Polymerization..... 113

3.6 Semi-interpenetrating Polymer Networks of Methyl Cellulose and Polyacrylamide Prepared by Frontal Polymerization..... 119

-CHAPTER IV-..... 130

Conclusions..... 130

4.1 Synthesis of β-Cyclodextrin-based supramolecular poly(N-isopropylacrylamide) hydrogels..... 130

4.2 Synthesis of Sliding Crosslinked Thermoresponsive materials made of Poly(N-Isopropylacrylamide) and Acrylamide-γ-Cyclodextrin..... 131

4.3 Synthesis and characterization of oxypropylated cork and preparation and characterization of PLA films 132

4.4 Synthesis of β-cyclodextrin-based oligomers of lactic acid and preparation of PLA films with β-CD-OLA as plasticizers..... 133

4.5 Semi-Interpenetrating Polymer Networks Based on Crosslinked Poly(N-Isopropyl Acrylamide) and methylcellulose prepared by Frontal Polymerization..... 134

4.6 Semi-interpenetrating Polymer Networks of Methyl Cellulose and Polyacrylamide Prepared by Frontal Polymerization..... 134

- Acknowledgments-..... 136

-Introduction-

This thesis collects three years of work dedicated to the development of new polymeric systems based on the use of raw materials derived from biomasses.

European Directive 2009/28/EC defines biomass as the biodegradable fraction of products, waste and residues of biological origin from agriculture (including plant and animal), forestry and related industries, as well as the biodegradable part of industrial and urban waste.

The interest in this resource has increased considerably over time. Biomasses are a very versatile renewable energy source with low environmental impact and are less expensive than fossil ones. Furthermore, the use of biomasses leads to environmental advantages, since, unlike the latter, during combustion biomasses release into the atmosphere a quantity of carbon dioxide corresponding to that previously absorbed by them during their life, thus not increasing the total average amount of CO_2 on a short time scale.

This manuscript is divided into two parts: the first one describes the works (some already published by me and my group) in which cyclodextrins are chosen for the synthesis and characterization of crosslinked or non-crosslinked hydrogels, and polypseudorotaxane hydrogels. Moreover, they were also used for the synthesis of a new class of cork-based materials, and for the synthesis of cyclodextrin-based lactic acid oligomers. The second one, report the experimental work on methyl cellulose as starting material for the obtainment of hydrogels having a semi-interpenetrating polymer network architecture.

-Abbreviations-

AA	Acrylic acid
AβCD	Acryloyl-β-cyclodextrin
AγCD	Acryloyl-γ-cyclodextrin
AcEt	Ethyl acetate
ADA	Adamantane
AmPS	Ammonium persulfate
APS	Aliquot persulfate
α-, β-, or γ-CD	α-, β-, or γ- Cyclodextrin
CD	Cyclodextrin
CH_2Cl_2	Dichloromethane
CST	Critical Solution Temperature
DMA	Dynamic Mechanical Analysis
DMA/LiCl	Dimethylacetamide/Lithium chloride
DMSO	Dimethyl sulfoxide
DP	Degree of Polymerization
DSC	Differential Scanning Calorimetry
E	Young's modulus
EPH	Epichloridrine
FDA	Food and Drug Administration
FT-IR	Fourier Transform Infrared Spectroscopy
HEMA	2-Hydroxyethyl methacrylate
HP-βCD	2-Hydroxypropyl-βCD
HPMC	Hydroxypropyl methylcellulose

IL	Ionic Liquids
IPN	Interpenetrating Polymeric Network
LCST	Lower Critical Solution Temperature
KOH	Potassium hydroxide
MBAm	N,N′-methylene-bisacrylamide
MC	Methylcellulose
NIPAAm	N-isopropylacrylamide
NMMO	N-methylmorpholine-N-oxide
NMP	N-methyl pyrrolidone
OLA-β-CD	Oligomers of lactic acid-β-cyclodextrin
PBS	Poly(butylene succinate)
PDLA	Poly(D-lactide)
PEG	Poly(ethylene glycol)
PET	Poly(ethylene terephthalate)
PICs	Inclusion Complexes Polymers
PLA	Poly Lactic Acid
PLLA	Poly (L-lactide)
PNIPAAm	Poly(N-isoproprylacrylamide)
PO	Propylene Oxide
PS	Polystyrene
PVA	Poly(vinyl alcohol)
ROP	Ring opening polymerization
SAXS	Small Angle X-ray Scattering
SBE-βCD	Sulfobutylether-βCD
SIPN	Semi-Interpenetrating Polymeric Network

$SnOct_2$	Tin (II) octanoate
SR%	Swelling Ratio %
T_g	Glass Transition Temperature
TBAF/DMSO	Tetrabutylammonium trihydrate fluoride/dimethyl sulfoxide
TEMED	Tetramethylenediamine
TETDPPS	Trihexyltetradecylphosphonium persulfate
TGA	Thermogravimetric analysis
THF	Tetrahydrofuran
UCST	Upper critical solution temperature
XRD	X-ray diffraction

-CHAPTER I-

State of Art

1.1 Cyclodextrin

1.1.1 Introduction

Cyclodextrins (CDs) are synthetic substances obtained from the enzymatic degradation of one of the most important polysaccharides, starch. CDs, sometimes called Schardinger sugars or cycloamylose dextrins, were discovered unexpectedly by Vielliers in 1891, [1, 2] who called these compounds “cellulosing”.

Later on, Franz Schardinger, considerate the founder of CD chemistry, during his study on microorganisms responsible for the deterioration of starch-containing foods, obtained two distinct crystalline substances with properties similar to dextrins (already known as partial degradation products of starch), which he called α- and β-dextrin.[1] The cycloalkyls were separated by selective precipitation with organic solvents or by high temperature chromatography on a cellulose column. Afterward Schardinger, who gave a detailed description about preparation and separation of CDs, other scientists gave significant contributions to CDs science. In the 1930s, Freudenberg and his collaborators explained the cyclic structure of α- and β-dextrin [3], consisting of glucopyranose units linked (α-1→4). More recently, Kurkov and Loftsson improved the CD science.[4]

1.1.2 Structure and properties

CDs consisting of six, seven, or eight glucose units are called α-, β-, or γ-CDs, respectively. CDs have a toroidal shape, caused by the spatial arrangement of the various functional groups of glucose units (Figure 1.1). Consequently, all the secondary hydroxyl groups (corresponding to the C2 and C3 carbon atoms of the glucose units) look out one of the faces, while the primary hydroxyls are located at the other face of the cavity. The rotation of these secondary hydroxyl groups reduces the effective dimensions of the cavity, making it more open towards the secondary hydroxyls (Figure 1.2).[5]

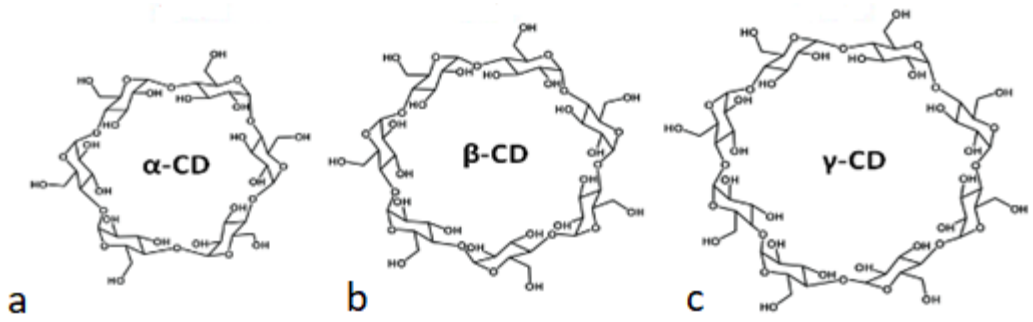

Figure 1.1: Molecular structure of (a) α, (b) β, and (c) γ-CDs.

The presence of –OH groups at the ends of the cone makes CDs polar, therefore soluble in water, while the spatial arrangement confers a non-polar character inside the cavity. These peculiar properties permit to host hydrophobic molecules inside the cavity through an encapsulation process called host-guest complexation, whereas polar interactions between polar hosts and –OH of the primary hydroxyls by the formation of hydrogen bridges can be simultaneously established. This encapsulation phenomenon depends considerably on dimensions of both CDs cavity (which is function of the glucose unit number), and guest molecules. [6-9]

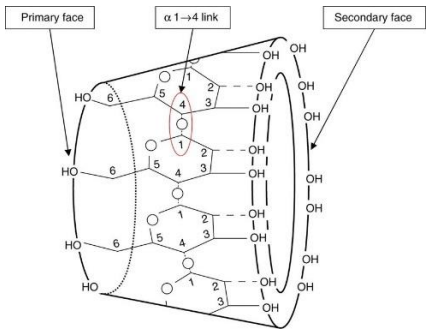

Figure 1.2: Structure of γ-CD toroid showing spatial arrangement.

1.1.3 Physic-chemical properties

The three classes of cyclodextrins differ in size of the ring and therefore of the cavity, equal to 5.70, 7.80 and 9.50 Å, respectively, and for the solubility in water, equal to 145 g/l for α, 18.5 g/l for the β, and 232 g/l for γ. At room temperature they are odorless, white crystalline

powders with a slightly sweet taste. Cyclodextrins are insoluble in alcohols, ketones, ethers, chlorinated hydrocarbons, aliphatic and aromatic hydrocarbons.[10]

Other physical properties of α-, β- and γ-CD are listed in Table 1.1.

Table 1.1: Physical properties of the most important cyclodextrins.

	α-CD	**β-CD**	**γ-CD**
Formula	$C_{36}H_{60}O_{30}$	$C_{42}H_{70}O_{35}$	$C_{48}H_{80}O_{40}$
Molecular mass	972.85	1135.00	1297.14
Solubility in water (25°C), g/100mL	14.5	1.85	23.2
Crystal water, wt%	10.2	13.2-14.5	8.13-17.7
a_D^{20}, °	148.0	162.0	177.0
mp, °C	>200°C	>200°C	>200°C
pKa value (25°C)	12.331	12.202	12.081

Cyclodextrins are chiral, non-reducing oligosaccharides. The acid treatment, for example using periodate, leads to the splitting of the CD in glucose units. The latter is the only degradation product of all cyclodextrins. The hydrolysis rate is superior for γ-, and lower for α-CD. All cyclodextrins are very stable and highly soluble in alkaline solution (pH> 14). It is possible to increase the solubility of CDs in water, increasing pH. Cyclodextrins are stable up to 250°C in nitrogen atmosphere. [10]

It is possible to obtain numerous cyclodextrin-derivatives, starting from the native ones, through reactions that involve the hydroxyl groups of the glycoside units. For this purpose, it is necessary the presence of regioselective reagents, reaction conditions, purification and isolation methods for the separation of products. The main reactions are of two types:

1) electrophilic additions to the hydroxyl, which lead to the formation of ether or ester bonds with alkyl halides, epoxides, carboxylic acids, etc.

2) nucleophilic attacks on C-OH by halides, amines, azides, etc.

Thanks to the ability of cyclodextrins and its derivatives to form covalent and supramolecular interactions, they are excellent precursors for compounds such as catenans, rotaxanes and polyrotaxanes.

1.1.4 Inclusion complex

As previously mentioned, the encapsulation process occurs according to a host-guest mechanism in which a guest molecule is inserted into the hydrophobic cavity of the cyclodextrin (host). The inclusion complex formation, in aqueous solution, takes place without formation or cleavage of covalent bonds; the guest molecule kicks out the water molecules from the cavity. It is accepted that the forces involves in a complex formation are, in general: [11-13]

a) van der Waals interactions (or hydrophobic interactions) between the hydrophobic surface of the CD cavity and the host molecules;
b) hydrogen bond formation between CD hydroxyl groups and functional polar groups of host molecules;
c) high energy release during the complex training process;
d) release of deformation energy in the ring structure of the CD.

The most important factors that guarantee the stability of the inclusion complex are:

- Geometric factors: if the guest is too small, it passes without difficulty through the cavity and the bond will be weak or not occur. Is also possible that the complex formation occurs with molecules larger than the cavity, but, in this case, only a limited number of groups or side chains can penetrate the CD cavity.
- Polarity of the guest molecules: complexes are formed if the guest molecule is less polar than water ones. The greater the hydrophobic character of host molecule, the more stable the complex is.
- Medium: the majority of the inclusion complexes is formed in water, but in some cases it is possible to have a complex also in an organic solution.[1, 14]
- Temperature: generally, the stability of the inclusion complex decreases with the increase of the temperature. The changes of entropy and enthalpy depend on the equilibrium constant, which in turn depends on temperature.[15]

The stoichiometric ratio between the cyclodextrin and the guest to form the inclusion complex, usually, is equal to 1:1. But sometimes, it is possible to obtain a stoichiometric ratio equal to 1:2 or 2:1 (Figure 1.3). It depends principally on guest molecule nature. [15-17]

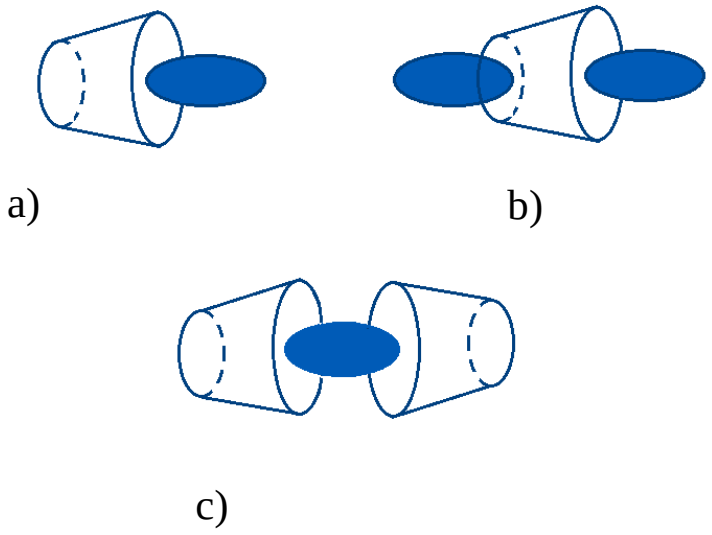

Figure 1.3: Stoichiometry of the inclusion complex between CDs and a guest molecule. Molar ratio can be: a) 1:1; b) 2:1; c) 1:2.

Thanks to their ability to form host-guest inclusion complexes, to non-toxic nature and high availability and their low price, the use of cyclodextrins is increased in many research fields, as polymer science,[18-22] analytical chemistry,[23-27] food science and packaging,[28-31] and pharmaceutical applications.[32-34]

1.2 Cyclodextrins and polymers

Cyclodextrins and their derivates have demonstrated to be excellent candidates as building blocks for the design of a wide range of new polymeric networks and assemblies, like hydrogels, nano/microparticles and micelles. These materials are mainly studied for pharmaceutical and biomedical applications, such as the controlled release and target delivery of bioactive substances (e.g., low molecular weight drugs, peptides, proteins, and genetic material) and for tissue engineering and diagnostics.[35] In addition, some of them show a response to external stimuli, resulting to be sensitive to pH, temperature or mechanical

stress. To date, these materials can be divided in chemically (covalently) crosslinked, or physically assembled. [36] Among those covalently crosslinked, it is possible to have two types of materials based on cyclodextrins:

- crosslinked cyclodextrins: the first CD-containing polymer network was synthetized in the 1980's. Cyclodextrins (α, β or γ) were polymerized to each other with the use of epichloridrine (EPH) as a bifunctional crosslinker resulting in the formation of polymeric hydrogels (Figure 1.4).[37] Numerous studies showed the ability of these networks to complex a wide variety of weakly water-soluble molecules.[38, 39] The crosslinking of CDs, in addition to the use of the bifunctional agent EPH, can also be obtained through the use of other bifunctional compounds such as diepoxides, [40] diisocyanates [41, 42] and anhydrides. [43, 44] Derivatives of the CDs, including methyl-CD, sulfobutylether-βCD (SBE-βCD), and 2-hydroxypropyl-βCD (HP-βCD), can also be used for the formation of networks capable of absorbing significant amounts of water up to 10 times with respect to their dry weight.[45]

- Cyclodextrin-based Polymeric Systems: to improve the mechanical properties of these CDs polymers, the polymerization was carried out in presence of both EHP cross-linking agents, (or diisocyanates, etc.), and some water-soluble polymers, such as poly(vinyl alcohol) (PVA), hydroxypropyl methylcellulose (HPMC) or poly(N-isoproprylacrylamide) (PNIPAAm).[40, 46, 47]

  For example, PNIPAAm-β-CD gels have been synthesized by reacting PNIPAAm functionalized with carboxyl groups and amine-functionalized EPH-cross-linked β-CDs. Thanks to the peculiar property of PNIPAAm (explained in paragraph 1.2.2), the resulting β-CD-PNIPAAm gels have been used for the realization of systems able not only to complex hydrophobic fluorescent molecules, but also to modulate this complexation reaction based on temperature.[48]

  In addition to the polymerization of CDs with low molecular weight crosslinking agents, covalently crosslinked systems have been developed starting from modified or unmodified CDs and from a wide variety of polymers. In many cases, CD has been used as a cross-linking agent as in the case of the synthesis of poly(acrylic acid) (PAA) and β-CD networks.[49, 50]

The most widely strategy for preparing CD/polymer systems is the chemical copolymerization (or induced radiation) of vinyl- or (meth)acryloyl-modified CD monomers with other commonly used vinyl monomers, such as acrylic acid (AA), 2-hydroxyethyl methacrylate (HEMA), and N-isopropylacrylamide (NIPAAm).[51-54]

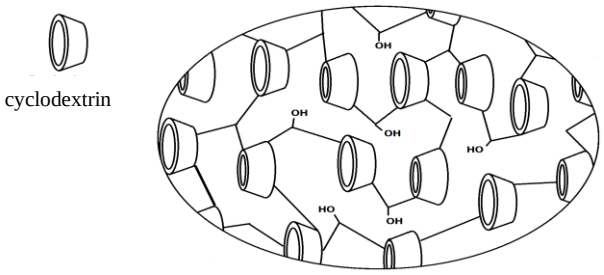

Figure 1.4: Polymerized CDs.

In addition to those permanently crosslinked, it is possible to obtain networks held together by strong physical interactions. These systems have various advantages, compared to those chemically crosslinked, for example they do not require the use of toxic crosslinking agents and the reaction conditions are mild (low temperature and pressure). Among these, there are the Inclusion Complexes Polymers (PICs). These PICs have a crosslinked structure that is formed thanks to the non-covalent host-guest interactions between polymer and cyclodextrin. The interactions are reversible, so the bonds are formed and/or broken. Crosslinking agents are not used and, for this reason, PICs are suitable for biomedical and pharmaceutical applications; these systems are also referred to as "self-assembling". One of these systems was obtained by Li and collaborators in 2008, exploiting the formation of the host-guest complex between adamantane (ADA) and β-CD, grafted onto two different polymeric chains (Figure 1.5). [55]

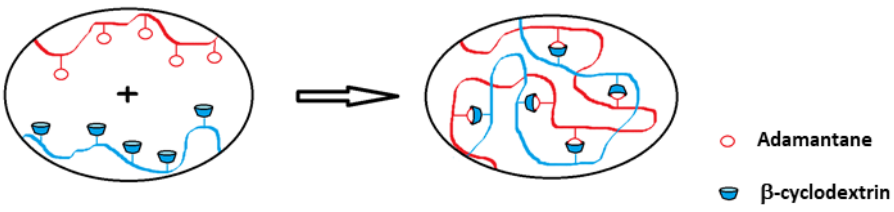

Figure 1.5: Formation of the host-guest complex between the adamantane (ADA) and the β-CD.

1.2.1 Cyclodextrins and polyrotaxanes

In general, rotaxanes are molecules made up of one or more axes passing through one or more rings, and in which the terminal part of these axes is blocked, at both ends, by bulky terminal groups (the so-called stoppers) (Figure 1.6b). It is about of mechanically interlocked molecules. Rotaxanes are stable entities because, even if they do not contain covalent bonds, a large amount of energy is needed to separate the ring from the axis (Figure 1.6e).

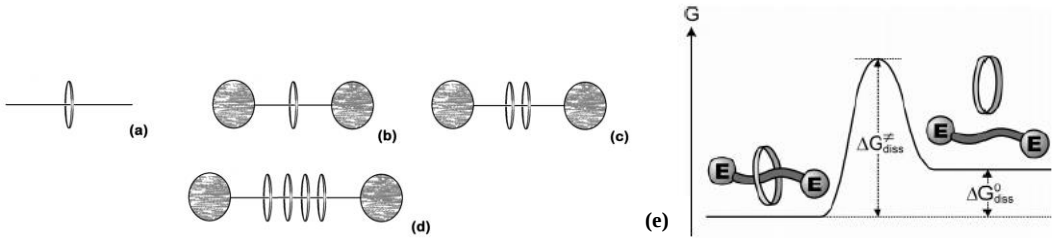

Figure 1.6: Schematic representation of some rotaxanes. a) pseudorotaxanes. b) [2] rotaxane. c) [3] rotaxane. d) [5] rotaxane; e) amount of energy needed to separate the rings from the axis.

Since their discovery, about 50 years ago, rotaxanes have acquired more interest for their peculiar abilities in synthesis of sophisticated devices. [56-59]

When the axis that penetrates the ring is a polymer, it is called polyrotaxane. Polyrotaxanes (PRs) are one of the most investigated types of supramolecular polymers. Depending on the structure, two types of polyrotaxane can be distinguished:

- the main chain consists of monomeric units, covalently linked to each other, which pass through the macrocyclic rings (Figure 1.7a).

- the supporting structure of the polymer consists of chains formed by the macrocycles covalently linked together (Figure 1.7b). [60]

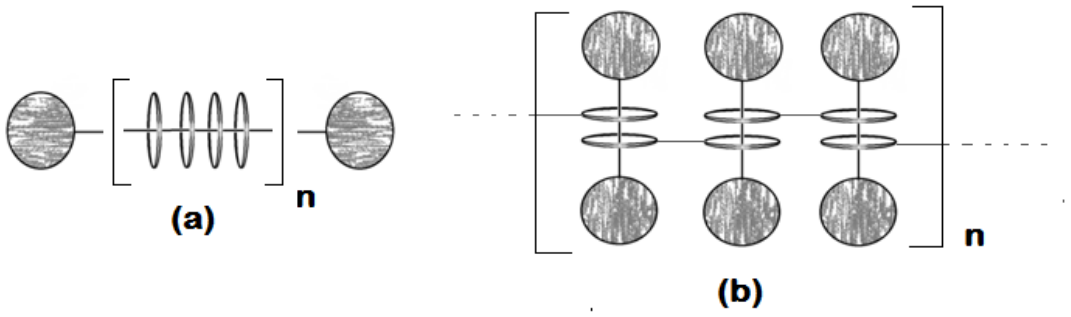

Figure 1.7: Representation of the two types of polyrotaxanes. a) the main chain is penetrated of several macrocyclic rings, b) different chains, with a certain number of rings inserted inside it, are covalently linked together.

Between the polymer and the macrocycle, a dynamic interaction is established, determined by weak interactions, which allow the macrocycle to run along the chain without slipping off. The physical characteristics of a polyrotaxane depend on the "inclusion ratio", which corresponds to the number of macrocyclic rings inserted in a polymeric chain. Varying the inclusion ratio, the mechanical and rheological properties differ, which in turn varies according to the length of the polymer chain.[4, 61, 62] From this point of view, it is very interesting to investigate the mechanical properties of crosslinked polyrotaxanes, as they have crosslinking points with a high degree of freedom (the rings flow without particular impediments), unlike those with classical crosslinking, chemical or physical type, in which the cross-linking points are fixed or slightly mobile.[4]

The cyclodextrin-based polyrotaxanes are among the most studied, as they lead to the formation of particularly stable complexes. The scientific literature has shown that cyclodextrins are able to complex not only with a small hydrophobic molecules, but also with linear polymers, as a polypseudorotaxane derived from the formation of the inclusion complex between the α-CDs and the poly(ethylene glycol) (PEG), studied by A. Harada and M. Kamachi in 1990. [63] Since then, numerous polyrotaxanes based on cyclodextrins have been synthesized and studied, obtaining in most cases insoluble compounds in water. However, not all polymers form stable inclusion complexes with all three cyclodextrins; for example, PEG forms stable inclusion complexes only with α-CDs, but not with β or γ-CD. This leads to the conclusion that each polymer shows a certain affinity towards to a specific cyclodextrin, due to the dimensions of both components. [4]

1.2.2 Cyclodextrins and hydrogels

Gels are materials, physically or chemically crosslinked, that have the peculiar capacity to swell or deswell when immersed in an aqueous solution or in a biological fluid, without dissolving in it. [64] This ability is made possible thanks to their three-dimensional crosslinked structure that works as an elastic network. In the case where the medium is water, it is named hydrogel. These materials can absorb a large amount of water (up to over 90% of their started weight) due to the presence of hydrophilic groups present in the hydrogel structure. In fact, among the hydrophilic groups and the water molecules present between the meshes of the polymer lattice, thermodynamically favored interactions are established (Figure 1.8).

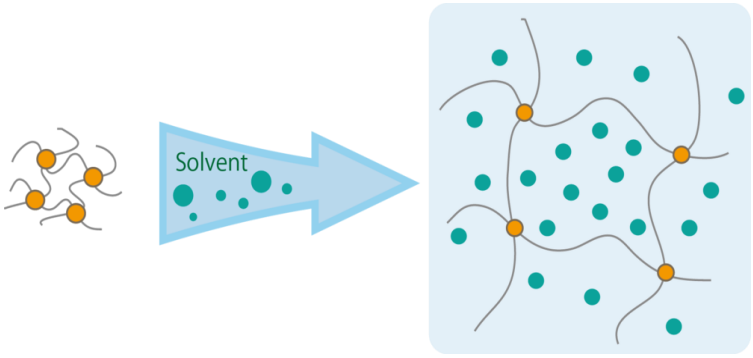

Figure 1.8: Volume variation of a mesh of the polymer lattice after the diffusion of solvent molecules within it.

The amount of swelling depends on:

- number of hydrophilic groups present in the hydrogel: the number higher, the higher the number of interactions between water molecules and hydrogel.

- degree of crosslinking: the swelling capacity decreases as it increases because of the narrower meshes of the network.

Hydrogels can be classified in five general classes based on:

1. Origin: natural or synthetic. Natural hydrogels have generally poor mechanical properties. They are often biocompatible and biodegradable. This class includes polysaccharides such as alginate, chitosan and dextran, or proteins such as collagen. [65] Synthetic polymers have well-defined structures that can be modified to produce materials with specific characteristics. In recent years, synthetic hydrogels have

gradually replaced natural hydrogels due to their long life, high water absorption capacity and high mechanical properties.[65]

2. Preparation method: homopolymeric hydrogels, copolymeric hydrogels and IPN (Interpenetrating Polymeric Network) hydrogels. The first type of hydrogel derives from the polymerization of a single type of monomer. The second ones are obtained by copolymerization reaction of two or more monomers containing at least one hydrophilic group. The macromolecular chain may assume a statistical (random), block or alternate configuration. IPN hydrogels are constituted of two independent, synthetic and/or natural crosslinked polymers, having a structure held together by the entanglements between the polymeric lattices and, often, by weak interactions such as hydrogen bonds. Semi-IPN hydrogels, consisting of a cross-linked and a non-crosslinked polymer, also belong to this class.

3. Electric charge: it is possible to distinguish amphoteric electrolyte (ampholytic) hydrogels containing both acidic and basic groups, ionic (including anionic or cationic) hydrogels, non-ionic (neutral) and zwitterionic (polybetaines) hydrogels containing both anionic and cationic groups in each structural repeating unit.

4. Crosslinking nature: physical or chemical gels can be identified. Physical gels, also called reversible gels, are the hydrogels having a physical type of cross-linking, in which the structure is held together by reversible interactions such Van der Walls or hydrogen bond interactions. The chemical or permanent gels, on the other hand, are characterized by a covalent crosslinking.

5. Structural configuration: based on physical structure, crystalline, semi-crystalline and amorphous hydrogels can be classified.

An interesting class of hydrogels are those with stimulus response, called also “smart”. These materials respond to a variety of environmental stimuli, and undergo changes in mechanical strength, network structure, growth actions and permeability. The hydrogels are subject to evident volume variations induced by external stimuli of a chemical (pH, ionic strength, chemical agents) or physical nature (pression, temperature, light, magnetic and electrical fields) (Figure 1.9). [66]

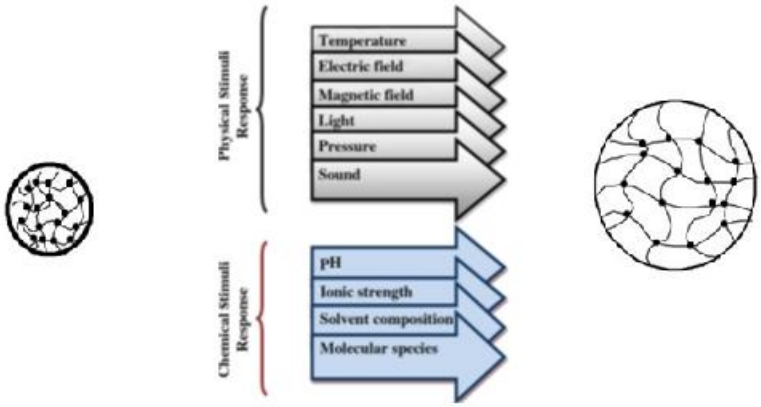

Figure 1.9: Representation of the swelling of a hydrogel in response to external stimuli of a physical and chemical nature.

Thermo-responsive hydrogels are among the most studied, thanks to the simple experimental protocol and for their potential application in the bio-medical field. These materials change their structural properties when subjected to temperature variations. The temperature at which this change occurs is known as critical solution temperature (CST) and describes thermo-responsive polymer systems. Polymeric hydrogels can have an upper critical solution temperature (UCST); in this case they will be in the swollen state above this temperature, while those having a lower critical solution temperature (LCST) will be in the swollen state below it (Figure 1.10). There are also hydrogels that have both CSTs and are contracted (or swollen) in the interval between the two temperatures. When the hydrogel is in water, the volume change is due to the competition between the intermolecular hydrogen bonds and the possible intramolecular interactions between the water molecules, which controls swelling and solvation, and the polymer. [67-72]

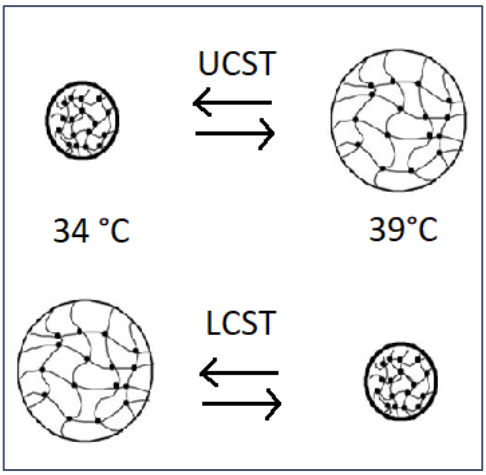

Figure 1.10: Example of swelling/deswelling process for thermoresponsive hydrogel crosslinked network.

Poly(N-isopropylacrylamide) (pNIPAAm) is one of the more studied thermosensitive hydrogels. It exhibits an LCST at about 30 °C and, since this value is near to both room and physiological temperatures, it is an excellent candidate in many application fields. Recently, pNIPAAm-based hydrogels have been used in tissue engineering: for the construction of artificial muscles and as structural supports, but also as substrates for cell cultures. Its use combined with cyclodextrins, for the synthesis of environmentally sensitive hydrogels in the biomedicine and pharmaceutical fields, is very interesting, thanks to responsiveness and the capacity to deliver drugs. [73-77]

To improve mechanical properties of these systems, especially in compression and elongation stress, a new type of materials deriving from a polyrotaxane and called Slide-Ring Gel (also called "topological gels") has been designed. This gel is characterized by a sliding crosslinking, form by two macrocycles covalently linked to each other, in a figure-of-eight shape (Figure 1.11a), inside which the macromolecular chain passes and is able to move freely. The sliding mechanism can be put in analogy with a pulley, on which a rope slides (figure 1.11b).

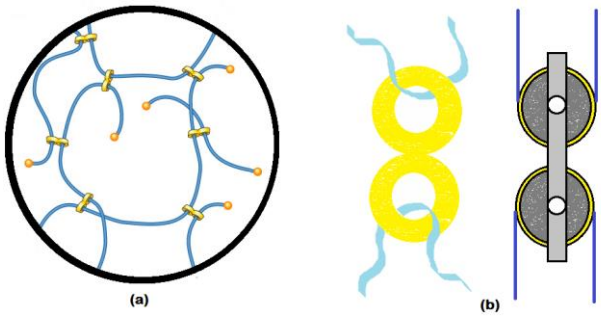

Figure 1.11: a) Representation of slide ring gel b) Analogy between a figure-eight shape (left) and a pulley (right).

The peculiarity of this mechanism is that, given the absence of covalent bonds or attractive physical interactions, the chains have a certain mobility around the cross-linking points, therefore when the gel is subjected to mechanical stresses, such as elongation (Figure 1.12), the tension concentrated on the nodes of the lattice is dissipated by the eight-shaped points, which act as pulleys allowing the chains to slide, avoiding any breakage of the structure; this is called the "pulley" effect.

This characteristic gives the topological gels exceptional elastic properties, such as high tensile strength: in fact, they can withstand an elongation equal to tenth of times their initial length without undergoing obvious deformations or resist a swelling with a volume change equal to many thousands of times the initial shape.

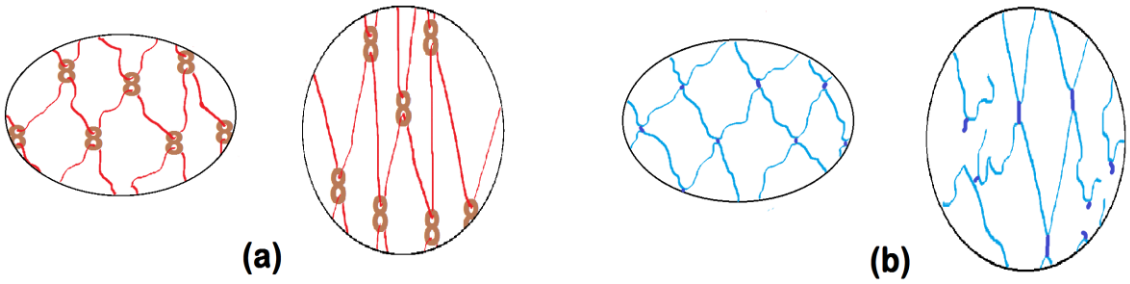

Figure 1.12: Comparison between a slide-ring gel and a chemical gel subjected to traction. a) to the left a slide-ring gel at rest, to the right the same subjected to traction. b) On the left a chemical gel at rest, on the right the same subjected to traction.

1.3 Cyclodextrins and biopolymers

1.3.1 Poly(lactic acid)

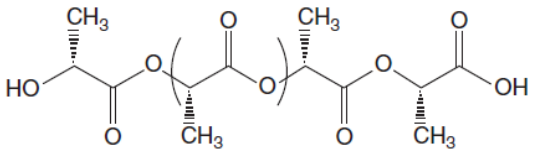

Figure 1.13: Structure of poly(lactic acid).

Poly(Lactic Acid) (PLA), shown in figure 1.13, belongs to the family of aliphatic polyesters, and is obtained by the fermentation of different biomasses (the most commonly used is corn starch). [78] PLA is a rigid thermoplastic polymer that can be semi-crystalline or totally amorphous.[79] This polymer also has other important properties such as transparency, good thermal, mechanical and processing properties (properties analogous to polyethylene terephthalate (PET) or polystyrene (PS)). The polymer degrades rapidly in the environment and the by-products, having very low toxicity, can be easily converted into carbon dioxide and water, i.e. it is biodegradable and compostable.

The starting monomer is lactic acid and it is synthesized through a fermentation process that uses 100% renewable resources per annum.[80] The lactide (cyclic derivate of lactic acid) is obtained by an oligomerization and consequently by a cyclization and purification of lactic acid (Figure 1.14a). Based on the starting configuration of lactic acid (L or D), it is possible to obtain lactide with three different stereoisomeric forms: L-lactide, meso-lactide and D-lactide (Figure 1.14b). The D and L forms are optically active, while the meso form is optically inactive.

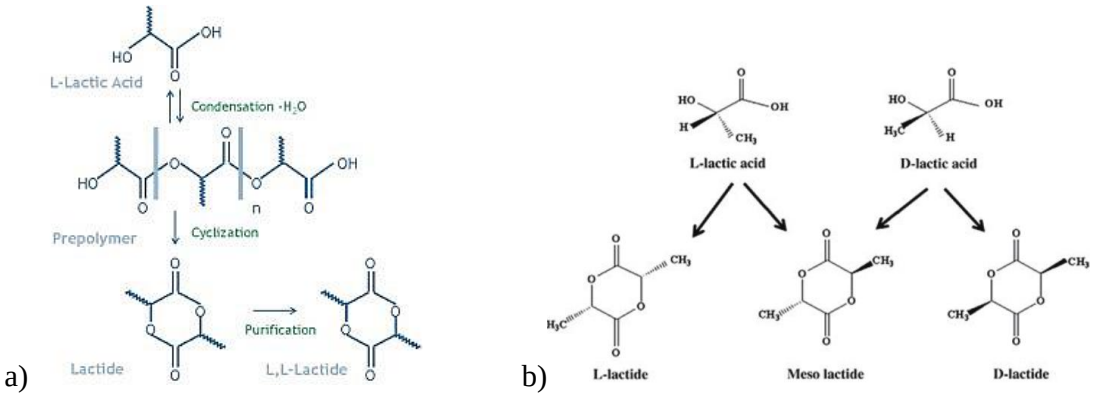

Figure 1.14: a) Lactide synthesis chart and b) L-lactide, Meso-lactide and D-lactide isomers.

The polymerization of different lactide, leads to the formation of final polymers containing different isomeric ratios and with different molecular weights. As can be seen from figure 1.15, highly pure L and D lactides form poly (L-lactide) (PLLA) and poly (D-lactide) (PDLA), respectively, which are stereoregular isotactic polymers. These are semi-crystalline polymers with a high melting point of about 180 °C and a glass transition temperature between 55-60 °C. The degree of crystallinity depends on many factors, such as molecular weight, temperature, and processing protocol and time. Instead, the D, L-lactide, on the other hand, leads to the obtainment of a product having an atactic structure, the poly (D, L-lactide) (PDLLA), which is amorphous. [78]

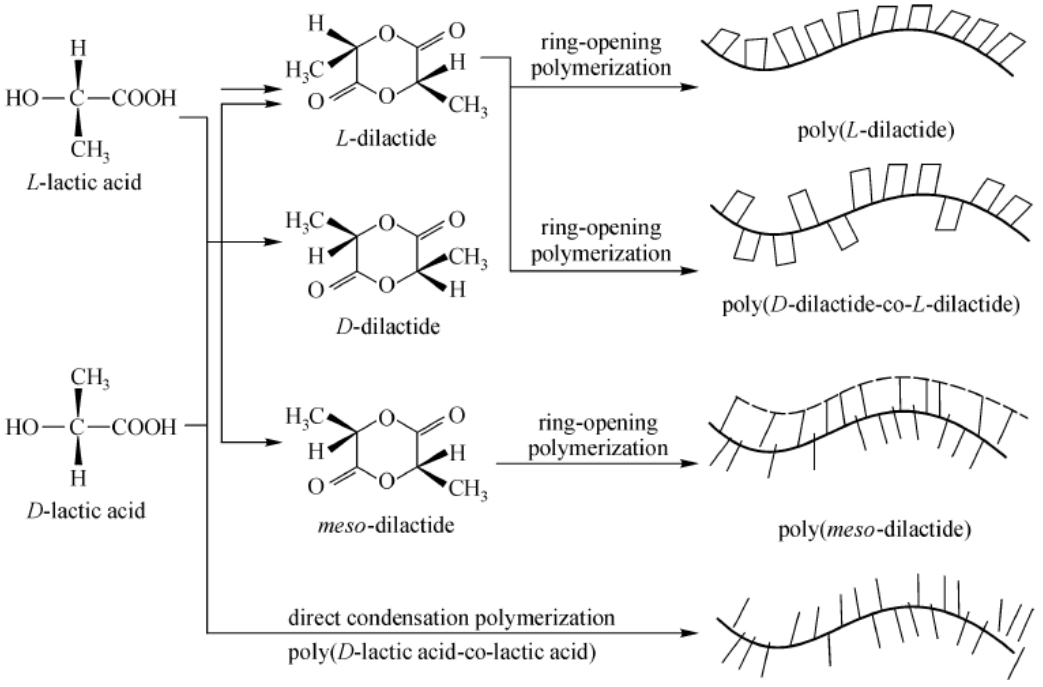

Figure 1.15: Polymerization routes for L-lactide, D-lactide and D, L-lactide. [81]

It is possible to obtain poly(lactic acid) by three different synthesis ways (Figure 1.16):[80, 82]

1. Direct condensation polymerization: in this case, the polymerization, takes place by direct condensation of lactic acid molecules and the product is a fragile and low molecular weight polymer. It is then possible to increase the molecular weight by using external coupling agents to lengthen the chain. This step presents several pros and cons: among the pros, there are the low costs for small amounts of agent used; it is possible to carry out the reaction with the melt without phase separation and increases the possibility of synthesis of different copolymers. Among the cons, there are: the presence of oligomers inside the obtained polymer, presence of residual metallic impurities, unreacted chain extension agents and poor biodegradability due to some extensive agents. Examples of these latter are isocyanates, anhydrides and epoxides. Using adjuvants as esterification-promoting agents, there is the formation of a highly pure product in which there are no residual oligomers or catalysts; however this involves a further extra work and cost increase due to neutralization and purification steps. [83]

2. Azeotropic dehydration and condensation: in this case, high molecular weight polymer is obtained (about 300 000 Daltons)[80, 82] avoiding the use of chain extenders or adjuvants. The process protocol provides in a first step the distillation of the lactic acid for a few hours at reduced pressure and a temperature of 130 °C to eliminate the condensation water. Then, the diphenyl ether and the catalyst are added and finally, purification of the PLA is performed. It is necessary to add a high amount of catalyst, essential to reach the appropriate reaction rate. The disadvantage is related to the use of high quantities of catalyst due the formation of many residues, often causing hydrolysis and degradation during processing. the catalyst is then deactivated by treatment with phosphoric acid or using strong acids such as sulfuric acid.

3. Ring opening polymerization (ROP) of lactide: this polymerization way allows to obtain high molecular weights, above 100 000 Daltons.[80, 84-86] The ROP can produce a family of polymers that differ in the molecular weight distribution, the quantity and the sequence of the lactide D in the polymer. The reaction mechanism can change depending on the type of initiator. It is possible:

- Cationic polymerization;
- Anionic polymerization;
- Insertion-coordination mechanism;
- Enzymatic polymerization;
- Solid state polymerization.

The cationic polymerization mechanism consists in an initial electrophilic activation of the bond due to protonation or alkylation of carboxylic oxygen. [87] After which there is the nucleophilic attack of another monomer, and the process proceeds until there is termination due to a nucleophile, like water. This mechanism involves a nucleophilic substitution on chiral carbon; the disadvantage of this mechanism is due to the temperature as the PLLA can be obtained only if the temperatures are below 50 °C. At higher temperatures, in fact, there is a racemization process that does not produce good mechanical and physical properties in the final polymer. Even at low temperatures, however, low yields and a low molecular weight are obtained. For this reason, this method is not used in industrial preparations.

In the anionic one, metal alkoxides are used as catalysts of the polymerization reaction. Phenoxides and carboxylates can also be used at high temperatures. Both the activation and propagation stages are based on a nucleophilic attack of an anion in the CO group of the lactide, followed by the breaking of the CO-O bond. Even in this type of mechanism there may be secondary reactions that cause racemization.

In the ROP, metal alkoxides are used as reaction catalysts. Lactide acts like a ligand that coordinates the metallic atom with carbonyl oxygen. [88] This coordination improves the electrophilicity of the CO group and the nucleophilicity of the O-R group, so that the insertion of the lactone into the oxygen-metal bond can occur. Typical initiators of this mechanism are the magnesium, aluminum, tin, zirconium and zinc alkoxides. Zinc and Tin (II) bring polymers to a higher level of purity. At present, the most used compound is Tin (II) octanoate ($SnOct_2$) thanks to its solubility, high catalytic activity and ability to favor the formation of high molecular weight polymers with low level of racemization (<1%). Furthermore, this catalyst has low toxicity levels and has been recognized by the Food and Drug Administration (FDA) as suitable for use in biomedical and food. [89]

Enzymatic polymerization is an environmentally friendly process. Besides the use of renewable resources, it uses very mild reaction conditions, with low temperatures,

ambient pressure and absence of solvents. All with high regioselectivity and the possibility of reusing the catalyst. [90]

Solid state polymerization has aroused much interest as it occurs in the absence of a solvent. The problem is represented by the cost of the process, which turns out to be very expensive and non-eco-sustainable. [91]

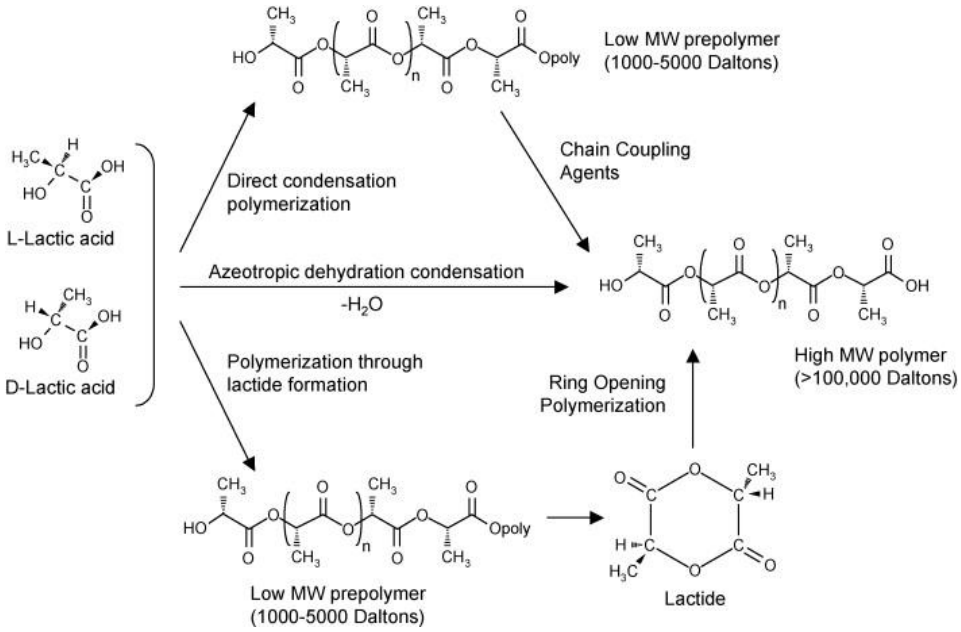

Figure 1.16: Synthesis of PLA.

1.3.1.1 Properties and applications

In general, the properties of polymers depend on some characteristics, such as molecular weight, stereochemistry and process conditions. In particular, for PLA the various differences are mainly related to the different proportions among L-, D- and meso-lactide. The melting point, the degree of crystallinity and the mechanical strength are particularly affected. Varying the proportion between D- and L-lactide isomers, the degree of crystallinity of the polymer can be tuned: it is possible to obtain either a totally amorphous PLA or a polymer with more than 40% crystallinity. The degree of crystallinity, then, affects many properties, one is the tendency of the polymer to give degradative hydrolysis. In fact, a highly crystalline PLA takes months, if not years, to be completely degraded to lactic acid, while an amorphous polymer can be degraded in a few weeks. This is due to the water resistance of the crystalline regions. Polymers with more than 93% L-lactide are crystalline while the polymers

containing lesser amount of this isomer are amorphous. The glass transition temperature is between 50 and 80 °C.

Barrier properties are particularly important for PLA, given its various applications in the field of food packaging. On this regard, they have been extensively studied with respect to carbon dioxide, oxygen and water vapor. [80] PLA shows coefficients of permeability to carbon dioxide and oxygen more or less similar to those of polystyrene, but lower than those of PET. An increase in the degree of crystallinity causes a decrease in permeability, as the diffusion occurs in the amorphous part. Although lactic acid polymers are polar materials, their water vapor permeability coefficients do not vary significantly with relative humidity.[80] The decrease in the permeability coefficient to water vapor, which is observed with increasing temperature, makes PLA interesting for a potential use in multilayer applications, in order to counterbalance the general decrease in barrier properties with increasing temperature.

PLA is a good material from the point of view of processability, in fact it can be manipulated and converted into molded parts, foams, films and fibers by conventional processing techniques. [92] Depending on molecular weight and stereochemical composition, it is possible to obtained PLA with good mechanical characteristic as a tensile strength as high as 50-70 MPa and an elastic modulus of 3.0-4.0 GPa. Furthermore, PLLA shows melting point of 170-180°C, which is higher than many other biopolymers, such as poly(butylene succinate) (PBS) and its copolymers. In addition to these good features, PLA also has some shortcomings that limit its use to some specific areas of industry. One of the major limitations of PLA is intrinsic fragility, showed by limited elongation at break together with low impact resistance. Despite showing comparable tensile strength and modulus to poly(ethylene terephthalate) (PET), elongation at break is less than 10% and the impact strength is less than 20 J/m. Another limit is the rather slow crystallization rate, which leads to a low degree of combination crystallinity with a low heat deflection temperature (HDT). [93]

A possible solution to overcome the problem is the addition of plasticizers that allow to modify the mechanical properties. These acts generally causing the decrease of the glass transition temperature and the Young's modulus, improving the elastic behavior. The selection of the plasticizer is based on various parameters, one of which is compatibility with the polymer matrix. After processing, in fact, if the selected plasticizer is not completely compatible with PLA, the material will undergo phase separation later in time. This will lead to a double negative effect: on the one hand, the surface migration of the plasticizer, on the other a return to the fragile behavior of the polymer. The presence of crystalline domains can negatively affect the distribution and compatibility of the plasticizer. [94]

Among the most commonly used plasticizers the same lactic acid is present, [95] which has the advantage of being very compatible with the polymeric matrix. Unfortunately, given its small size, lactic acid has a high mobility and therefore tends to migrate in the surface. Over the years, several alternatives have been studied such as glucose mono esters and partial fatty acid esters, [95] glycerol esters, [96] citrates, [97] citrate oligomers, [98] and also low molecular weight polymers as poly(ethylene glycol), [99, 100] poly(propylene glycol). [101]

The most promising plasticizer are represented by the lactic acid oligomers (OLA), as in addition to high compatibility with the polymeric matrix, they possess a low volatility and therefore a lower migration capacity. The use of OLAs as PLA plasticizers has shown excellent results as regards the thermal (lowering of T_g) and mechanical properties (decrease in Young's modulus). [102]

1.3.2 Cork

The term cork is the name commonly used to indicate the bark of the cork tree (Quercus Suber L.), an evergreen tree that grows in the western Mediterranean region (Figure 1.17). [103] No other tree in the world gives rise to the thick layers of suberized bark generated by the Quercus suber, even though other species can generate suberized tissues. Cork is widely used, especially in the food industry as stoppers for wine and champagne, but it is also used in the construction field as insulation materials, panels for domestic and office interiors and in the fashion field. [104]

Figure 1.17: *Quercus Suber L.*

Quercus suber grows in woods characterized by sandy soils, with low levels of nitrogen and phosphorus but rich in potassium, with a pH between 5-6 and a temperature that should never fall below 5 °C. For this reason, the cork oak is found naturally almost throughout the Mediterranean (Table 1.2). [105]

Table 1.2: distribution of the areas in which there are forests of Quercus suber.

Region and country	Area (ha)	Percent of total
Mediterranean Europe		
France	110 000	5
Italy	90 000	4
Portugal	660 000	30
Spain	440 000	20
Subtotal	1 300 000	59
North Africa		
Algeria	460 000	21
Morocco	350 000	16
Tunisia	90 000	4
Subtotal	900 000	41
Total	2 200 000	100.00

The porous structure of cork is responsible for the unique properties of this material, such as its remarkable elasticity, low density, impermeability to liquids and gases, low thermal and acoustic conductivity, thermal resistance, resistance to combustion and decomposition. [104] The industrial processing of cork (primarily the production of cork stoppers) produces significant amounts of residues, such as cork powder that is generated during the production of granulated cork for agglomerated materials. The cork powder particles have an inadequate size distribution due to their use in the manufacture of agglomerates and are currently mainly burned to produce energy. Huge quantities of cork by-products are therefore potentially available for alternative uses to combustion. [104]

1.3.2.1 Structure and composition

Cork is formed by hexagonal prismatic cells that are organized in rows and assembled in parallel in a compact arrangement. In adjacent rows, the bases of the prism are not coincident and are in staggered positions, aligned in the radial direction (Figure 1.18).

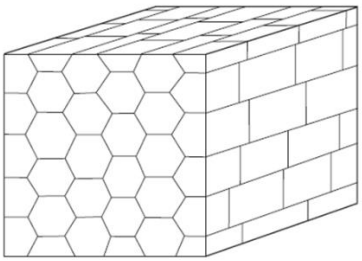

Figure 1.18: three-dimensional cork structure.

The chemical components are in the faces and in the borders of the cells, forming a solid three-dimensional matrix that surrounds the empty cells filled with air. Many of the specific properties of cork depend on this type of structure and are directly related to its chemical composition. [106] Cork is a barrier that protects the physiologically active tissues of the tree trunk from the external environment, in fact it limits the loss of water, controls the transfer of gas and does not allow the passage of large molecules and micro-organisms.

From a chemical point of view, all plants are made up of two types of components:

a) structural: formed by macromolecules, which form the cell wall and define its structure. They are insoluble and cannot be removed without affecting the structure and properties of the cell;
b) non-structural: low molecular weight organic compounds that can be solubilized with appropriate solvents.

In cork, the structural components of the cell wall are, in order of importance: suberin, lignin, cellulose and hemicellulose. [106]

The term suberin is used to define a complex of different components including esters of saturated and unsaturated carboxylic acids capable of forming a layer impermeable to water. It is present in many plant species but, in the case of cork, it is the main structural component of the cells and constitutes about 50% of the total material (Figure 1.19).

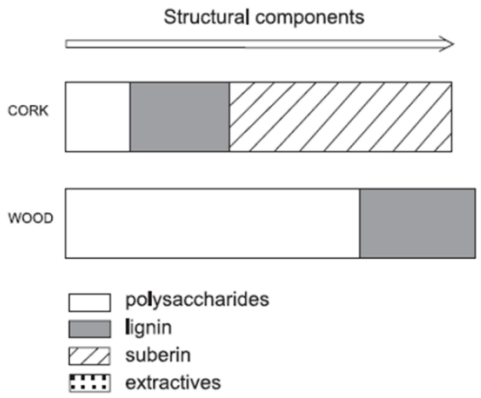

Figure 1.19: Representation of the chemical composition of cork and cork oak wood.

The monomeric composition of suberin varies among plant species but, in general, is composed of two chemically different domains: an aliphatic and an aromatic one. The interest in suberin is that it is an abundant source of hydroxylated fatty acids, α, ω- dicarboxylic acids and their dihydroxy- or epoxy derivatives, compounds that are not very abundant in nature. [107] It is difficult to define a precise monomeric unit of suberin since the spatial arrangement of these units cannot be precisely defined, even when their relative abundance is known. This latter aspect depends on the depolymerization methods used to isolate the aliphatic fraction (named dep-suberin) whereas about the aromatic domain, its identification/quantification is complex due to its macromolecular nature and the structural similarity with lignin. To illustrate the macromolecular structure of suberin many models have been designed: recently, one has been hypothesized in which the suberin aliphatic domain, composed of long chain branched polyester units, are linked through glycerol units (Figure 1.20). [108] From the earliest studies, glycerol has been found in suberin depolymerization extracts but its role as a fundamental structural component has only been demonstrated with more recent studies. [109] The aromatic domain has a structure like lignin, separated in space by aliphatic domains, and is composed of cross-linked coumaric acid and amide units. [109]

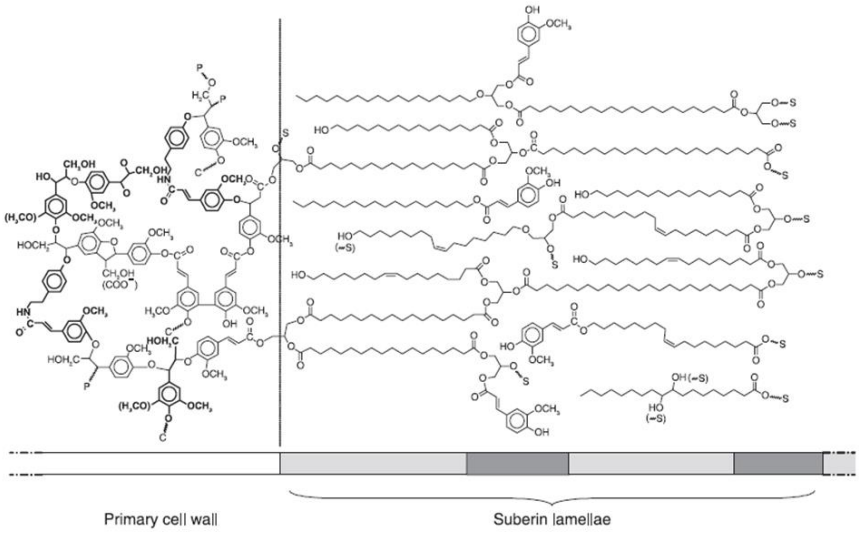

Figure 1.20: Suberin structure model. (C: carbohydrates, P: phenol; S: suberin)

In general, the analysis of the composition is carried out following the depolymerization of suberin through the splitting of esters. The methods used involve both an alkaline hydrolysis and alcoholism. Alkaline methanolysis with anhydrous sodium methoxide is the most common depolymerization method that produces the components of aliphatic acid in the form of methyl esters.

In table 1.3 the distribution of species in the aliphatic and aromatic domains referred to the two most important sources of suberin, Quercus suber and Betula pendula are showed.

Table 1.3: distribution of species in the Quercus suber and Betula pendula.

	Quercus suber	*Betula pendula*
References	[7, 8, 12, 51, 60, 61, 68]	[37, 63]
Aliphatic alcohols	0.4–4.7	–
Fatty acids	**2.5–14.9**	**7.4–12.3**
C(16:0)	0–0.5	–
di(OH)-C(16:0)	0–0.9	–
C(18:1)	0–1.8	–
9,10-di(OH)-C(18:0)	0–6.6	–
9,10-epoxi-C(18:0)	0–2.2	–
C(20:0)	0–0.3	–
di-OH-C(20:0)	0–10.1	–
C(22:0)	0–2.5	–
C(24:0)		–
C(26:0)	0–2	–
ω-Hydroxyfatty acids	**36.0–61.7**	**76.7–79.7**
C(16:0)	0–1.2	
9,16-di-OH(C16:0)	0	3.2–3.7
C(18:0)	0–0.6	
C(18:1)	0–18.2	11.1–12.2
9,10-epoxy-C(18:0)	0–5.5	37.0–39.2
9,10-di(OH)-C(18:0)	0–12.7	8.4–8.6
9,10-(OH,OMe)-C(18:0)	0–7.5	
C(20:0)	0–2.2	2.8
C(20:1)	0–1.2	
C(22:0)	0–28.6	13.6–13.9
C(24:0)	0–4.6	
C(26:0)	0–4.4	
α,ω-Dicarboxylic acids	**6.1–53.3**	**10.4–12.9**
C(16:0)	0–3.1	
C(18:0)	0–0.5	0–0.9
C(18:1)	0–9.1	3.4–4.7
9,10-epoxy-(C18:0)	0–37.8	
9,10-di(OH)-C(18:0)	0–7.7	
9,10-(OH,OMe)-C(18:0)	0–20	
C(20:0)	0–4.9	
C(20:1)	0–0.3	
C(22:0)	0–7.1	6.1–8.2
C(24:0)	0–1.1	
Aromatic compounds	**0.1–7.9**	–
Ferulic acid	0.1–7.9	–

1.3.2.2 Functionalization of cork

As previously described, cork consists mainly of suberin and polysaccharides. The hydroxyl functionalities of these structures can be exploited to make changes on the cork. In particular, the reaction between cork powder, obtained from processing waste, and propylene oxide (PO) was studied. [110]

Using a nucleophilic catalyst, strong Brønsted bases such as KOH, it is possible to deprotonate the OH groups of the substrate, which initiate the anionic polymerization of propylene oxide. In this way the insertion of poly-PO chains on the starting macromolecules can occur. This reaction is a process of extending the chain that transforms the cork powder

into a liquid viscous polyol, a product having many OH groups as the initial substrate. This branching mechanism produces oligomeric diols (Figures 1.21, 1.22). [104]

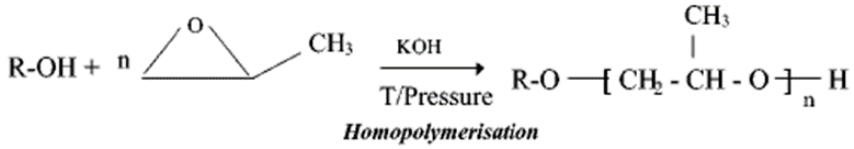

Figure 1.21: polymerization reaction of PO.

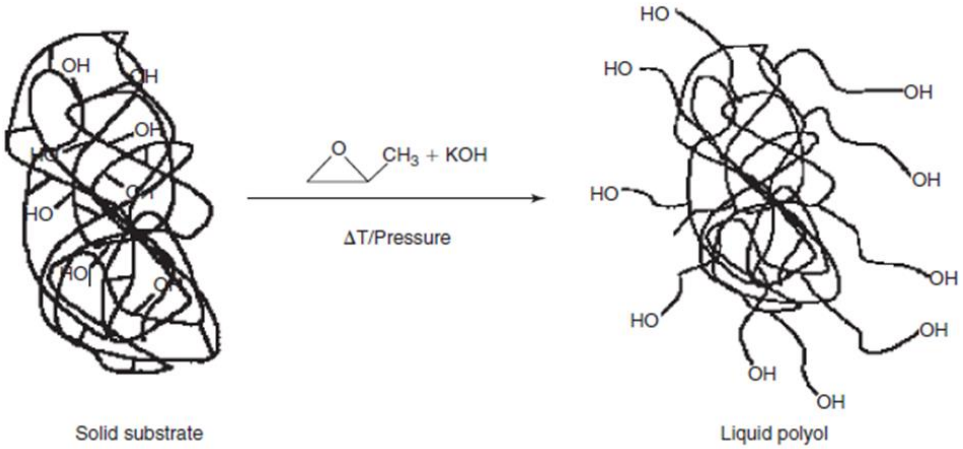

Figure 1.22: Reaction scheme of cork modification with addition of propylene oxide; 130 °C, 10 bar PO.

1.4 Methyl cellulose

1.4.1 Cellulose

Cellulose is the most well-known organic polymer derived from biomass. Given its abundance, it is considered an inexhaustible polymer raw material with fascinating structure and properties. It was first discovered by the French chemist Anselme Payen in 1839, during an acid-alkaline process of the plant tissues.[111, 112] From the elemental analysis, he observed that cellulose had a structure similar to starch. Before its discovery, cellulose was used in form of wood, cotton and other plants for a variety of uses in different fields like building materials, and clothing. The first cellulose-based polymeric material was synthesized in 1870 by the Hyatt Manufacturing Company, known with the name of celluloid (cellulose nitrate), obtained by a reaction between cellulose and nitric acid.[113] In 1920, Hermann Staudinger determined the cellulose structures through acetylation and deacetylation reaction of the cellulose and concluded that the d-glucose units were covalently linked together to form long molecular chains.[114]

1.4.2 Structure and properties

Cellulose is derived from D-glucose units, bound through β-glycosidic bonds (1→4) to form linear polymer chains with many hydroxy groups. In each chain there is a non-reducing end, where the carbon C1 is involved in the glycosidic bond, and a reducing end, where C1 attaches a hydroxyl group, thus allowing the opening of the glucopyranose ring (Figure 1.22). The degree of polymerization (DP) of cellulose chain varies with the origin and treatment of the raw material. In the case of wood pulp DP ranges from 300 to 1700 monomeric units, while for cotton and other vegetable fibers DP values are between 800 and 10000, depending on the treatment; similar DP values are observed in bacterial cellulose. Sometimes two glucopyranosyl rings are known as the constituent units of the polymer, known as cellobiose (Figure 1.23).

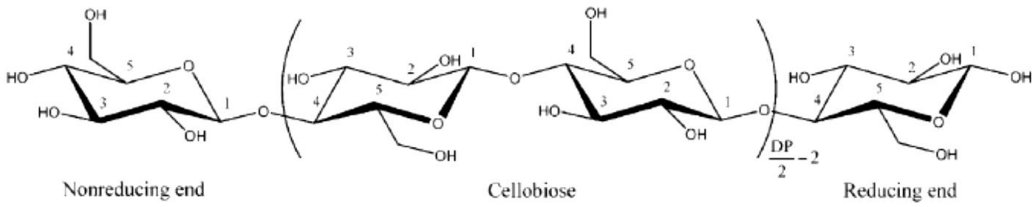

Figure 1.23: Cellulose structure.

The glucopyranosyl rings adopt a chair conformation, with a rotation of 180° respect to each other. The three hydroxyl groups in each ring are arranged in equatorial position respect to the middle plane while the hydrogen atoms are in axial position. The presence of hydroxyl groups allows the formation of a complex network made of intra- and inter-molecular hydrogen bonds that stabilize the single chain (Figure 1.24). In this way, more chains aggregate giving rise to the crystalline systems typical of cellulose fibers. [115, 116]

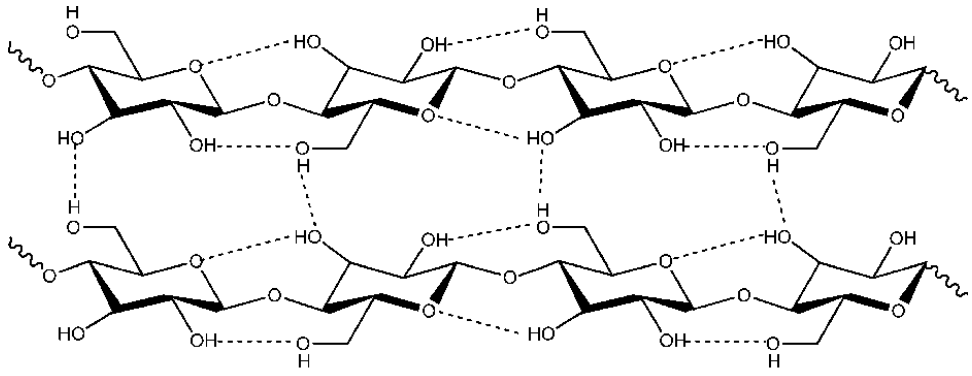

Figure 1.24: Inter-intramolecular hydrogen bonds in cellulose.

This hydrogen bond network makes cellulose insoluble in both water and organic solutions, but at the same time, confers to polymer excellent properties thanks to the presence of crystalline domains. It exhibits a theoretical Young module (E), calculate by x-ray diffraction (XRD), of about 140 GPa.

Generally, in plants, about 36 cellulose fibers chains tend to bond together leading to the formation of large units, called protofibrils, that have a diameter of about 3.5 nm. These structures, in turn, tend to pack further, forming structures of ever larger dimensions, called microfibrils (d= 4-35 nm, based on the type of cellulose source considered), which continue

packing until the known cellulose fibers are generated (Figure 1.25). [116] Although the packing of the cellulosic chains allows for an orderly structure with high crystallinity, there are amorphous areas randomly located along the microfibrils that cause a fiber distortion as the internal forces are lost.

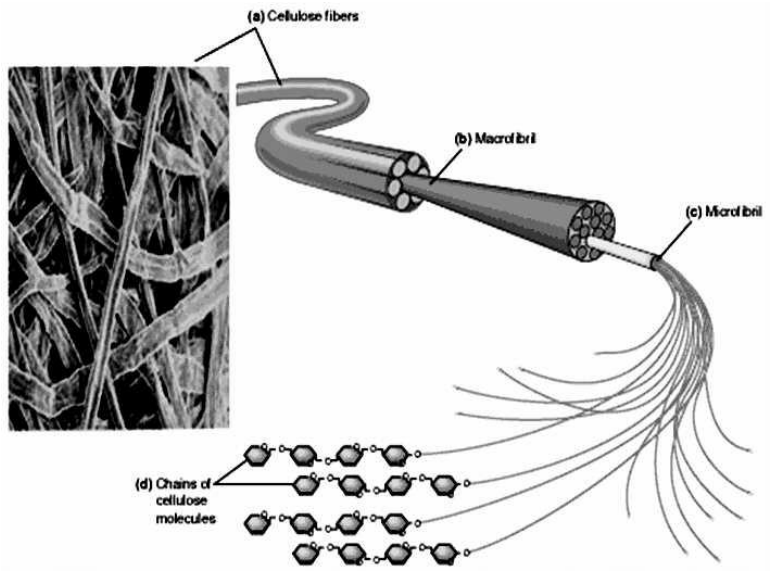

Figure 1.25: Cellulose fibrous structure.

The strong interactions between the cellulose chains can be interrupted by using appropriate solvents that split the adducts. One of the most commonly systems, used as cellulose solvent, consists of a solution of lithium chloride in dimethylacetamide (DMA/LiCl). [117, 118] This system has been extensively studied by the scientific community. [119-124] In recent years, additional systems have been developed such as tetrabutylammonium trihydrate fluoride in dimethyl sulfoxide (TBAF/DMSO) [125] or systems in which solvents contain a metal such as cuprammonic hydroxide, [126] and again N-methylmorpholine-N-oxide (NMMO), ionic liquids (IL) and alkaline systems/urea (or thiourea). [127]

1.4.3 Cellulose derivates

The hydroxyl groups (-OH) of cellulose can be partially or fully reacted with various reagents to afford derivatives with useful properties like mainly cellulose esters and cellulose ethers (-OR). It is possible to obtain different types of esters such as aliphatic, aromatic esters through in situ activation with tosylchloride, N,N-carbonyl diimidazole and iminium chloride in

homogeneous acylation with DMA/LiCl or DMSO/TBAF. [112] In this way, a wide range of products with different substituents is obtained, with various properties (bioactivity, thermal behavior and dissolution capability). In figure 1.26, a schematic representation of different esterification route is shown.

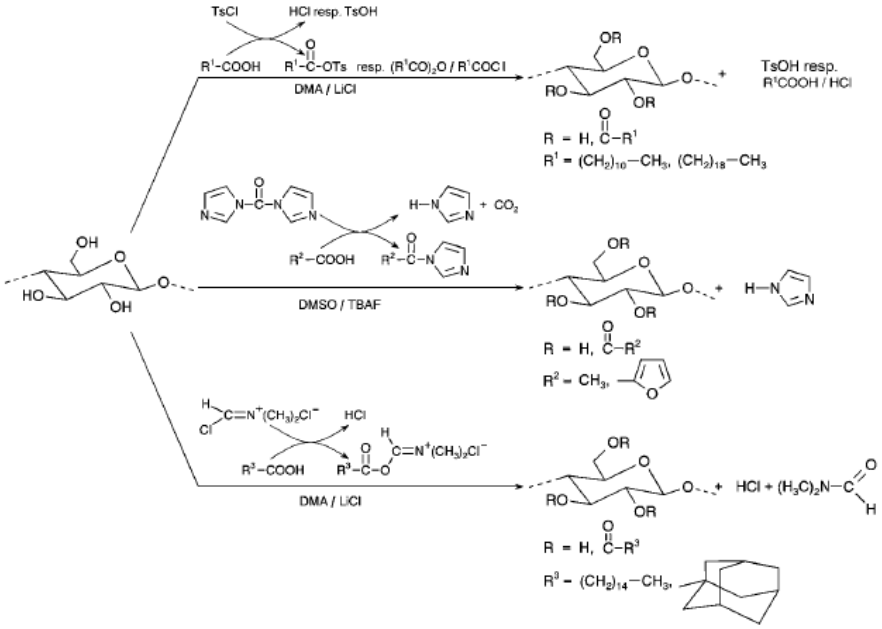

Figure 1.26: Schematic representation of esterification by in situ activation with a) tosyl chloride b) N,N-carbonyldiimidazole c) iminium chloride. [112]

As regards cellulose ethers, it is possible to synthesize a wide range of products including trityl, [128] methoxy substituted, [129, 130] as well as allyl, silyl and benzyl ethers, [131] which in addition to their use as substrates, can act as protecting groups. The reactivity of cellulose with high crystallinity produces materials that are not very soluble in water. Therefore, to obtain more soluble products it is necessary to destroy the crystalline domains by treatment with an aqueous solution of sodium hydroxide. [132] In figure 1.27 a schematic synthesis of the most known ethers is represented.

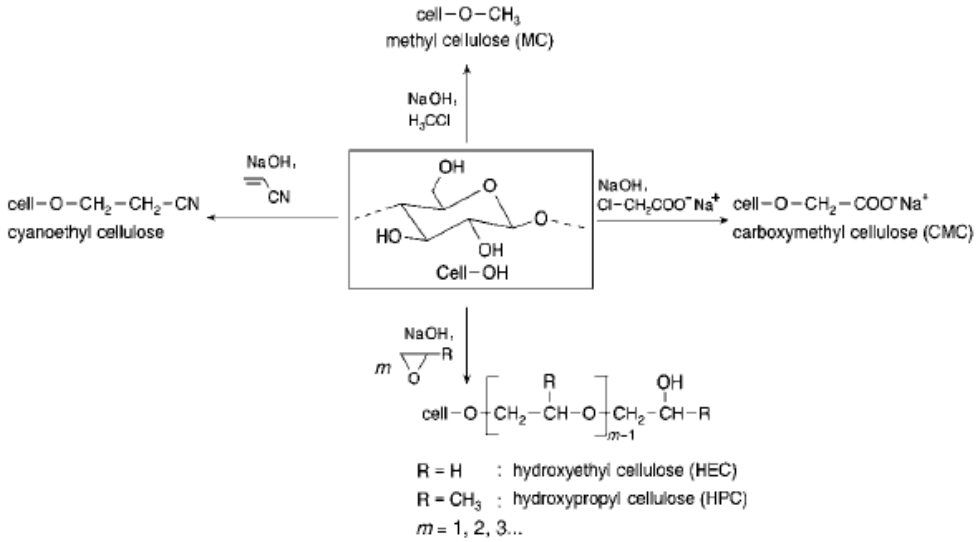

Figure 1.27: Example of the most common cellulose ethers.

1.4.4 Methyl cellulose (MC)

Methylcellulose (MC) is the easiest derivative of cellulose, in which the hydroxyl groups are replaced by methoxy groups (Figure 1.28). [133] On a commercial scale, it is obtained through the Williamson heterogeneous etherification process, which consists in the reaction of alkali-cellulose with methyl chloride. [134] In this way, a cellulose with a heterogeneous distribution of substituents along the polymer chains is achieved. The degree of substitution (DS), which corresponds to the number of hydroxyl groups replaced per monomer unit, ranges from 1.7 to 3.

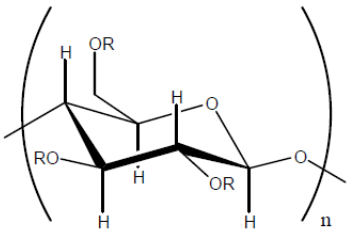

R= CH3 or H

Figure 1.28: Methylcellulose structure.

MC is odorless, tasteless, biocompatible and non-toxic like cellulose. It has unique properties which make it very interesting for multiple uses in different sectors like that biomedical, pharmaceutical, food-industry and cosmetic. [135-137] The most important property of MC is the capacity to form a gel with temperature increase (thermo-gelation process). This process

takes place thanks to the presence of highly substituted areas called "hydrophobic zones" and of less substituted areas called "hydrophilic zones. [133] Only the aqueous MC solutions form a gel at high temperatures, typically above 50 ° C. MC that are prepared under homogeneous reaction conditions do not show this thermo-gelation property.

Initially, at low temperatures the macromolecules are in a hydration state therefore the interactions between the cellulose chains are minimized. As the temperature increase, above a critical temperature called Lower Critical Solution Temperature (LCST), the macromolecules gradually lose the hydration water, and this causes the sol-gel transition. This transition is completely reversible, in fact by cooling the solution, the gel liquefies and the system becomes liquid again. For MC, the LCST is included between 40-50°C. [133-138]

The gelation process of aqueous methylcellulose solution was studied from Sekiguchi et al. by using different characterization techniques such as infrared spectroscopy (IR), differential scanning calorimetry (DSC), and small angle X-ray scattering (SAXS). [139] This study showed that the gelation behavior is different when comparing a regioselective substituted 2,3-di-O-methylcellulose series (called 2,3MC-n, where n = 1-3) and a randomly replaced series (called R-MC). This indicates that a different cooperation between the hydrophobic interaction among the methyl groups and the hydrogen bonds between the hydroxyl groups in C6 of different MC chains exists, and this depends on the position of the methyl groups in the chain. [139]

1.4.5 Cellulose-derivates: hydrogels

In recent years, many researchers have dedicated much efforts and time to the search of alternative materials, deriving from natural and eco-sustainable sources, compared to those of a synthetic nature for the synthesis of polymeric hydrogels with stimulus and non-stimulus responses and good mechanical properties. The chemical bases of hydrogel are explained in chapter 1, paragraph 1.2.2. Recent literature collects advances on hydrogel materials based on pure cellulose, but also cellulose hybrid composites and hydrogels. It is possible to obtain hydrogels using different cellulose-derivates, like methylcellulose (MC), hydroxypropyl cellulose (HPC), hydroxypropylmethyl cellulose (HPMC) and carboxymethyl cellulose (CMC) through physical crosslinking and chemical crosslinking. The water-soluble cellulose derivatives, being mostly biocompatible, can be used especially in the food industry as thickeners, binders, emulsifiers, film formers, suspension aids, surfactants, lubricants and stabilizers, but also additives in formulations pharmaceutical and cosmetic products. [140]

For example, MC hydrogels are used in the biotechnological field as coating materials for polystyrene dishes and are used as incubator cells to cultivate human embryonic stem cells (hES) for the formation of embryonic bodies (EB) in liquid suspension culture. [141]

It is possible to synthesize hydroxypropyl cellulose (HPC) microgels with temperature-responsive properties, through chemical crosslinking in a water-surfactant dispersion (dodecyl trimethylammonium). [142] From this study, it was found that the size and distribution of the particle size of the microgel depend on different parameters including the surfactant concentration, the HPC concentration and the reaction temperature. It has been discovered that microgels are formed only above a critical micellar concentration (cmc) of the surfactant. For the HPC concentration, it was found that the increase from 0.1 to 0.3% by weight, the size distribution becomes significantly larger. Finally, the reaction temperature plays an important role for the dimensional distribution in the microgel: as the temperature rises above the LCST, the particle size increases rapidly. [142]

By reacting MC with a small amount of ethylene glycol (EG), hydroxypropylmethyl cellulose (HPMC) is obtained. This cellulose-derivative has been very studied for the creation of biomaterials. These materials have good biocompatibility and are very interesting due to the rheological properties shown. An interesting modification of these, envisages the introduction of silane groups to give Si-HPMC. This is a non-toxic and biocompatible material, so it can be widely used in biomedical areas, such as scaffolds for cell cultures, bone implants and cartilage substituents. [137]

Carboxymethyl cellulose (CMC) is a negatively charged polyelectrolyte. Polyelectrolytes are soluble in water, but when they form a complex with another system charged in the opposite way become insoluble in aqueous solution. For these reasons, a polymeric material made of a polyelectrolyte system can be employed in amphoteric films, fibers, and hydrogels. An example of smart hydrogel is represented by CMC-chitosan hydrogel, which results to have an electrical stimulus response based on the pH of the solution. [143]

1.4.6 Cellulose and cellulose-derivates interpenetrating polymer networks (IPNs)

An interpenetrating polymeric network (IPN) is a polymer formed by two or more networks that are at least partially interconnected on a molecular scale but not covalently bound together. The two or more networks can be figured out as intertwined and cannot be separated,

except with the breaking of covalent bonds, even if they are not linked by any chemical bond. While in the semi-interpenetrating polymer network (SIPN) only one of the components must be crosslinked and form the network, in which a second component can be linear or branched but not crosslinked. In principle, SIPN networks can be separated from constituent polymeric networks without breaking chemical bonds; they are mixtures of polymers. [144] The difference between IPN and SIPN is show in figure 1.29.

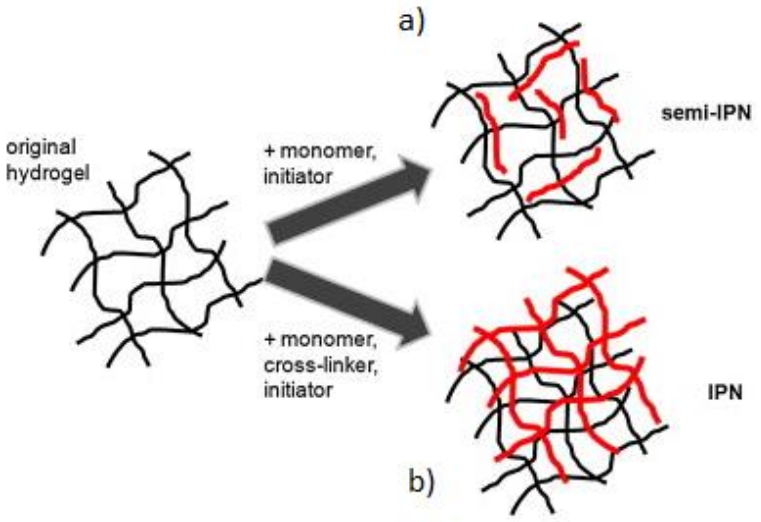

Figure 1.29: Schematic representation of: a) semi-interpenetrating polymer network (semi-IPN) and interpenetrating polymer network (IPN).

From the point of view of chemical synthesis, IPN hydrogels can be classified into:

- simultaneous IPN: a solution of the precursors of both networks is prepared and the two networks are synthesized simultaneously with different non-interfering polymerization methods (e.g. chain and step-growth polymerization) (Figure 1.30a). [145-147]

- Sequential IPN: in this case one of the networks is already formed and is allowed to swell in a solution containing the mixture of monomer, initiator and activator, with or without crosslinker (Figure 1.30b). If a crosslinking agent is present, an IPN is obtained while, in its absence, a semi-IPN. [148, 149]

It is possible to pass from a semi-IPN to an IPN by selective crosslinking of the linear polymer chains of the second network (Figure 1.30c). [150-152]

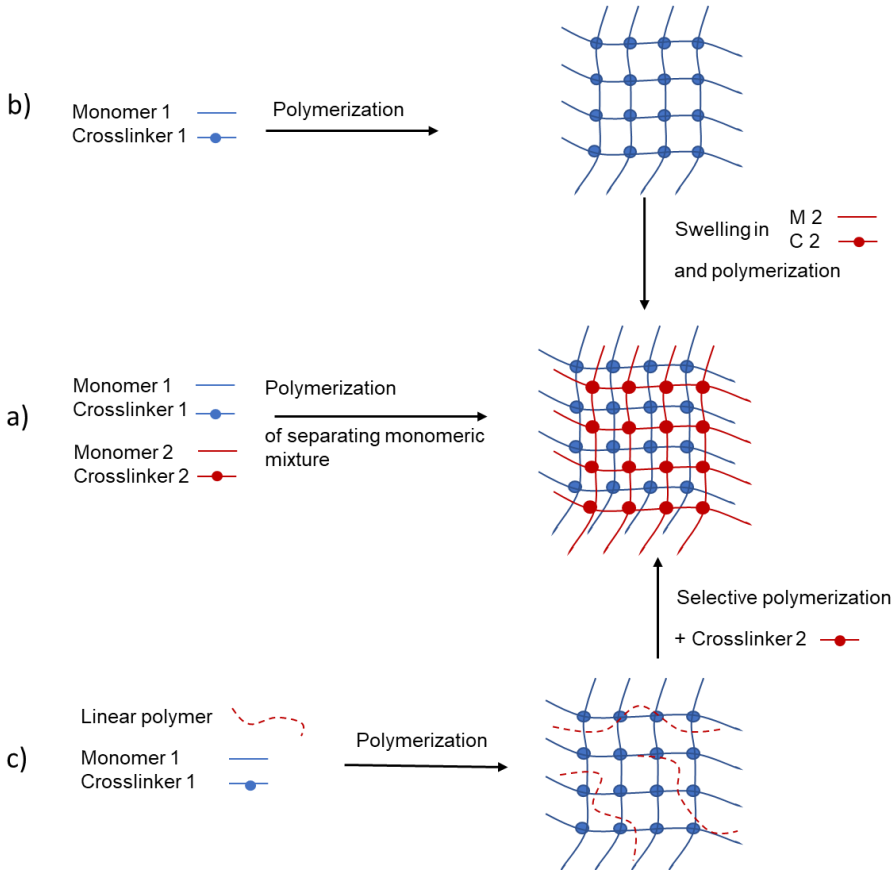

Figure 1.30: Schematic representation of the IPN formation: (a) simultaneous strategy; (b) sequential strategy; (c) selective crosslinking of a linear polymer.

Over the years, various IPN and semi-IPN cellulose-based or its derivatives have been synthesized. Double-network hydrogels (DN) with high mechanical strength were prepared with bacterial cellulose (BC) and gelatin, [153] or IPN cellulose-based with poly (N-isopropylacrylamide) were synthesized by in situ polymerization reaction of the second monomeric mixture. These hydrogels have demonstrated high mechanical strength and adjustable thermal sensitivity, which strongly depend on the weight ratio between the two polymers networks. [140] Recently, semi-IPN hydrogels composed of a chitosan network and a linear chain of acrylamide-graft-hydroxyethyl cellulose (AAm-g-HEC), trapped inside the lattice, have been synthesized for the release of sodium diclofenac. [154] Other materials made of chitosan and cellulose or cellulose derivates have been synthesized in many ways, for different uses. [155-158]

Several other polysaccharides, or their derivatives, have been used in the preparation of hydrogel semi-IPN or IPN composites. [159] Among these, IPN composite hydrogels consisting of sodium alginate (SA) and numerous synthetic polymers containing different end

groups, such as the carboxyl one, have showed new properties such as super-porosity, [152] electrical sensitivity, [160] drug-controlled release, [161] multi-response stimulus. [162, 163] IPNs in which SA is present have gained wide interest in industrial applications such as actuators or as muscle substituents. Moreover, the ability to respond to the electrical stimulus has made these materials excellent candidates in the production of components of artificial organs, such as the contractile structure similar to a muscle, sensors and systems of release of drugs modulated by electric current. [160]

Among the synthetic monomers, those most used for the synthesis of hydrogel IPN and semi-IPN are acrylamide (AAm), [164-169] N-isopropylacrylamide (NIPAAm), [170, 171] N, N-dimethylacrylamide [172] and 2- hydroxyethyl methacrylate (HEMA). [173, 174]

IPNs have been developed to improve different properties compared to the individual polymers that compose the IPN. The main advantages are, in addition to greater material density, better mechanical properties, more controllable physical properties and (commonly) more frequent drug loading than single-network hydrogels. [149, 175] For example, in the case of the IPN made up of chitosan/PNIPAAm, the load capacity of the IPN is improved compared to the pure PNIPAAm hydrogel, while retaining the strong thermosensitivity of the PNIPAAm network. [171] In many cases, semi-IPN can keep rapid kinetic response rates at pH or temperature more effectively, while retaining the benefits of IPN in controlled drug delivery (pore size change, drug release slowdown).

1.5 Frontal polymerization

Frontal polymerization (FP) is a non-conventional technique of macromolecular synthesis based on the conversion of the monomer into a polymer by means of a hot moving reaction front able to sustain itself. FP needs that the reaction is exothermic: the heat released during the polymerization feeds the hot front that propagates from one end to the other of the reacting system. Initially the front is generated by an external source of energy (for example a welder) which is put in contact with one end of the reactor (e.g., a cylindrical test tube) containing the monomeric mixture in which the initiator and/or the catalyst are dissolved. Once the reaction is ignited, if the heat released by the polymerization is large, the reaction goes to completeness without the need of a continuous supply of external energy. The polymerization takes place in the area below the front, and as the reaction progresses, both the formed polymer and the monomer that still must react will be present in the reactor, as shown in Figure 1.31.

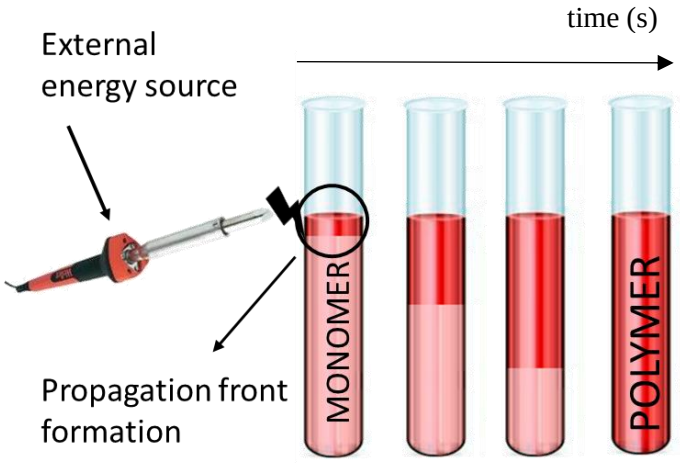

Figure 1.31: Schematic representation of FP synthesis protocol.

In addition to thermal frontal polymerization, [176] there are two other types:

- Photo-assisted FP (Photo-frontal Polymerization), in which the propagation front needs an external UV radiation source for propagation; [177]

- Isothermal FP (Isothermal Frontal Polymerization), which depends on the gel effect, called also Trommsdorff-Norrish, [178] and occurs when the monomer and initiator diffuse inside a polymeric germ. [179]

Compared to the classic thermal polymerization, FP has the following advantages:

- simplified protocol;
- minimum energy consumption;
- possibility of operating in the absence of solvents;
- direct use of monomers without the elimination of the inhibitor;
- high conversions;
- short reaction times;

The two main parameters of interest in FP are the maximum front temperature (T_{max}) and its velocity (V_f). The first is determined by monitoring the temperature trend as a function of time through the position of a thermocouple inside the reaction mixture, away from the ignition zone (the temperature profile is shown in Figure 1.31). It can be seen in the graph that for a certain period of time the temperature does not undergo appreciable changes, but once the front crosses the zone in which the thermocouple is placed, it undergoes a sharp increase reaching the maximum value Tmax; the temperature of the front varies according to the system studied. In the case in which other concomitant reactions take place in addition to FP, an increase is observed (or, more rarely, a temperature decreases) even in areas far from the front (the first section of the graph in figure 1.32 is not horizontal).

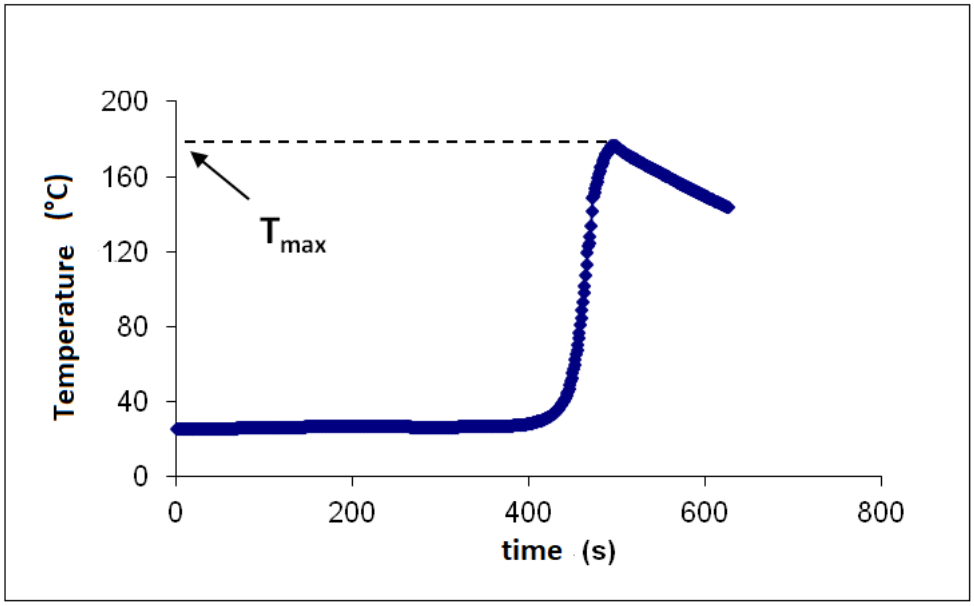

Figure 1.32: FP Temperature profile as a function of time.

Given the high temperature reached, FP often guarantees large conversion.

The other main parameter V_f is measured and calculated simply by marking the position from the beginning of the formation of the front and for regular time intervals. For a pure FP (in which the conversion is due to the FP itself and not to any secondary reactions) the velocity is constant, while in the case of undesirable concomitant reactions the temperature, in the areas far from the front, and the speed are not.

Sometimes, it is possible that phenomena which lead to the slowing down and in some cases to the stopping of the polymerization reaction may occur. The most common of these phenomena is called fingering, which happens when a polymer is denser than the corresponding monomer and/or melts at the temperature of the front. In these cases, there is the formation of descending drops of hot material, similar to fingers, which contaminate the lower areas of the monomer that has not yet reacted, thus causing the removal of heat from the front and the triggering of local spontaneous polymerizations. This phenomenon can be reduced or prevented taking some precautions, like increasing the viscosity of the medium by adding suitable additives or increasing the amount of crosslinking agent.

The monomers used in FP are divided into three main categories, depending on the characteristics of the resulting polymers: [180]

- Monomers that form thermoplastic polymers. This class includes those highly reactive monomers that are present in the molten state at the maximum temperature of the front. Examples of this class are acrylic monomers such as benzyl acrylate, hexyl acrylate and butyl methacrylate. [180] Some of these monoacrylate monomers give the phenomenon of fingering.

- Monomers that form thermosetting polymers. In multifunctional monomers or systems where crosslinking systems are present, the polymerization develops in three dimensions, giving rise to highly crosslinked polymers. The passage of the warm front allows polymerization to take place simultaneously with cross-linking, avoiding diffusive problems. Examples of monomers are triethyleneglycoldimethacrylate (TEGDMA) and diethylenglyl dimethacrylate (DEGDMA).

- Monomers that form phase-separated polymers. These monomers have limited miscibility with the respective polymer. During polymerization the system passes from a condition of homogeneity to one of heterogeneity due to the insolubility of the growing polymer in the monomer mixture. The insoluble polymer particles coagulate and adhere to the reactor, in this way a very clear monomer-polymer interface is created, at this point the heat can easily propagate to the areas where it has not reacted and complete the polymerization. Examples of this type are all monomers containing carboxylic groups, such as acrylic and methacrylic acids. [181] These monomers can also give rise to fingering.

The minimum general conditions for obtaining a stable front are still under study, as each monomer requires a perfect combination of the initial concentration of monomer and initiator, initial temperature, reactor geometry but above all the following points are of fundamental importance:

- The monomer and any solvent must have a high melting and boiling point to avoid melting or boiling during the passage of the front. The presence of bubbles interferes with propagation and leads to the formation of an inhomogeneous product. The formation of bubbles, in some cases, is due to the decomposition of the initiator, which can lead to the formation of gases such as carbon dioxide and nitrogen. To avoid this, for example, persulfate-based initiators can be used.

- The polymerization rate must be practically zero at room temperature, while it should increase drastically at the front temperatures. In this way bulk polymerizations are avoided, and the polymerization reaction is triggered only if the right amount of thermal energy is applied.

- The thermal energy developed by the polymerization reaction must be enough to guarantee the self-maintenance of the front. In some cases, the high dispersion of the energy released by the exothermicity of the reaction can be avoided by using larger diameter reactors, pre-heating the reagents or using insulation systems.

The first polymer to be synthesized by FP, from Chechilo and Enikolopyan in 1972, was poly (methyl methacrylate), under adiabatic conditions and at high pressures. [176] Subsequently, this technique was extensively studied by various research groups. Pojman et al. used FP for the synthesis of epoxy resins, vinyl polymers [182] and subsequently thermochromic compounds [183] (compounds able to change color with temperature). Morbidelli et al. used FP to obtain polymer blend of poly (methyl methacrylate)/polystyrene. [184] The FP technique was also used for the synthesis of copolymers: for example, Washington and Steinbock used FP to obtain thermosensitive polymers. [185] Crivello used FP to polymerize diglycidyl ethers, [186] Chen et al. they synthesized different systems including poly (2-hydroxyethyl acrylate), [187] poly (N-methylolacrylamide), [188] poly (N-vinylpyrrolidone), [189] cross-linked polymers of epoxy/polyurethane resin [190] and nanocomposites polyurethane/nano silica hybrids. [191] Mariani et al. have extensively studied FP, applying it to different monomeric systems including polyurethanes, [192] thermosensitive hydrogels of poly (N-isopropylacrylamide) and poly (-vinyl caprolactam) [193] containing graphene, nanocomposites containing Polyhedral Oligomeric Silsesquioxane (POSS) [194] and montmorillonite [195] superabsorbent hydrogels [196] and organic-inorganic hybrid polymers. [197]

References

1. J. Martin, E.J.D.-M., A. G. Asuero, *Cyclodextrins: Past and Present*2018.

2. Crini, G., *Review: A history of cyclodextrins.* Chemical Reviews, 2014(21): p. 10940-10975.

3. F. Cramer , H.H., *Inclusion compounds of cyclodextrins.* Die Naturwissenschaften, 1967(54): p. 625-632.

4. S.V.Kurkov, T.L., *Cyclodextrins.* International Journal of Pharmaceutics, 2013. **453**(1): p. 167-180.

5. V.N. Maistrenko , V.N.G., E.Y. Sangalov *Voltammetry of host-guest complexes.* Journal of Analytical Chemistry, 1995(50): p. 528-533.

6. F. Van de Manakker, K.B., N.E. Morabit, S.C. De Smedt, C.F. van Nostrum, W.E. Hennink, *Protein-Release Behaviour of Self-Assembled PEG-β-Cyclodextrin/PEG-Cholesterol Hydrogels.* Advanced Functional Materials, 2009. **19**(18): p. 2992-300.

7. O. F. Silva, N.M.C., J. J. Silber, R. H. de Rossi, M. A. Fernandez, *Supramolecular assemblies obtained by mixing different cyclodextrins and AOT or BHDC reverse micelles.* Langmuir, 2014. **30**(12): p. 3354-3362.

8. R. Gramage-Doria, D.A., D. Matt,, *Metallated cavitands (calixarenes, resorcinarenes, cyclodextrins) with internal coordination sites.* Coordination Chemistry Reviews, 2013. **257**(3): p. 776-816.

9. Q.D. Hu, G.P.T., P.K. Chu, *Cyclodextrin-based host-guest supramolecular nanoparticles for delivery: from design to applications.* Accounts of chemical research, 2014. **47**(7): p. 2017-2025.

10. Wimmer, T., *Cyclodextrins*, in *Ullmann's Encyclopedia of Industrial Chemistry*2000, Wiley Online Library.

11. S. S. Jambhekar, P.B., *Cyclodextrins in pharmaceutical formulations II: Solubilization, binding constant, and complexation efficiency.* Drug Discovery Today, 2016. **21**(2): p. 363-368.

12. S. Li, W.C.P., *Cyclodextrins and their applications in analytical chemistry.* ChemicalReviews, 1992. **92**: p. 1457-1470.

13. Caira, M.R., *Structural aspects of crystalline derivatized cyclodextrins and their inclusion complexes.* Current Organic Chemistry, 2011. **15**(6): p. 815-830.

14. Gelb R.I., S.L.M., Radeos M., Edmonds R.B., Laufer A.A., *Cyclohexaamylose complexation with organic solvent molecules.* Journal of the American Chemical Society, 1982. **104**: p. 6283-6288.

15. Connors, K.A., *The stability of cyclodextrin complexes in solution.* Chemical Reviews, 1997. **97**: p. 1325-1357.

16. R.A. Rajewski, V.J.S.J.o.P.S., *Pharmaceutical applications of cyclodextrins. 2. In vivo drug delivery.* 1996. **85**(11): p. 1142-1169.

17. D.D.Pendergast, *Stability constants of α-cyclodextrin complexes of disubstituted benzenes: Interpretation of structural effects in terms of a binding*, 1983, University of Wisconsin-Madison

18. A.Z.M. Badruddoza, Z.B.Z.S., D.W.J. Tay, K. Hidajat, M. S. Uddin, *Endocrine disrupters and toxic metal ions removal by carboxymethyl-β-cyclodextrin polymer grafted onto magnetic nanoadsorbents. Journal of Chemical Engineering.* 2013. **27**(1): p. 69-73.

19. Nuvoli, D., et al., *Synthesis and characterization of poly(2-hydroxyethylacrylate)/β-cyclodextrin hydrogels obtained by frontal polymerization.* Carbohydrate Polymers, 2016. **150**: p. 166-171.

20. Pack, D.W., et al., *Design and development of polymers for gene delivery.* Nature Reviews Drug Discovery, 2005. **4**(7): p. 581-593.

21. Sanna, D., et al., *β-Cyclodextrin-based supramolecular poly(N-isopropylacrylamide) hydrogels prepared by frontal polymerization.* Carbohydrate Polymers, 2017. **166**: p. 249-255.

22. Tabary, N., et al., *Determination of the glass transition temperature of cyclodextrin polymers.* Carbohydrate Polymers, 2016. **148**: p. 172-180.

23. D. Kaceriakova, I.S., *Utilization of cyclodextrins in gas chromatography: preparation of capillary columns with cyclodextrin stationary phases.* Chem Listy, 2014. **108**(5): p. 462-469.

24. López-Nicolás, J.M., P. Rodríguez-Bonilla, and F. García-Carmona, *Cyclodextrins and Antioxidants.* Critical Reviews in Food Science and Nutrition, 2014. **54**(2): p. 251-276.

25. Rodríguez-Bonilla, P., et al., *Development of a reversed phase high performance liquid chromatography method based on the use of cyclodextrins as mobile phase additives to determine pterostilbene in blueberries.* Journal of Chromatography B, 2011. **879**(15): p. 1091-1097.

26. Rocco, A., A. Maruška, and S. Fanali, *Cyclodextrins as a chiral mobile phase additive in nano-liquid chromatography: comparison of reversed-phase silica monolithic and particulate capillary columns.* Analytical and Bioanalytical Chemistry, 2012. **402**(9): p. 2935-2943.

27. Xiao, Y., et al., *Recent development of cyclodextrin chiral stationary phases and their applications in chromatography.* Journal of Chromatography A, 2012. **1269**: p. 52-68.

28. Ammar, H.O., et al., *Chitosan/cyclodextrin nanoparticles as drug delivery system.* Journal of Inclusion Phenomena and Macrocyclic Chemistry, 2012. **72**(1): p. 127-136.

29. Çelik, S.E., et al., *Spectroscopic study and antioxidant properties of the inclusion complexes of rosmarinic acid with natural and derivative cyclodextrins.* Spectrochimica Acta Part A: Molecular and Biomolecular Spectroscopy, 2011. **78**(5): p. 1615-1624.

30. Medronho, B., et al., *Inclusion complexes of rosmarinic acid and cyclodextrins: stoichiometry, association constants, and antioxidant potential.* Colloid and Polymer Science, 2014. **292**(4): p. 885-894.

31. Szente, L. and J. Szejtli, *Cyclodextrins as food ingredients.* Trends in Food Science & Technology, 2004. **15**(3): p. 137-142.

32. Bazhban, M., M. Nouri, and J. Mokhtari, *Electrospinning of cyclodextrin functionalized chitosan/PVA nanofibers as a drug delivery system.* Chinese Journal of Polymer Science, 2013. **31**(10): p. 1343-1351.

33. Larrañeta, E., et al., *Hydrogels based on poly(methyl vinyl ether-co-maleic acid) and Tween 85 for sustained delivery of hydrophobic drugs.* International Journal of Pharmaceutics, 2018. **538**(1): p. 147-158.

34. Kandoth, N., et al., *A Cyclodextrin-Based Nanoassembly with Bimodal Photodynamic Action.* Chemistry – A European Journal, 2012. **18**(6): p. 1684-1690.

35. van de Manakker, F., et al., *Cyclodextrin-Based Polymeric Materials: Synthesis, Properties, and Pharmaceutical/Biomedical Applications.* Biomacromolecules, 2009. **10**(12): p. 3157-3175.

36. J. Szeman, E.F., J.Szejtli, *Water Soluble Cyclodextrin Polymers: Their Interaction with Drugs.* Inclusion Phenomena in inorganic, 1987. **5**: p. 427-431.

37. F. Van de Manakker, T.V., C. F. van Nostrum, W. E. Hennink, *Cyclodextrin-Based Polymeric Materials: Synthesis Properties and Pharmaceutical/Biomedical Applications.* Biomacromolecules, 2009. **10**(12): p. 3158-3175.

38. Szeman, J., et al., *Water soluble cyclodextrin polymers: Their interaction with drugs.* Journal of inclusion phenomena, 1987. **5**(4): p. 427-431.

39. Mura, P., et al., *Characterization of physicochemical properties of naproxen systems with amorphous β-cyclodextrin-epichlorohydrin polymers.* Journal of pharmaceutical and biomedical analysis, 2002. **29**(6): p. 1015-1024.

40. Rodriguez-Tenreiro, C., et al., *Estradiol sustained release from high affinity cyclodextrin hydrogels.* European Journal of Pharmaceutics and Biopharmaceutics, 2007. **66**(1): p. 55-62.

41. Ma, M. and D. Li, *New organic nanoporous polymers and their inclusion complexes.* Chemistry of materials, 1999. **11**(4): p. 872-874.

42. Binello, A., et al., *Synthesis of cyclodextrin-based polymers and their use as debittering agents.* Journal of applied polymer science, 2008. **107**(4): p. 2549-2557.

43. Girek, T., et al., *Polymerisation of β-cyclodextrin with succinic anhydride. Synthesis, characterisation, and ion flotation of transition metals.* Carbohydrate Polymers, 2005. **59**(2): p. 211-215.

44. Girek, T., D.-H. Shin, and S.-T. Lim, *Polymerization of β-cyclodextrin with maleic anhydride and structural characterization of the polymers.* Carbohydrate Polymers, 2000. **42**(1): p. 59-63.

45. Leprêtre, S., et al., *Prolonged local antibiotics delivery from hydroxyapatite functionalised with cyclodextrin polymers.* Biomaterials, 2009. **30**(30): p. 6086-6093.

46. Fenyvesi, E., et al. *Controlled release of drugs from CD polymers substituted with ionic groups*. in *Proceedings of the Eighth International Symposium on Cyclodextrins*. 1996. Springer.

47. Liu, Y.Y., et al., *A cyclodextrin microgel for controlled release driven by inclusion effects.* Macromolecular rapid communications, 2004. **25**(22): p. 1912-1916.

48. Nozaki, T., Y. Maeda, and H. Kitano, *Cyclodextrin gels which have a temperature responsiveness.* Journal of Polymer Science Part A: Polymer Chemistry, 1997. **35**(8): p. 1535-1541.

49. Bibby, D.C., N.M. Davies, and I.G. Tucker, *Investigations into the structure and composition of β-cyclodextrin/poly (acrylic acid) microspheres.* International Journal of Pharmaceutics, 1999. **180**(2): p. 161-168.

50. Bibby, D.C., N.M. Davies, and I.G. Tucker, *Poly (acrylic acid) microspheres containing β-cyclodextrin: loading and in vitro release of two dyes.* International Journal of Pharmaceutics, 1999. **187**(2): p. 243-250.

51. dos Santos, J.-F.R., et al., *Poly (hydroxyethyl methacrylate-co-methacrylated-β-cyclodextrin) hydrogels: Synthesis, cytocompatibility, mechanical properties and drug loading/release properties.* Acta Biomaterialia, 2008. **4**(3): p. 745-755.

52. Liu, Y.-Y. and X.-D. Fan, *Synthesis and characterization of pH-and temperature-sensitive hydrogel of N-isopropylacrylamide/cyclodextrin based copolymer*. Polymer, 2002. **43**(18): p. 4997-5003.

53. Janus, L., et al., *New sorbents containing beta-cyclodextrin. Synthesis, characterization, and sorption properties.* Reactive and Functional polymers, 1999. **42**(3): p. 173-180.

54. Wang, Q., et al., *Preparation and characterization of a positive thermoresponsive hydrogel for drug loading and release.* Journal of applied polymer science, 2009. **111**(3): p. 1417-1425.

55. Li, L., et al., *Polymer networks assembled by host− guest inclusion between adamantyl and β-cyclodextrin substituents on poly (acrylic acid) in aqueous solution.* Macromolecules, 2008. **41**(22): p. 8677-8681.

56. A. Luttringhaus, F.C., H. Prinzbach, F.M. Henglein, Liebigs Ann. Chem, 1958. **613**: p. 185.

57. Wasserman, E., J. Am. Chem. Soc., 1960. **82**: p. 4433.

58. I.T. Harrison, S.H., J. Am. Chem. Soc., 1967. **89**: p. 5723.

59. Schill, G., *Catenanes, Rotaxanes, and Knots.* Academic Press: New York, 1971.

60. Takata, T., *Polyrotaxane and Polyrotaxane Network: Supramolecular Architectures Based on the Concept of Dynamic Covalent Bond Chemistry.* Polymer Journal, 2006. **38**(1): p. 1-20.

61. H. W. Gibson, M.C.B., P. T. Engen, *Rotaxanes, CatenanesPolyrotaxanes, Policatenanes, and related materials.* Progress in Polymer Science, 1994. **19**: p. 843.

62. F. Yuen, K.C.T., *Ciclodextrin-Assisted assembly of stimuli-responsive polymers in aqueous media.* Soft Matter, 2010. **6**: p. 4613-4630.

63. A. Harada, M.K., *Complex formation between poly(ethylene glycol) and α-cyclodextrin.* Macromolecules, 1990. **23**(10): p. 2821-2823.

64. A. K. Bajpai, S.K.S., S. Bhanu, S. Kankane, Prog. Polym. Sci, 2008. **33**: p. 1088-1118.

65. L. Klouda, A.G.M., *Thermoresponsive hydrogels in biomedical applications - a review.* European Journal of Pharmaceutics and Biopharmaceutics, 2008. **68**: p. 34-45.

66. M. C. Koetting, J.T.P., S. D. Steichen, N. A. Peppas, *Stimulus-Responsive Hydrogels: Theory Modern Avances and Applications, Materials Science and Engineering.* Reports, [s.n.], Elsevier, 2015: p. 1-49.

67. M. Constantin, M.C., P. Ascenzi, G. Fundueanu, *LCST versus volume phase transition temperature in thermoresponsive drug delivery systems.* EXPRESS Polymer Letters, 2011. **10**: p. 839-848.

68. F. Ganji, S.V.-F., E. Vasheghani-Farahani, *Theoretical Description of Hydrogel Swelling: A Review.* Iranian Polymer Journal, 2010. **19**(5): p. 375-398.

69. S. K. H. Gulrez, S.A.-A., G. O' Phillips, *Progress in Molecular and Environmental Bioengineering-From Analysis and Modeling to Technology Applications*, in *Hydrogels: Methods of Preparation Characterisation and Applications*2011.

70. Y. Y. Liu, Y.H.S., J. Lü, *Preparation, properties and controlled release behaviors of pH-induced thermosensitive amphiphilic gels.* Biomaterials, 2006. **27**(21): p. 4016-24.

71. M. C. Koetting, J.T.P., S. D. Steichen, N. A. Peppas, *Stimulus-Responsive Hydrogels: Theory Modern Avances and Applications, Materials Science and Engineering.* Elsevier, 2015: p. 1-49.

72. L. Klouda, A.G.M., *Thermoresponsive hydrogels in biomedical applications.* European Journal of Pharmaceutics and Biopharmaceutics, 2008. **68**: p. 34-45.

73. E. Calò, V.V.K., *Biomedical applications of hydrogels: A review of patents and commercial products.* European Polymer Journal, 2015(65): p. 252-267.

74. R. Yoshida, T.O., R.M.Ottenbrite, *Stimuli-Responsive Hydrogels and Their Application to Functional Materials, Biomedical Applications of Hydrogels.* 2010

75. W. Yuan, J.S., W. Guo, *Thermoresponse and light-induced reversible self-assembly/disassembly of supra-amphiphiles from azobenzene- and β-cyclodextrincontaining copolymers.* Mater. Lett., 2014. **134**: p. 259-262.

76. L. Fan, Y.Z., C. Luo, F. Lu, H. Qiu, M. Sun, *Synthesis and characterization of magnetic β-cyclodextrin-chitosan nanoparticles as nano-adsorbents for removal of methyl blue.* Int. J. Biol. Macromol. , 2012. **50**(2): p. 444-450.

77. B.L. Tardy, S.T., H.H. Dam, H. Ejima, A. Blencowe, G.G. Qiao, et al., *Nanoparticles assembled via pH-responsive reversible segregation of cyclodextrins in polyrotaxanes.* Nanoscale 8, 2016. **34**: p. 15589-15596.

78. Garlotta, D., *A Literature Review of Poly(Lactic Acid).* Journal of Polymers and the Environment, 2001. **9**(2).

79. D. E. Henton, P.G., J. Lunt, and J. Randall, *Polylactic Acid Technology Natural Fibers, Biopolymers, and Biocomposites.* 2005.

80. R. Auras, B.H., S. Selke *An overview of polylactides as packaging materials.* Macromol. Biosci., 2004. **4**: p. 835-864.

81. Cheng, Y., et al., *Polylactic acid (PLA) synthesis and modifications: a review.* Frontiers of Chemistry in China, 2009. **4**(3): p. 259-264.

82. Hartmann, H., *High molecular weight polylactic acid polymers*. 1st edition ed. Biopolymers from Renewable Resources, ed. K.D.L. Springer-Verlag1998.

83. S. Zhang, F.L., and D. Wei, *ACI Mater. J.* 2007. **5**: p. 227.

84. R. Mehta , V.K., H. Bhunia , S. N. Upahyay, *Synthesis of polylactic acid: A review.* J. Macromol. Sci., Polym. Rev., 2005. **45**: p. 325-349.

85. A. Sodergard , M.S., *Properties of lactic acid based polymers and their correlation with composition.* Prog. Polym. Sci., 2002. **27**: p. 1123-1163.

86. K.M. Stridsberg , M.R., A.C. Albertsson, *Controlled ring-opening polymerization: Polymers with designed macromolecular architecture.* Adv. Polym. Sci., 2001. **157**: p. 41-65.

87. D. Bourissou, B.M.-V., A. Dumitrescu , M. Graullier, F. Lacombe, *Controlled Cationic Polymerization of Lactide.* Macromolecules, 2005. **38**: p. 9993-9998.

88. O.T. du Boullay , E.M., B. Martin-Vaca , F.P. Cossıo , D. Bourissou, J Am Chem Soc., 2006. **128**: p. 16442-16443.

89. Kricheldorf, H.R., *Syntheses of Biodegradable and Biocompatible Polymers by Means of Bismuth Catalysts.* Chem. Rev., 2009. **109**: p. 5579-5594.

90. J. Kadokawa, S.K., *Curr. Opin. Chem. Biol.* 2010. **14**: p. 145-153.

91. S.I. Moon, C.W.L., I. Taniguchi, M. Miyamoto, Y. Kimura, *Melt/solid polycondensation of L-lactic acid: an alternative route to poly(L-lactic acid) with high molecular weight.* Polymer, 2001. **42**(11): p. 5059-5062.

92. L.T. Lim, R.A., M. Rubino and , . *Processing technologies for poly(lactic acid).* Prog. Polym. Sci., 2008. **33**: p. 820-852.

93. M. Wang, Y.W., Y.D. Li, J.B. Zeng, *Progress in Toughening Poly(Lactic Acid) with Renewable Polymers.* Polymer Reviews, 2017. **57**(4): p. 557-593.

94. N. Ljungberg , T.A., B. Wesslen, *Film extrusion and film weldability of polylactic acid, plasticized with triacetine and tributyl citrate.* J. Appl. Polym. Sci., 2003. **88**: p. 3239-3247.

95. Jacobsen, S. and H.-G. Fritz, *Plasticizing polylactide—the effect of different plasticizers on the mechanical properties.* Polymer Engineering & Science, 1999. **39**(7): p. 1303-1310.

96. Oksman, K., M. Skrifvars, and J.-F. Selin, *Natural fibres as reinforcement in polylactic acid (PLA) composites.* Composites Science and Technology, 2003. **63**(9): p. 1317-1324.

97. Ljungberg, N. and B. Wesslen, *Tributyl citrate oligomers as plasticizers for poly (lactic acid): thermo-mechanical film properties and aging.* Polymer, 2003. **44**(25): p. 7679-7688.

98. Ljungberg, N. and B. Wesslén, *Preparation and properties of plasticized poly (lactic acid) films.* Biomacromolecules, 2005. **6**(3): p. 1789-1796.

99. Paul, M.-A., et al., *New nanocomposite materials based on plasticized poly (L-lactide) and organo-modified montmorillonites: thermal and morphological study.* Polymer, 2003. **44**(2): p. 443-450.

100. Hu, Y., et al., *Crystallization and phase separation in blends of high stereoregular poly (lactide) with poly (ethylene glycol).* Polymer, 2003. **44**(19): p. 5681-5689.

101. Kulinski, Z., et al., *Plasticization of poly (L-lactide) with poly (propylene glycol).* Biomacromolecules, 2006. **7**(7): p. 2128-2135.

102. Martin, O. and L. Avérous, *Poly(lactic acid): plasticization and properties of biodegradable multiphase systems.* Polymer, 2001. **42**(14): p. 6209-6219.

103. S.P. Silva , M.A.S., E.M. Fernandes, V.M. Correlo , L.F. Boesel , R.L. Reis, *Cork: Properties, capabilities and applications.* Inter. Mater. Rev., 2005: p. 345-365.

104. Gandini, A. and M.N. Belgacem, *Chapter 11 - Lignins as Components of Macromolecular Materials*, in *Monomers, Polymers and Composites from Renewable Resources*, M.N. Belgacem and A. Gandini, Editors. 2008, Elsevier: Amsterdam. p. 243-271.

105. Ciesla, W.M., *Non-wood forest products from temperate broad-leaved trees.* 2002.

106. Pereira, H., *Cork: Biology, Production and Uses.* Elsevier, 2007.

107. Gandini, A., C. Pascoal Neto, and A.J.D. Silvestre, *Suberin: A promising renewable resource for novel macromolecular materials.* Progress in Polymer Science, 2006. **31**(10): p. 878-892.

108. Graça, J. and S. Santos, *Suberin: A Biopolyester of Plants' Skin.* Macromolecular Bioscience, 2007. **7**(2): p. 128-135.

109. Neto, C.P., et al., *Isolation and Characterization of a Lignin-Like Polymer of the Cork of Quercus suber L,* in *Holzforschung - International Journal of the Biology, Chemistry, Physics and Technology of Wood*1996. p. 563.

110. Evtiouguina, M., et al., *The oxypropylation of cork residues: preliminary results.* Bioresource Technology, 2000. **73**(2): p. 187-189.

111. Payen, A., *Sur un moyen d'isoler le tissue élémentaire des bois.* CR Hebd. Seances Acad. Sci, 1838. **7**: p. 1125.

112. Klemm, D., et al., *Cellulose: Fascinating Biopolymer and Sustainable Raw Material.* Angewandte Chemie International Edition, 2005. **44**(22): p. 3358-3393.

113. Schönbein, C., *Notiz über eine Veränderung der Pflanzenfaser und einiger andern organischen Substanzen.* Ber. Naturforsch. Ges. Basel, 1847. **7**: p. 27.

114. Staudinger, H., *Über polymerisation.* Berichte der deutschen chemischen Gesellschaft (A and B Series), 1920. **53**(6): p. 1073-1085.

115. Sarko, A. and R. Muggli, *Packing analysis of carbohydrates and polysaccharides. III. Valonia cellulose and cellulose II.* Macromolecules, 1974. **7**(4): p. 486-494.

116. Gardner, K. and J. Blackwell, *The structure of native cellulose.* Biopolymers: Original Research on Biomolecules, 1974. **13**(10): p. 1975-2001.

117. Burchard, W., et al., *Cellulose in Schweizers Reagens: ein stabiler, polymerer Metallkomplex hoher Kettensteifheit.* Angewandte Chemie, 1994. **106**(8): p. 936-939.

118. Dawsey, T. and C.L. McCormick, *The lithium chloride/dimethylacetamide solvent for cellulose: a literature review.* Journal of Macromolecular Science—Reviews in Macromolecular Chemistry and Physics, 1990. **30**(3-4): p. 405-440.

119. Burchard, W., *Solubility and solution structure of cellulose derivatives.* Cellulose, 2003. **10**(3): p. 213-225.

120. Fink, H.-P., et al., *Structure formation of regenerated cellulose materials from NMMO-solutions.* Progress in Polymer Science, 2001. **26**(9): p. 1473-1524.

121. Klemm, D., et al., *Comprehensive cellulose chemistry. Volume 1: Fundamentals and analytical methods*1998: Wiley-VCH Verlag GmbH.

122. Heinze, T. and A. Koschella. *Carboxymethyl ethers of cellulose and starch–a review.* in *Macromolecular Symposia*. 2005. Wiley Online Library.

123. Klemm, D., et al., *Bacterial synthesized cellulose—artificial blood vessels for microsurgery.* Progress in Polymer Science, 2001. **26**(9): p. 1561-1603.

124. Drechsler, U., S. Radosta, and W. Vorwerg, *Characterization of cellulose in solvent mixtures with N-methylmorpholine-N-oxide by static light scattering.* Macromolecular Chemistry and Physics, 2000. **201**(15): p. 2023-2030.

125. Ciacco, G.T., et al., *Application of the solvent dimethyl sulfoxide/tetrabutyl-ammonium fluoride trihydrate as reaction medium for the homogeneous acylation of Sisal cellulose.* Cellulose, 2003. **10**(2): p. 125-132.

126. Saalwächter, K., et al., *Cellulose solutions in water containing metal complexes.* Macromolecules, 2000. **33**(11): p. 4094-4107.

127. Edgar, K.J., et al., *Advances in cellulose ester performance and application.* Progress in Polymer Science, 2001. **26**(9): p. 1605-1688.

128. Green, J.W. and R. Whistler, *Methods of carbohydrate chemistry.* Methods in Carbohydrate. Chemistry, Acad. emic Press, New York, 1963: p. 9-21.

129. Kern, H., et al., *Synthesis, control of substitution pattern and phase transitions of 2, 3-di-O-methylcellulose.* Carbohydrate research, 2000. **326**(1): p. 67-79.

130. Gömez, J.A.C., U.W. Erler, and D.O. Klemm, *4-methoxy substituted trityl groups in 6-O protection of cellulose: Homogeneous synthesis, characterization, detritylation.* Macromolecular Chemistry and Physics, 1996. **197**(3): p. 953-964.

131. Kondo, T. and A. Isogai, *A. Ishizu, and J. Nakano.* J. Appl. Polym. Sci, 1987. **34**: p. 55-63.

132. Fox, S.C., et al., *Regioselective esterification and etherification of cellulose: a review.* Biomacromolecules, 2011. **12**(6): p. 1956-1972.

133. Desbrieres, J., M. Hirrien, and S. Ross-Murphy, *Thermogelation of methylcellulose: rheological considerations.* Polymer, 2000. **41**(7): p. 2451-2461.

134. Arisz, P.W., H.J. Kauw, and J.J. Boon, *Substituent distribution along the cellulose backbone in O-methylcelluloses using GC and FAB-MS for monomer and oligomer analysis.* Carbohydrate research, 1995. **271**(1): p. 1-14.

135. Jagur-Grodzinski, J., *Polymeric gels and hydrogels for biomedical and pharmaceutical applications.* Polymers for Advanced Technologies, 2010. **21**(1): p. 27-47.

136. Yoon, D.S., et al., *A microfluidic gel valve device using reversible sol–gel transition of methyl cellulose for biomedical application.* Microsystem technologies, 2006. **12**(3): p. 238-246.

137. Bourges, X., et al., *Synthesis and general properties of silated-hydroxypropyl methylcellulose in prospect of biomedical use.* Advances in colloid and interface science, 2002. **99**(3): p. 215-228.

138. Klouda, L. and A.G. Mikos, *Thermoresponsive hydrogels in biomedical applications.* European Journal of Pharmaceutics and Biopharmaceutics, 2008. **68**(1): p. 34-45.

139. Sekiguchi, Y., C. Sawatari, and T. Kondo, *A gelation mechanism depending on hydrogen bond formation in regioselectively substituted O-methylcelluloses.* Carbohydrate Polymers, 2003. **53**(2): p. 145-153.

140. Chang, C., K. Han, and L. Zhang, *Structure and properties of cellulose/poly (N-isopropylacrylamide) hydrogels prepared by IPN strategy.* Polymers for Advanced Technologies, 2011. **22**(9): p. 1329-1334.

141. Yang, M.-J., et al., *Novel method of forming human embryoid bodies in a polystyrene dish surface-coated with a temperature-responsive methylcellulose hydrogel.* Biomacromolecules, 2007. **8**(9): p. 2746-2752.

142. Lu, X., Z. Hu, and J. Gao, *Synthesis and light scattering study of hydroxypropyl cellulose microgels.* Macromolecules, 2000. **33**(23): p. 8698-8702.

143. Shang, J., Z. Shao, and X. Chen, *Electrical behavior of a natural polyelectrolyte hydrogel: chitosan/carboxymethylcellulose hydrogel.* Biomacromolecules, 2008. **9**(4): p. 1208-1213.

144. McNaught, A.D. and A. Wilkinson, *Compendium of chemical terminology. IUPAC recommendations.* 1997.

145. Wang, J.J. and F. Liu, *Enhanced adsorption of heavy metal ions onto simultaneous interpenetrating polymer network hydrogels synthesized by UV irradiation.* Polymer bulletin, 2013. **70**(4): p. 1415-1430.

146. Mark, H.F., *Encyclopedia of polymer science and technology, concise*2013: John Wiley & Sons.

147. Myung, D., et al., *Progress in the development of interpenetrating polymer network hydrogels.* Polymers for Advanced Technologies, 2008. **19**(6): p. 647-657.

148. Chivukula, P., et al., *Synthesis and characterization of novel aromatic azo bond-containing pH-sensitive and hydrolytically cleavable IPN hydrogels.* Biomaterials, 2006. **27**(7): p. 1140-1151.

149. Hoare, T.R. and D.S. Kohane, *Hydrogels in drug delivery: Progress and challenges.* Polymer, 2008. **49**(8): p. 1993-2007.

150. Dragan, E.S., et al., *Macroporous composite IPN hydrogels based on poly (acrylamide) and chitosan with tuned swelling and sorption of cationic dyes.* Chemical Engineering Journal, 2012. **204**: p. 198-209.

151. Dragan, E.S., M.M. Perju, and M.V. Dinu, *Preparation and characterization of IPN composite hydrogels based on polyacrylamide and chitosan and their interaction with ionic dyes.* Carbohydrate Polymers, 2012. **88**(1): p. 270-281.

152. Yin, L., et al., *Synthesis, characterization, mechanical properties and biocompatibility of interpenetrating polymer network–super-porous hydrogel containing sodium alginate.* Polymer International, 2007. **56**(12): p. 1563-1571.

153. Nakayama, A., et al., *High mechanical strength double-network hydrogel with bacterial cellulose.* Advanced Functional Materials, 2004. **14**(11): p. 1124-1128.

154. Ahmed, A.A.-K., H.B. Naik, and B. Sherigara, *Synthesis and characterization of chitosan-based pH-sensitive semi-interpenetrating network microspheres for controlled release of diclofenac sodium.* Carbohydrate research, 2009. **344**(5): p. 699-706.

155. Rokhade, A.P., S.A. Patil, and T.M. Aminabhavi, *Synthesis and characterization of semi-interpenetrating polymer network microspheres of acrylamide grafted dextran and chitosan for controlled release of acyclovir.* Carbohydrate Polymers, 2007. **67**(4): p. 605-613.

156. Rokhade, A.P., et al., *Novel interpenetrating polymer network microspheres of chitosan and methylcellulose for controlled release of theophylline.* Carbohydrate Polymers, 2007. **69**(4): p. 678-687.

157. Angadi, S.C., L.S. Manjeshwar, and T.M. Aminabhavi, *Interpenetrating polymer network blend microspheres of chitosan and hydroxyethyl cellulose for controlled release of isoniazid.* International journal of biological macromolecules, 2010. **47**(2): p. 171-179.

158. Cai, Z. and J. Kim, *Cellulose–chitosan interpenetrating polymer network for electro-active paper actuator.* Journal of applied polymer science, 2009. **114**(1): p. 288-297.

159. Dragan, E.S., *Design and applications of interpenetrating polymer network hydrogels. A review.* Chemical Engineering Journal, 2014. **243**: p. 572-590.

160. Kim, S.J., et al., *Bending behavior of hydrogels composed of poly (methacrylic acid) and alginate by electrical stimulus.* Polymer International, 2004. **53**(10): p. 1456-1460.

161. Wang, Q., J. Zhang, and A. Wang, *Preparation and characterization of a novel pH-sensitive chitosan-g-poly (acrylic acid)/attapulgite/sodium alginate composite hydrogel bead for controlled release of diclofenac sodium.* Carbohydrate Polymers, 2009. **78**(4): p. 731-737.

162. Dumitriu, R.P., G.R. Mitchell, and C. Vasile, *Multi-responsive hydrogels based on N-isopropylacrylamide and sodium alginate.* Polymer International, 2011. **60**(2): p. 222-233.

163. Lin, H., et al., *Synthesis and characterization of pH-and salt-responsive hydrogels based on etherificated sodium alginate.* Journal of applied polymer science, 2010. **115**(6): p. 3161-3167.

164. Zhou, C. and Q. Wu, *A novel polyacrylamide nanocomposite hydrogel reinforced with natural chitosan nanofibers.* Colloids and Surfaces B: Biointerfaces, 2011. **84**(1): p. 155-162.

165. Xia, Y.-q., et al., *Hemoglobin recognition by imprinting in semi-interpenetrating polymer network hydrogel based on polyacrylamide and chitosan.* Biomacromolecules, 2005. **6**(5): p. 2601-2606.

166. Varaprasad, K., et al., *Poly (acrylamide-chitosan) hydrogels: Interaction with surfactants.* International Journal of Polymeric Materials, 2010. **59**(12): p. 981-993.

167. Martinez-Ruvalcaba, A., et al., *Swelling characterization and drug delivery kinetics of polyacrylamide-co-itaconic acid/chitosan hydrogels.* Express Polym Lett, 2009. **3**(1): p. 25-32.

168. Ekici, S. and D. Saraydin, *Synthesis, characterization and evaluation of IPN hydrogels for antibiotic release.* Drug Delivery, 2004. **11**(6): p. 381-388.

169. Bonina, P., T. Petrova, and N. Manolova, *pH-sensitive hydrogels composed of chitosan and polyacrylamide–preparation and properties.* Journal of Bioactive and Compatible Polymers, 2004. **19**(2): p. 101-116.

170. Wang, M., Y. Fang, and D. Hu, *Preparation and properties of chitosan-poly (N-isopropylacrylamide) full-IPN hydrogels.* Reactive and Functional polymers, 2001. **48**(1-3): p. 215-221.

171. Alvarez-Lorenzo, C., et al., *Temperature-sensitive chitosan-poly (N-isopropylacrylamide) interpenetrated networks with enhanced loading capacity and controlled release properties.* Journal of Controlled Release, 2005. **102**(3): p. 629-641.

172. Babu, V.R., K. Hosamani, and T. Aminabhavi, *Preparation and in-vitro release of chlorothiazide novel pH-sensitive chitosan-N, N′-dimethylacrylamide semi-interpenetrating network microspheres.* Carbohydrate Polymers, 2008. **71**(2): p. 208-217.

173. Kim, S.J., et al., *Synthesis and characteristics of semi-interpenetrating polymer network hydrogels based on chitosan and poly (hydroxy ethyl methacrylate).* Journal of applied polymer science, 2005. **96**(1): p. 86-92.

174. Han, Y.A., E.M. Lee, and B.C. Ji, *Mechanical properties of semi-interpenetrating polymer network hydrogels based on poly (2-hydroxyethyl methacrylate) copolymer and chitosan.* Fibers and Polymers, 2008. **9**(4): p. 393-399.

175. Peak, C.W., J.J. Wilker, and G. Schmidt, *A review on tough and sticky hydrogels.* Colloid and Polymer Science, 2013. **291**(9): p. 2031-2047.

176. Chechilo, N., R. Khvilivitskii, and N. Enikolopyan. *Propagation of the polymerization reaction*. in *Dokl Akad Nauk SSSR*. 1972.

177. Ivanov, V.V. and C. Decker, *Kinetic study of photoinitiated frontal polymerization.* Polymer International, 2001. **50**(1): p. 113-118.

178. Norrish, R. and R. Smith, *Catalysed polymerization of methyl methacrylate in the liquid phase.* Nature, 1942. **150**(3803): p. 336.

179. Lewis, L.L., et al., *Isothermal frontal polymerization: Confirmation of the mechanism and determination of factors affecting the front velocity, front shape, and propagation distance with comparison to mathematical modeling.* Journal of Polymer Science Part A: Polymer Chemistry, 2005. **43**(23): p. 5774-5786.

180. Pojman, J.A., V.M. Ilyashenko, and A.M. Khan, *Free-radical frontal polymerization: self-propagating thermal reaction waves.* Journal of the Chemical Society, Faraday Transactions, 1996. **92**(16): p. 2825-2837.

181. Pojman, J.A., et al., *Factors affecting propagating fronts of addition polymerization: velocity, front curvature, temperatue profile, conversion, and molecular weight distribution.* Journal of Polymer Science Part A: Polymer Chemistry, 1995. **33**(4): p. 643-652.

182. Pojman, J.A., G. Curtis, and V.M. Ilyashenko, *Frontal polymerization in solution.* Journal of the American Chemical Society, 1996. **118**(15): p. 3783-3784.

183. Nagy, I.P., L. Sike, and J.A. Pojman, *Thermochromic composite prepared via a propagating polymerization front.* Journal of the American Chemical Society, 1995. **117**(12): p. 3611-3612.

184. Tredici, A., et al., *Polymer blends by self-propagating frontal polymerization.* Journal of applied polymer science, 1998. **70**(13): p. 2695-2702.

185. Washington, R.P. and O. Steinbock, *Frontal polymerization synthesis of temperature-sensitive hydrogels.* Journal of the American Chemical Society, 2001. **123**(32): p. 7933-7934.

186. Crivello, J.V., *Design and synthesis of multifunctional glycidyl ethers that undergo frontal polymerization.* Journal of Polymer Science Part A: Polymer Chemistry, 2006. **44**(21): p. 6435-6448.

187. Chen, S., et al., *Facile synthesis of poly (hydroxyethyl acrylate) by frontal free-radical polymerization.* Journal of Polymer Science Part A: Polymer Chemistry, 2007. **45**(5): p. 873-881.

188. Chen, L., et al., *First solvent-free synthesis of poly (N-methylolacrylamide) via frontal free-radical polymerization.* Journal of Polymer Science Part A: Polymer Chemistry, 2007. **45**(18): p. 4322-4330.

189. Cai, X., S. Chen, and L. Chen, *Solvent-free free-radical frontal polymerization: A new approach to quickly synthesize poly (N-vinylpyrrolidone).* Journal of Polymer Science Part A: Polymer Chemistry, 2008. **46**(6): p. 2177-2185.

190. Chen, S., et al., *Epoxy resin/polyurethane hybrid networks synthesized by frontal polymerization.* Chemistry of materials, 2006. **18**(8): p. 2159-2163.

191. Chen, S., et al., *Polyurethane–nanosilica hybrid nanocomposites synthesized by frontal polymerization.* Journal of Polymer Science Part A: Polymer Chemistry, 2005. **43**(8): p. 1670-1680.

192. Fiori, S., et al., *First synthesis of a polyurethane by frontal polymerization.* Macromolecules, 2003. **36**(8): p. 2674-2679.

193. Alzari, V., et al., *Stimuli responsive hydrogels prepared by frontal polymerization.* Biomacromolecules, 2009. **10**(9): p. 2672-2677.

194. Mariani, A., et al., *Polymeric nanocomposites containing polyhedral oligomeric silsesquioxanes prepared via frontal polymerization.* Journal of Polymer Science Part A: Polymer Chemistry, 2007. **45**(19): p. 4514-4521.

195. Mariani, A., et al., *Synthesis and characterization of epoxy resin-montmorillonite nanocomposites obtained by frontal polymerization.* Journal of Polymer Science Part A: Polymer Chemistry, 2007. **45**(11): p. 2204-2211.

196. Scognamillo, S., et al., *Thermoresponsive super water absorbent hydrogels prepared by frontal polymerization.* Journal of Polymer Science Part A: Polymer Chemistry, 2010. **48**(11): p. 2486-2490.

197. Scognamillo, S., et al., *Hybrid organic/inorganic epoxy resins prepared by frontal polymerization.* Journal of Polymer Science Part A: Polymer Chemistry, 2010. **48**(21): p. 4721-4725.

-MAIN PURPOSES-

The main objective of this research work was to study and synthesize different types of materials starting from the use of different biomasses, deriving from the processing waste of raw materials such as cork or from food waste such as corn. The use of these resources allows to obtain materials with a high added value, as it gives a second life to waste materials that would normally be abandoned or destined to produce energy.

One of the biomasses used during this PhD were cyclodextrins, a very versatile family of cyclic oligosaccharides. Different types of polymeric systems were obtained with CDs: in the first case, hydrogels with a temperature stimulus response were obtained, characterized by an absorption capacity higher than that of traditional hydrogels; these materials have been synthesized by frontal polymerization, an unconventional synthesis technique which allows to obtain advantages in terms of time, energy saving and synthetic protocol. In the second case, the CDs were used for the synthesis of hydrogels with a temperature stimulus response but characterized by a sliding crosslinking. These materials were synthesized by classic batch polymerization. the hydrogels obtained were characterized from a mechanical point of view through dynamo mechanical analysis (DMA), but also from a thermal point of view through differential scanning calorimetry analysis (DSC) and the swelling properties of the hydrogels were studied (SR%).

Furthermore, the CDs were used for the synthesis of new materials. In the first one, the CDs were reacted with oxypropylated cork (obtained from the processing waste of this raw material of great economic value). While in the second one, CDs were used for the synthesis of lactic acid oligomers, that acting as a radical initiator allowed its insertion in the chain. This last part was carried out during the internship period abroad, carried out at the University of Alicante (SPAIN). The final materials (CDs-cork, CDs- OLA) were subsequently characterized from a structural point of view by analysis of infrared spectrophotometry (FT-IR), analysis by electronic microscope (SEM), nuclear magnetic resonance (NMR) and spectrophotometry mass (ESI-MS). Once characterized, they were dispersed within a polymer matrix (poly lactic acid, PLA) for the formation of films and the effects that these molecules played on the mechanical and thermal properties of the final polymer were studied. The films were subjected to mechanical dynamo analysis (DMA) and thermal analysis (DSC).

Methyl cellulose, a simpler derivative of cellulose, is another biomass treated during the research work. This material has been used to obtain a particular type of crosslinking hydrogel called semi-interpenetrating polymers network, SIPN. This type of materials were synthesized by front polymerization and the samples were characterized from a thermal (by DSC analysis), mechanical (dynamo mechanical analysis) and swelling point of view.

-CHAPTER II-

Experimental Part

2.1 Synthesis of β-Cyclodextrin-based supramolecular poly(N-isopropylacrylamide) hydrogels

2.1.1 Starting materials

N-Isopropylacrylamide (NIPAAm, MW=113.16 g/mol), N,N′-methylene-bisacrylamide (MBAM, MW=154.17 g/mol), dimethylsulfoxide (DMSO) were purchased from Sigma Aldrich; acryloyl-β-cyclodextrin (AβCD) was from Shandong Binzhou Zhiyuan Biotechnology. All materials were used as received with-out further purification. Aliquat persulfate (APS, MW=1198.01 g/mol) was synthesized according to the literature. [198]

2.1.2. Hydrogels synthesis

In a common glass test tube (i.d.= 1.5cm, length= 16cm), a suitable amount of AβCD (Table 2.1) was dissolved into 2.5 ml of DMSO. 3.0 g of NIPAAm (25.8 mmol) were added and the glass tube was ultrasonicated for 10 min at room temperature. Finally, 1.0 mol% of APS (referred to total moles of NIPAAm), as the radical initiator, were added. Furthermore, when covalently crosslinked hydrogels were synthesized, MBAm (0.5 mol%), as the crosslinker, was also added to their action mixture. A thermo couple was located at about 1 cm from the bottom of the tube and connected to a digital temperature recorder (Delta Ohm 941661C). Front started by heating the external wall of the tube with a soldering iron tip in correspondence of the upper surface of the solution, until the formation of the front became evident.

Table 2.1. Composition*, FP parameters and T_g values of the polymer samples synthesized in this work.

Sample code	**NIPAAm** (mol%)	**AβCD** (mol%)	**MBAm** (mol%)	**T_{max}** (°C)	**V_f** (cm/min)	**T_g** (°C)
M1	98.5	0.0	0.5	121	0.8	124
AM1	98.4	0.1	0.5	117	0.8	110
AM2	98.3	0.2	0.5	117	0.8	112
AM3	98.0	0.5	0.5	119	0.9	115
AM4	97.5	1.0	0.5	121	1.0	121
AM5	96.5	2.0	0.5	121	1.2	122
A1	98.5	0.5	0.0	118	0.9	138
A2	98.0	1.0	0.0	119	0.9	135
A3	97.0	2.0	0.0	121	1.1	142

*all samples contain 1 mol% of initiator APS.

Front velocities (V_f's) were determined by measuring the front position (easily visible through the glass wall of test tubes) as a function of time. T_{max} measurements were performed by using a K-type thermocouple connected to the above digital thermometer used for temperature reading and recording (sampling rate: 1 Hz). For all samples, T_{max} (± 10 °C) and V_f (±0.05 cm/min) were measured. After polymerization, all samples were washed in water for 3 days to remove DMSO.

2.1.3 Differential scanning calorimetry

DSC analyses were performed by using a DSC Q100 Waters TA Instruments calorimeter, with a TA Universal Analysis 2000 software. Hydrogels were subjected to a heat scan, from -60 to 180 °C, with a scan rate of 20 °C/min in inert atmosphere (nitrogen flow: 50 mL/min), in order to establish the T_g values. All hydrogel samples were dried in a vacuum oven at 100 °C overnight before analysis.

2.1.4 Swelling measurements

All samples were cut into small pieces having similar shape and size and immersed in distilled water for three days in order to completely remove DMSO. After this period, hydrogels were allowed to swell in distilled water until reaching swelling equilibrium (ca. 1 day).

Their swelling behavior as a function of temperature was measured in water from 4 to 35 °C by heating them in a thermostatic bath at the rate of 1 °C/day. SR% was calculated by applying the following equation (1):

$$SR\% = \frac{Ms-Md}{Md} * 100 \qquad (1)$$

where Ms and Md are the sample masses in the swollen and in the dry state, respectively.

2.2 Synthesis of Sliding Crosslinked Thermoresponsive materials made of Poly(N-Isopropylacrylamide) and Acrylamide-γ-Cyclodextrin.

2.2.1 Starting materials

Ammonium persulfate (AmPS, MW= 228.20 g/mol), N-isopropylacrylamide (NIPAAm, MW= 113.16 g/mol), N,N′-methylene-bisacrylamide (MBAm, MW= 154.17 g/mol), tetramethylenediamine (TEMED, MW= 116.20 g/mol, d= 0.775 g/mL); triethylamine (MW= 101.19 g/mol, d= 0.796 g/mL) acryloyl chloride (MW= 90.51 g/mol, d= 1.114 g/mL) were purchased from Sigma Aldrich. N-methyl pyrrolidone (NMP) was purchased from Sigma-Aldrich and distilled on molecular sieves before use. γ-cyclodextrin (γ-CD, MW: 1297.14 g/mol) was kindly supplied by IMCD Italia S.p.A. Mono-6-amino-deoxy-6-γ-cyclodextrin was obtained according to the literature (MW: 1296.1). [199]

2.2.2 Synthesis of Acrylamide-γ-Cyclodextrin

15 g of mono-6-amino-deoxy-6-γ-cyclodextrin (0.015 mol), previously dried in oven at 60 °C for 1 h, were put in a 250 mL round bottom flask with 200 mL of dry N-methylpyrrolidone

and dissolved through vigorous stirring at room temperature. Then, 1.9 mL of triethylamine (0.015 mol) were added. The mixture was cooled down to 0 °C, and 1.22 mL (0.015 mol) of acryloyl chloride were added dropwise under stirring in argon atmosphere. The system was left overnight at room temperature. After, 400 mL of cold methanol were added to precipitate triethylammonium chloride, which was eventually eliminated by centrifugation. The resulting liquid phase was poured in a large amount of acetone, in order to precipitate the desired product. The obtained white solid, AγCD (MW= 1024.89 g/mol), was recovered by centrifugation and washed three times with acetone to eliminate residual NMP. Yield: 36% (white-pale yellow powder). ^{1}H NMR (D_2O 400 MHz), δ: 6.46 − 5.92($C_\alpha H$= $C_\beta H2$), δ: 5.04(C_1H); ^{1}H NMR (DMSO 400 MHz), δ: 6.37 − 5.21($C_\alpha H$ = $C_\beta H_2$), δ: 5.79(C_1H).

2.2.3 Synthesis of PNIPAAm Hydrogels Containing AγCD

Various NIPAAm aqueous solutions (10% w/v) were put in a glass test tube, together with a known amount of AγCD (ranging from 0.5 to 2.0 mol% of AγCD with respect to the molar amount of NIPAAm). Subsequently, APS and TEMED were added (1.00:1.22 mol/mol, respectively), varying the APS concentration from 0.25 to 1.0 mol% (with respect to the total molar amount of NIPAAm and AγCD). The polymerization reaction was carried out at 4 °C for 3 h. Yields were quantitative.

2.2.4 Synthesis of pNIPAAm Hydrogels Containing γCD or MBAm

NIPAAm aqueous solution (10% w/v) was mixed with 1 mol% of γ-CD (with respect to the molar amount of NIPAAm) in a glass test tube. Subsequently, APS and TEMED were added (1.00:1.22 mol/mol; 1 mol% of APS with respect to the total molar amount of NIPAAm and γ-CD). The polymerization reaction was performed at 4 °C for 3 h (hereinafter coded as sample DγCD). The same materials and method were exploited for synthesizing pNIPAAm hydrogels containing MBAm as a crosslinker, which replaces γ-CD (hereinafter coded as sample DMBAm). The obtained hydrogels were washed several times in distilled water. The compositions of all the synthesized samples are listed in Table 2.2. Yields were quantitative.

Table 2.2 Composition, T_g, LCST, and modulus values of the samples synthesized in the present work.

Sample	AγCD (mol%)	APS (mol%)	T_g (°C)	LCST (°C)	E (MPa)
$A_{0.5}$	0.5	0.25	138	34	16.8
A_1	1.0	0.25	152	35	21.8
A_2	2.0	0.25	149	37	25.5
$B_{0.5}$	0.5	0.50	148	35	11.9
B_1	1.0	0.50	148	35	18.5
B_2	2.0	0.50	153	37	21.3
$C_{0.5}$	0.5	1.00	145	35	17.0
C_1	1.0	1.00	152	35	16.0
C_2	2.0	1.00	152	38	17.0
	γ-CD (mol%)				
DγCD	1.0	1.00	–	–	–
	MBAM (mol%)				
DMBAM	1.0	1.00	124	32	–

2.2.5 Differential Scanning Calorimetry

DSC analyses were performed by using a DSC Q100 Waters TA Instruments calorimeter, equipped with TA Universal Analysis 2000 software. Two types of analyses were performed. The first one was carried out on hydrogels immediately after synthesis. To this aim, the obtained products were subjected to a heat scan, from 0 to 250 °C, with a heating rate of 20 °C/min in inert atmosphere (nitrogen flow: 50 ml/min), in order to evaluate the conversion. [197] The second analysis was carried out on samples after being washed in water and dried in a vacuum oven at 50 °C for 3 days: the resulting hydrogels were subjected to a heat/cool/heat cycle scan, from -80 to 250 °C, with a heating rate of 20 °C/min and a cooling rate of 10

°C/min in inert atmosphere (nitrogen flow: 50 ml/min), in order to evaluate the glass transition temperature (T_g).

2.2.6 Swelling Measurements

After synthesis, all samples were washed and swollen in distilled water for 2 weeks, in order to remove solvents and unreacted reagents and to reach swelling equilibrium. Then, they were cut into small pieces having similar shape and size and immersed in distilled water in a thermostatic bath; the temperature of water was increased from 20 to 40 °C at a rate of 1 °C/day. Their swelling behavior as a function of temperature was measured.

The swelling ratio (SR%) of hydrogels was calculated according to equation (1) described in the paragraph 2.1.4. The LCST of hydrogels was determined by the flex of the swelling curve in a plot of SR% as a function of temperature. The M_d-value for each sample was determined, at the end of the experiment, on the samples dried in a vacuum oven at 50 °C for 3 days.

2.2.7 Compression Tests

Compression tests were performed on cylindrical specimens (diameter: 15 mm, height: 10 mm) according to ISO 527-1 standard, using a Zwick-Roll Z010 apparatus equipped with a 5 kN load cell, at 23 °C and 50 % relative humidity, applying 0.05 N pre-load; the speed test was 2 mm/min. At least five tests were carried out for each material in order to have reproducible and significant data. Furthermore, cyclic compression tests were carried out, using the same apparatus: for these tests, the load was increased from 0 to 3 N at 0.2 N/min and then decreased using the same force decrement.

2.3 Synthesis of oxypropylated cork and preparation of PLA films

2.3.1 Starting materials

Cork powder, produced by Molinas cork factory; poly lactic acid (PLA), from Condencia Quimica; propylene oxide (PO, MW: 58.08 g/mol; d: 0.83 g/mL), dichloromethane (CH_2Cl_2, MW: 84.93 g/mol; d: 1.33 g/mL), acetic acid (MW: 60.05 g/mol; d: 1.05 g/mL) purchased from Sigma-Aldrich. Potassium hydroxide (KOH, MW: 56.11 g/mol) was purchased from

Honeywell Riedel-de Haën, hexane (MW: 86.18 g/mol; d: 0.66 g/mL) was purchased from VWR. α-cyclodextrin (α-CD, MW: 972.84 g/mol), β-cyclodextrin (β-CD, MW: 1134.98 g/mol), γ-cyclodextrin (γ-CD, MW: 1297.12 g/mol) were purchased Wacker chemical;

2.3.2 Oxypropylation reaction

15 g of cork powder was placed in a 50 mL autoclave; 14.1 mL of propylene oxide, 0.15 g of potassium hydroxide and α-cyclodextrin/ β-cyclodextrin/ γ-cyclodextrin were added in variable percentages, 88% series B, Table 2.3) and 20% compared to the weight of cork (series C, Table 2.3). The reaction was carried out at 142 °C, which resulted in an increase of the internal pressure up to 10-12 bar. The lowering of pressure, down to ca. 1 bar, indicated that the reaction has finished. The obtained product was solubilized in dichloromethane, neutralized with acetic acid and subsequently filtered. The product derived from the filtration was placed in a 50 mL flask; 30 mL of hexane was added and it was heated to reflux for 4 hours (x 2 times). The two hexane phases were recombined and the solvent was evaporated to recover the hexane-soluble phase which was then weighed. The insoluble phase was also dried and weighed.

Table 2.3: Composition of the sample in series A, B, C, D and E

Sample	Cork (g)	PO (mL)	α-CD (g)	β-CD (g)	γ-CD (g)
A1	1.5	14.1			
B1	1.5	14.1	1.32		
B2	1.5	14.1		1.32	
B3	1.5	14.1			1.32
C1	1.2	14.1	0.3		
C2	1.2	14.1		0.3	
C3	1.2	14.1			0.3
D1		14.1	1.32		

D2	14.1	1.32	
D3	14.1		1.32
E1	14.1		

2.3.3 Synthesis of PLA films

12 g of PLA were solubilized in CH_2Cl_2. 1.2 g of product A1 (10 wt% with respect to PLA) and 3.6 g of product B2 (30 wt% with respect to PLA) were added (compositions are reported in table 2.4). The solvent was evaporated, and the product obtained was extruded at a temperature of 140 °C. 1 g of the resulting product was solubilized in 20 mL of CH_2Cl_2, deposited in a petri dish (diameter: 11 cm) and the solvent was evaporated.

Table 2.4: Composition of PLA films.

Sample	**Composition**	
F1	PLA	
F2	PLA	10 % A1
F3	PLA	30 % A1
F4	PLA	10 % B2
F5	PLA	30 % B2

2.3.4 Solubility tests

Solubility tests were performed on samples of series A, B, C, E using 0.3 g of solute and 5 mL of solvent: water, methanol, acetone, tetrahydrofuran (THF) and hexane.

2.3.5 Differential Scanning Calorimetry

The DSC analyses were performed with a DSC Q100 Waters TA Instruments instrument and a TA Universal Analysis 2000 data processing software. The analyses were conducted in an inert nitrogen atmosphere, using hermetically sealed aluminum capsules, with sample quantities between 10 and 15 mg. For the analysis, a "heat/cool/heat" cycle was used which involves two analysis cycles from -90 to 250 °C with a heating rate of 20 °C/min and a cooling speed of 10 °C / min.

2.3.6 Thermogravimetric analysis

The TGA analysis of the F series (Table 2.4) were conducted with a LECO TGA-601 instrument. The characterization was carried out in the temperature range of 50 to 700 °C with a heating rate of 20 °C/min in a nitrogen atmosphere.

2.3.7 Dynamic mechanical analysis

The mechanical tests of the F series (Table 2.4) were studied through elongation tests with a DMA Q800 Water TA instrument. The elongation tests were carried out on samples with a rectangular shape (length: 3 cm; width: 0.5 cm) applying a pre-load force of 0.01 N with a ramp of 1 N/min starting from the pre-load value up to 18 N.

2.3.8 FT-IR spectroscopy

The IR analysis were carried out with an instrument Bruker. The characterization was performed in the solid state by depositing the sample directly in the instrument. 128 scans were performed for each sample.

2.3.9 Scanning electron microscope

The morphology of the F series samples has been studied using a scanning electron microscope, an instrument of the FEI Quanta line. The samples were fixed on a metal support and analyzed in high vacuum at 2 kV.

2.4 Synthesis of β-cyclodextrin-based oligomers of lactic acid and preparation of PLA films with OLA-β-CD as plasticizer

2.4.1 Starting materials

β-cyclodextrin (β-CD, MW: 1134.98 g/mol) was purchased from Shandong Binzhou Zhiyuan Biotechnology Co. Ltd. PLA, D-lactide and Tin (II) 2-ethylhexanoate ($SnOct_2$, MW: 405.12 g/mol), were kindly supplied by Condencia Quimica; dimethylsulfoxide (DMSO, MW: 78.10 g/mol, d= 1.1 g/mL), dichloromethane (CH_2Cl_2, MW: 84.93 g/mol, d= 1.33 g/mL), ethyl acetate (AcEt, MW: 88.11 g/mol, d= 0.90 g/mL) were purchased from Sigma Aldrich.

2.4.2 Synthesis of β-cyclodextrin-based oligomers of lactic acid

By microwaves. In a 100 ml flask, 5 g of anhydrous β-CD (4.4 mmol) was added and dissolved in 40 ml of DMSO. Once solubilized, the lactide (34.5 mmol) and $SnOct_2$ catalyst were added (0.1% mol with respect to lactide). The desired working power (or temperature) and time were set in the microwave oven and the reaction started. Once finished, the solution was precipitated with a mixture of CH_2Cl_2/AcEt in ratio 1:3. The precipitate was filtered under pression and dried to air.

By conventional method. In a 100 mL flask, 5 g of anhydrous β-CD (4.4 mmol) was solubilized in 20 mL of DMSO. Once solubilized, lactide (34.5 mmol) and $SnOct_2$ catalyst (0.1% mol with respect to lactide) were added. The solution was reacted for 6h at 80 °C. After the reaction was completed, the solution was precipitated in a mixture of CH_2Cl_2/AcEt 1:3. The precipitate was filtered and dried to air.

The NMR signals are listed in table 2.5.

Table 2.5: Chemical shift (δ) of β-cd and OLA-β-CD.

β-CD		**OLA-β-CD (D_2O) (MW: 1630 g/mol)**	
5.05	d, 7H, C(1)H	5.06	
3.94	t, 7H, C(3)H	4.94	m,12.41H, -COCH-(CH_3O)-; C'1H
3.86	m, 14H, C(5)(6)H	4.33	m, 4.65H, -COCH(CH_3)OH; C'6H
3.63	m, 7H, C(2)H	3.78-3.52	m, 40.45H, C2H,3H,4H,5H,6H

3.56	t, /H, C(4)H	1.47-1.26	m, 20.87H, -CH_3

2.4.3 FT-IR spectroscopy

The IR analysis were carried out with an instrument Jasco. The characterization was performed in the solid state by depositing the sample directly in the instrument. 128 scans were performed for each sample.

2.4.4 Scanning electron microscope

The morphology of samples has been studied using a scanning electron microscope, an instrument of the FEI Quanta line. The samples were fixed on a metal support and analyzed in high vacuum at 15.0 kV and at different amplifications size.

2.4.5 Differential Scanning Calorimetry

DSC measurements were performed by using a Q100 apparatus (Waters; TA Instruments) interfaced with a TA universal analysis 2000 software. Analyses were performed on dry samples using a heat–cool–heat cycle from -80 to 120 °C, with a heating rate of 20 °C/min in inert atmosphere (argon flow: 50 mL/min).

2.4.6 Mass spectroscopy

Mass spectra in the positive-ion mode were obtained on a Q Exactive Plus Hybrid Quadrupole-Orbitrap (Thermo Fisher Scientific) mass spectrometer. The samples were solubilized in ultra-pure water at the concentration of 1 ppm. The solutions were infused at a flow rate of 5.00 μL/min into the ESI chamber. The spectra were recorded in the m/z range 300−4000 at a resolution of 140 000 and accumulated for at least 5 min in order to increase the signal-to-noise ratio. The instrumental conditions used for the measurements were as follows: spray voltage 2300 V, capillary temperature 230 °C, sheath gas 10 (arbitrary units), auxiliary gas 3 (arbitrary units), sweep gas 0 (arbitrary units), and probe heater temperature 50 °C. ESI-MS spectra were analyzed by using Thermo Xcalibur 3.0.63 software (Thermo Fisher Scientific).

2.4.7 Preparation of films

PLA films were prepared by casting solution method. 1 g of PLA was solubilized in 15 mL of CH_2Cl_2, after its solution, an amount of OLA-β-CD was added and solubilized in the solution (Table 2.6). The final solution was deposited in a petri dish (diameter: 11 cm) and the solvent was evaporated for a night.

Table 2.6: Composition of PLA films.

Sample	PLA (g)	OLA-β-CD (wt%)*
F1	1	0
F2	1	5
F3	1	10
F4	1	15
F5	1	20
		β-CD
F6	1	15

* wt% respect PLA

2.4.8 Differential Scanning Calorimetry

For the films, DSC measurements were performed by using a Q100 apparatus (Waters; TA Instruments) interfaced with a TA universal analysis 2000 software. The analyses were performed on dry samples using a heat–cool–heat cycle from -70 to 200 °C, with a heating rate of 10 °C/min in inert atmosphere (argon flow: 50 ml/min).

2.4.9 Dynamic mechanical analysis

The mechanical tests of the films (Table 9) were studied through elongation tests with a DMA Q800 Water TA instrument. The elongation tests were carried out on samples with a rectangular shape (length: 3 cm; width: 0.5 cm). The samples were analyzed by a controlled

force method applying a force ramp from 0 to 18 N, with a speed ramp of 1 N/min and a preload force of 0.10 N. For each sample, Young's modulus (E), which corresponds to the first section of the stress/strain curve (0–5% strain) were determined.

2.5 Semi-Interpenetrating Polymer Networks Based on Crosslinked Poly(N-Isopropyl Acrylamide) and methylcellulose prepared by Frontal Polymerization

2.5.1 Starting Materials

N-isopropylacrylamide (NIPAAm, MW= 113.16 g/mol), methyl cellulose (MC, average Mn≈ 40,000, viscosity 400 cP), N,N′-methylene-bisacrylamide (MBAm, MW= 154.17 g/mol), as a crosslinker, and dimethyl sulfoxide (DMSO, FW=78.13 g/mol; d=1.101 g/mL) were purchased from Sigma Aldrich and used as received. Trihexyltetradecylphosphonium persulfate (TETDPPS, FW=1157 g/mol) was prepared following the method reported in our previous study.[200]

2.5.2 Synthesis of Trihexyltetradecylphosphonium Persulfate (TETDPPS)

1.8 g of trihexyltetradecylphosphonium chloride, dissolved in 20 mL of ethyl ether, were introduced in a separatory funnel and shaken with 30 mL of an aqueous solution containing 5 g of ammonium persulfate. The organic phase was recovered and washed three times with water. Then, anhydrous $MgSO_4$ was added to dry the organic portion and ethyl ether was removed under vacuum. The final product (TETDPPS) is a viscous colorless liquid. IR: 2925 cm^{-1}, CH_2 asymmetric stretching; 2854 cm^{-1}, CH_2 symmetric stretching; 1466 cm^{-1}, CH_3 scissoring; 1378 cm^{-1}, CH_3 symmetric bending; 1278 cm^{-1}, S=O symmetric stretching. Anal. calcd: C, 66.28; H, 11.82; O, 11.04; S, 5.53; P, 5.34. Found: C, 66.96; H, 11.89; S, 5.04; P, 5.67. [200]

2.5.3 Synthesis of PNIPAAm–MC Semi-Interpenetrating Polymer Networks

0.2 g of MC were dissolved in 5 mL of DMSO at 85 °C. 2.7 g of NIPAAm and a suitable amount of MBAm were added (Table 2.7). Then, the mixture was magnetically stirred at 85

°C for a few minutes. The resulting solution was removed from the hot bath and slowly cooled down to room temperature under mechanical stirring. 0.56 g of TETDPPS (2 mol% with respect to NIPAAm) were added. This mixture was put into a common glass test tube (i.d.= 1.5 cm, length= 16 cm) and a thermocouple was located at about 1 cm from the bottom of the tube and connected to a digital temperature recorder (Delta Ohm 9416, sampling rate: 1 Hz). FP was triggered by heating the external wall of the tube in correspondence of the upper surface of the viscous solution by using a soldering iron tip. The position of the front (easily visible through the glass wall of test tubes) as a function of time was also monitored. For all the samples, the maximum temperature reached by the front (T_{max}) and its velocity (V_f) were measured. After polymerization, the samples were cut into two parts: the first was directly used (hence obtaining gels containing DMSO) and the second was thoroughly washed with water (hydrogels) for several days at room temperature (i.e., lower than hydrogel LCST).

Table 2.7: FP parameters and glass transition temperatures of the samples synthesized.

Sample Code	**MBAm (mol%)**	**T_{max} (°C)**	**V_f (cm/min)**	**T_g (°C)**
FP1	0.0	116	0.6	89
FP2	0.1	110	0.7	107
FP3	0.5	97	0.5	107
FP4	1.0	107	0.5	110
FP5	2.0	110	0.6	116

2.5.4 FTIR-ATR Measurements

FTIR-ATR measurements were performed on the gels containing DMSO. Attenuated Total Reflectance (ATR) spectra were recorded at room temperature in the range of 4000– 600 cm^{-1} (16 scans and 4 cm^{-1} resolution), using a Frontier FT-IR/FIR spectrophotometer, equipped with a diamond crystal.

2.5.5 Dynamic-Mechanical Analysis

Dynamic-mechanical analyses on PNIPAAm-*g*-MC on both just polymerized gels (containing DMSO) and hydrogels (swollen in water up to equilibrium) were carried out at room temperature (T=25 °C), using a TA Instruments Q800 DMA equipped with a TA Universal Analysis 2000 software. To evaluate the tangent moduli and ultimate stresses, samples were analyzed with a compression clamp. Square samples (width ca. 1 cm, height ca. 0.5 cm) were obtained and put in the clamp tank. The analyses were performed with a controlled force method, using 0.01 N preload and a force ramp from 0 to 18 N, with an increment of 0.5 N/min. Tangent moduli were calculated at different percentages of strain and for each sample, three tests were performed.

2.5.6 Differential Scanning Calorimetry

DSC measurements on PM dry samples were performed by means of a Q100 Waters TA Instruments calorimeter, equipped with a TA Universal Analysis 2000 software. Analyses were performed in heat-cool-heat mode at 20 °C/min in inert atmosphere (argon flow: 40 mL/min), in the range between -80 and 150 °C. The first run was carried out to check the presence of any possible residual reaction heat, thus determining the degree of conversion; in all cases, this latter was almost quantitative (no residual heat was recorded). The glass transition temperature (T_g) was evaluated on the second heating scan.

2.5.7 Swelling Measurements

The hydrogel samples as derived from FP experiments were washed repeatedly in water, cut in different pieces of similar shape and size, and put in water at controlled temperature to reach the swelling equilibrium. The swelling behavior was measured as a function of temperature (from 4 to 45 °C). The temperature dependence was assessed by increasing it at a rate of 1.0 °C/day and weighing the samples at each temperature. The reported data are an average of three measurements (reproducibility was ca. ≈10%). The swelling ratio (SR%) of hydrogels was calculated according to equation (1) described in the paragraph 2.1.4.

2.6 Semi-interpenetrating Polymer Networks of Methyl Cellulose and Polyacrylamide Prepared by Frontal Polymerization

2.6.1 Starting materials

Methylcellulose (MC, Mn≈ 40,000 g/mol), acrylamide (AAm, FW= 71.07 g/mol), N-N'-methylene-bis-acrylamide (MBAm, FW= 154.17 g/mol), ammonium persulfate (AmPS, FW= 228.20 g/mol), glycerol (FW= 92.09 g/mol, d= 1.25 g/mol) were purchased from Sigma-Aldrich and used as received.

2.6.2 Monomer Mixtures Preparation

MC was poured into a common beaker containing 5 ml of water or glycerol and stirred at 80 8C until MC dissolution. Suitable amounts of AAm and MBAm were added (MBAm= 0.3 mol% referred to AAm; Table 2.8 and 2.9), and after their dissolution, the beaker was placed in an ice bath in order to cool it down to room temperature; AmPS was eventually added (0.3 mol% referred to AAm).

Table 2.8: Composition, Glass Transition Temperature, Young's Modulus, and Tangent Modulus of the Samples Synthesized in the Presence of Water (Sample code WX-Y-Z identifies solvent (water), AAm/MC weight ratio, MBAm mol% and a progressive identification number, respectively).

	Sample code	**MBAm (mol%)**	**T_g (°C)**	**E (kPa)**	**Et_{30} (kPa)***
W9 series	W9-0.1-1	0.1	156	2	100
	W9-0.5-2	0.5	145	10	200
	W9-1.0-3	1.0	156	40	300
	W9-2.0-4	2.0	134	30	300
	(AAm:MC= 9:1 w/w)				
W20 series	W20-0.1-1	0.1	165	3	20
	W20-0.5-2	0.5	174	5	60

	W20-1.0-3	1.0	150	20	200
	W20-2.0-4	2.0	182	10	70
	(AAm:MC= 20:1 w/w)				

Table 2.9: Composition, glass transition temperature, Young's modulus and tangent modulus of the samples synthesized in the presence of glycerol. (Sample code GX-Y-Z identifies solvent (glycerol), AAm/MC weight ratio, MBAM mol% and a progressive identification number, respectively).

	Sample code	**MBAm (mol%)**	**T_g (°C)**	**E (kPa)**	**Et_{30} (kPa)***
G9 series	G9-0.1-1	0.1	-	-	-
	G9-0.5-2	0.5	154	30	20
	G9-1.0-3	1.0	151	40	100
	G9-2.0-4	2.0	166	90	600
	(AAm:MC= 9:1 w/w)				
G20 series	G20-0.1-1	0.1	-	-	-
	G20-0.5-2	0.5	150	4	30
	G20-1.0-3	1.0	160	50	200
	G20-2.0-4	2.0	165	90	600
	(AAm:MC= 20:1 w/w)				

2.6.3 Frontal Polymerizations

The above mixtures were poured into a common glass test tube (i.d.= 1.5 cm, length= 16 cm); a thermocouple was located at about 1 cm from the bottom of the tube and connected to a digital temperature recorder (Delta Ohm 9416, sampling rate: 1 Hz). The front was started by heating the external wall of the tube in correspondence of the upper surface of the monomer mixture until the formation of the front became evident. T_{max} (±10 °C in glycerol and ±20 °C in water) and V_f (±0.5 in glycerol and ±0.7 cm/min in water) were measured as function of time. The reported data are the average of three run measurements. After polymerizations,

each sample was cut into three parts. The first one was directly used for the dynamic mechanical analyses. The second and third parts were washed with water and used: (a) for DSC analyses after having been dried and (b) for assessing the swelling behavior in water. Besides, further cylindrical specimens of all the investigated hydrogel formulations were prepared for tensile tests.

2.6.4 Differential Scanning Calorimetry

DSC measurements were performed by using a Q100 apparatus (Waters; TA Instruments) interfaced with a TA universal analysis 2000 software. Analyses were performed on washed and dry samples using a heat–cool–heat cycle from -100 to 250 °C, with a heating rate of 20 °C/min in inert atmosphere (argon flow: 40 ml/min).

2.6.5 Dynamic Mechanical Analysis

DMA measurements were performed on the gels swollen in water or glycerol, as directly obtained by FP (Tables 2.8 and 2.9). A Q800 TA Instruments analyzer interfaced with a TA universal analysis 2007 software was used. Referring to the samples obtained in water, since part of this solvent evaporated during FP because of the high Tmax reached, in order to have comparable samples, i.e., containing the same amount of water, a suitable amount of this solvent was added and allowed to be absorbed before the analyses. Samples were cut into square disks (width < 25 mm and thickness < 5 mm) and placed in a submersion compression clamp without the addition of further solvent. The samples were analyzed by a controlled force method applying a force ramp from 0 to 18 N, with a speed ramp of 1 N/min and a preload force of 0.010 N. For each sample, Young's modulus (E), which corresponds to the first section of the stress/strain curve (0–5% strain), and the tangent modulus (Et_{30}), which is defined as the slope of the tangent to the stress–strain curve at 30% of strain, were determined. The standard deviation for the samples synthesized in glycerol was always below 5%, while that of the samples prepared in water was below 10%.

2.6.6 Tensile Tests

Tensile tests were performed on cylindrical specimens (diameter: 15 mm), according to ISO 527-1 standard, using a Zwick- Roll Z010 apparatus, equipped with a 5 kN load cell, at 23 ±2 °C and 50 ±5% relative humidity; the speed test was 50 mm/min. At least four tests were carried out for each material in order to have reproducible and significant data.

2.6.7 Swelling Measurements

All samples were cut into small disks (2 cm thick) and placed in distilled water at room temperature. Each sample was weighed periodically until no weight change was observed (equilibrium state). The swelling ratio (SR%) of hydrogels was calculated according to equation (1) described in the paragraph 2.1.4. Reproducibility in swelling measurements was always within ±5%.

198. Masere, J., et al., Gas-free initiators for high-temperature free-radical polymerization. Journal of Polymer Science Part A: Polymer Chemistry, 2000. 38(21): p. 3984-3990.

199. Tang, W. and S.-C. Ng, Facile synthesis of mono-6-amino-6-deoxy-α-, β-, γ-cyclodextrin hydrochlorides for molecular recognition, chiral separation and drug delivery. Nature Protocols, 2008. 3(4): p. 691.

200. Mariani, A., et al., Phosphonium-based ionic liquids as a new class of radical initiators and their use in gas-free frontal polymerization. Macromolecules, 2008. 41(14): p. 5191-5196.

-CHAPTER III-

Results and discussion

3.1 Synthesis of β-Cyclodextrin-based supramolecular poly(N-isopropylacrylamide) hydrogels

As mentioned in paragraph 1.5, most of research studies performed on frontal polymerization deal with polymerizing systems containing covalent crosslinking agents. However, the amount of crosslinker generally used in FP experiments is sometimes quite large,[185, 196, 201-208] thus limiting the swelling extent potentially reachable and, in turn, the number of applications of the resulting material. We hypothesized that, in order to fully exploit frontal polymerization for the obtainment of hydrogel materials exhibiting large swelling capability, an approach that is different from the conventional ones should be used. In the present study, we investigated the effect of AβCD as non-conventional crosslinker, which may give rise to supramolecular crosslinking as depicted in Figure 3.1.

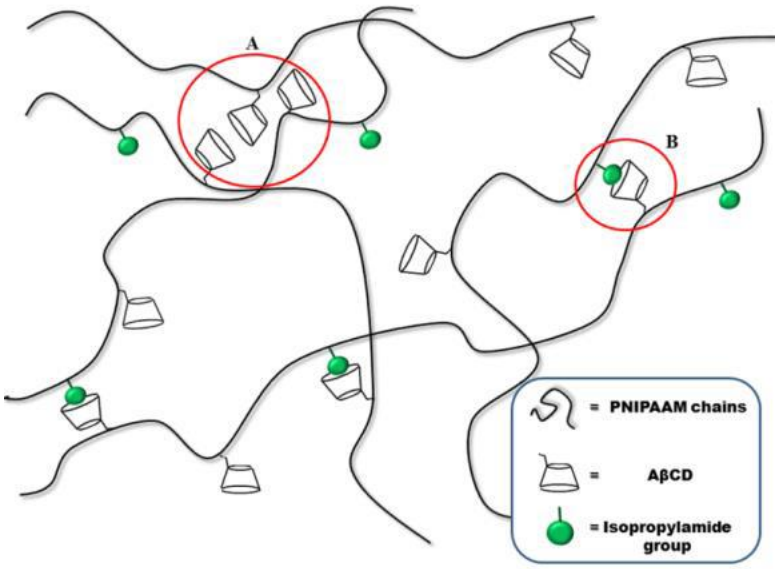

Figure 3.1: Supramolecularly crosslinked hydrogels due to both mutual CD interaction (A) and host-guest formation (B) with isopropylamide groups.

In addition, samples containing both AβCD and MBAm as a covalent (conventional) crosslinker were also synthesized for comparison. Since we found that front was not able to self-sustain without any crosslinker because of fingering occurrence, all experiments were performed in the presence of at least one (Table 3.1).

Table 3.1 Composition*, FP parameters and T_g values of the polymer samples synthesized in this work.

Sample code	NIPAAm (mol%)	AβCD (mol%)	MBAm (mol%)	T_{max} (°C)	V_f (cm/min)	T_g (°C)
M1	98.5	0.0	0.5	121	0.8	124
AM1	98.4	0.1	0.5	117	0.8	110
AM2	98.3	0.2	0.5	117	0.8	112
AM3	98.0	0.5	0.5	119	0.9	115
AM4	97.5	1.0	0.5	121	1.0	121
AM5	96.5	2.0	0.5	121	1.2	122
A1	98.5	0.5	0	118	0.9	138
A2	98.0	1.0	0	119	0.9	135
A3	97.0	2.0	0	121	1.1	142

Three series of samples were prepared. In the A series (grouping all samples that do not contain MBAm), the AβCD amount was varied from 0.5 to 2.0 mol% (ca. 5-20 wt.%). At variance, in the M and AM series (samples containing also MBAm), the AβCD amount was increased from 0 to 2.0 mol%, while the MBAm amount was kept constant at 0.5 mol% (Table 13). In order to avoid bubble formation, DMSO as a solvent boiling at high temperature was used.

However, by considering the A series, which gathers samples that do not contain any covalent crosslinker, no effect of the increased amount of cyclodextrin seems to occur or is hardly explainable (T_g values ranged from 135 to 142 °C without any apparent relationship with composition, Figure 3.2). Also, a comparison among the M, AM and A series is not straightforward. Indeed, if we compare the M1 sample (containing the covalent crosslinker only) to those belonging to the A series, we would conclude that the presence of even

relatively small amounts of cyclodextrin increase the glass transition temperature as a result of decreased chain mobility (Figure 3.2). Hypothesizing that, in the presence of covalent crosslinking, supramolecular CD aggregation might be partially prevented as a result of decreased mobility; we will investigate further on this point.

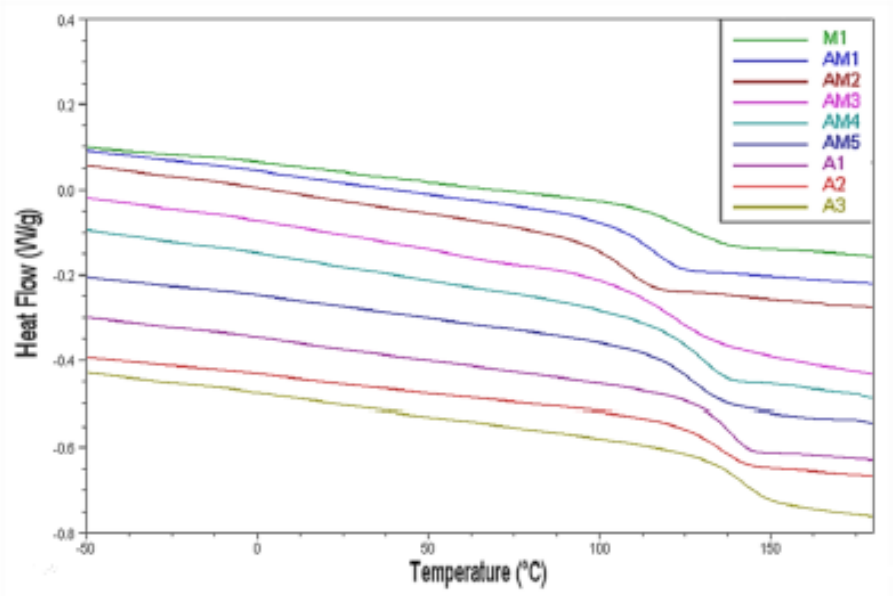

Figure 3.2: DSC heating runs for the samples containing both MBAm and AβCD.

However, the main scope of this work was the study of the effect of the presence of AβCD on the swelling behavior of PNIPAAm-based hydrogels.

In Figure 3.3, the trend of AM samples in water (pH = 5.5) as temperature increases from 4 to 35 °C is reported.

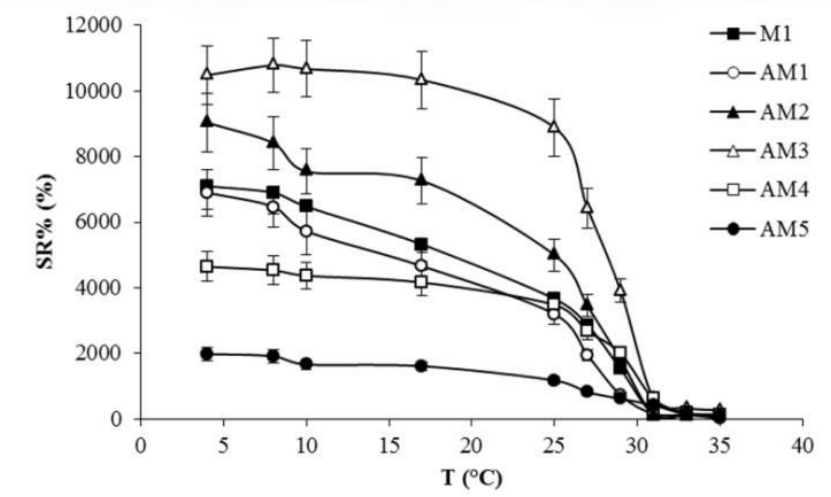

Figure 3.3: SR% as a function of temperature for samples containing both MBAm and AβCD.

All samples exhibit an evident lower critical solution temperature at ca. 28-30 °C, which is the typical value reported for PNIPAAm. [204] However, SR% is strongly influenced by the AβCD amount, as displayed in figure 3.4 for M and AM series samples at 4 °C. As can be seen, in the range of AβCD amount comprised between 0 and 0.5 mol% (samples M1 and AM3), SR% increases from ca. 7100 % to ca. 10500 %, respectively. On the other hand, when AβCD concentration exceeds 0.5 mol%, SR% decreases again down to ca. 1900 % (sample AM5).

This behavior can be explained by considering that, when the amount of cyclodextrin is relatively low, it partially prevents covalent crosslinking (due to the presence of MBAm), thus resulting in an increase of SR% as AβCD increases. However, when the threshold value of 0.5 mol% AβCD is overcome, the effect due to the supramolecular cyclodextrin interactions becomes prevalent and hydrogels swell less.

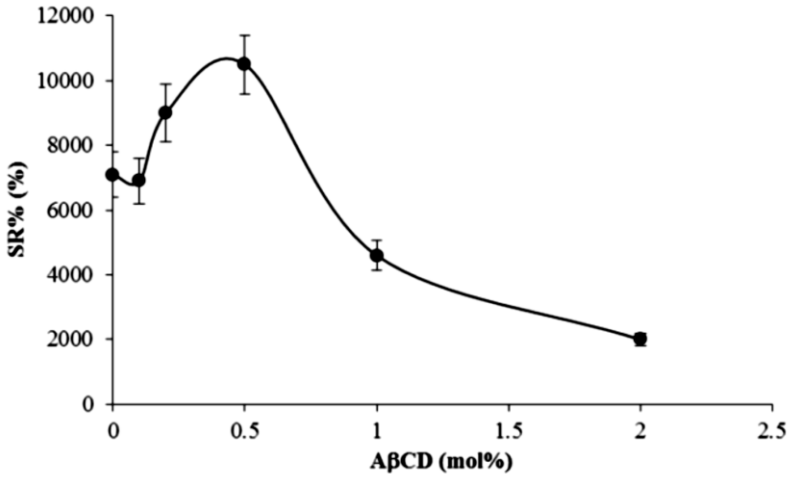

Figure 3.4: SR% as a function of AβCD amount at 4 ºC.

This behavior is also confirmed by the trend found for the A series, in which only AβCD was used as the crosslinker. Indeed, the larger the amount of cyclodextrin the lower SR%, at any temperature (Figure 3.5).

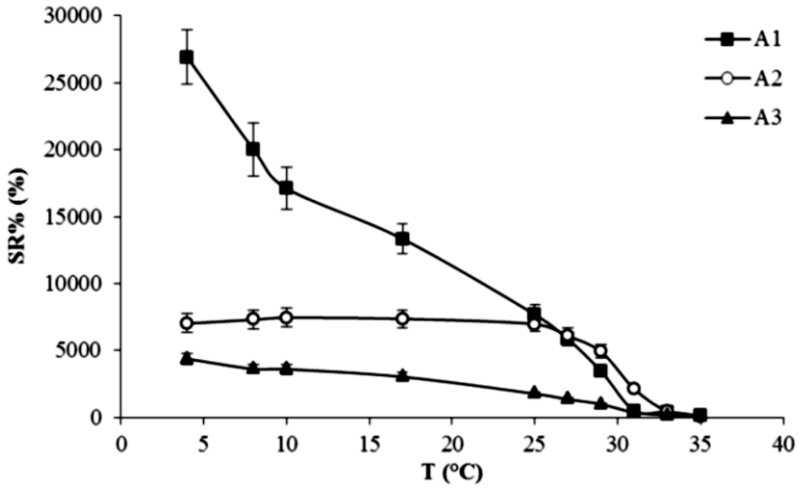

Figure 3.5: SR% as a function of temperature for samples containing AβCD only: A1= 0.5 mol%; A2= 1.0 mol%; A3= 2.0 mol%.

In detail, when the lowest amount of AβCD was used (0.5 mol%, sample A1) the hydrogel behaves as superabsorbent, it being characterized by an SR% as high as ca. 27000. By comparison, at the same temperature of 4 °C, SR% of samples A2 and A3 is ca. 7000 and 4400, respectively. This finding is a further evidence that, by using just little molar amounts of cyclodextrin as a supramolecular crosslinker, it is possible to obtain highly swelling hydrogels and, by changing its amount, SR% can be easily tuned. Furthermore, the use of a supramolecular crosslinker instead of a covalent one allows obtaining hydrogels characterized by much larger variation of SR%, thus showing potential in an increased number of applications.

It should also be pointed out that, at variance to what reported in our previous papers,[196, 203-205] these large degrees of swelling have been reached without using ionic monomers, which are less available and may be influenced by ionic force and pH in higher extent. Moreover, such a large degree of swelling is much larger than that reported by Liu and Fan (ca. 16000) who used a βCD derivative bearing a COOH group.[209]

Finally, since the presence of cyclodextrin does not result in any negative effect on the hydrogel swelling properties, and by considering its relative high weight amount, its low cost and large availability, its use as an additive able to partially replace NIPAAm, without resulting in negative effects, should be regarded as an advantage *per se*. In addition, the partial replacement of NIPAAm with a cyclodextrin, especially in the A series, makes pNIPAAm hydrogels safer and more compatible with their use in biomedical applications.

3.2 Synthesis of Sliding Crosslinked Thermoresponsive materials made of Poly(N-Isopropylacrylamide) and Acrylamide-γ-Cyclodextrin.

In order to prepare pNIPAAm-based PPRs, γ-CD was used, while their α and β counterparts were not considered suitable for this purpose. This is due to the relatively large size of γ-CD cavity, which allows NIPAAm to enter, hence giving rise to the corresponding inclusion complex. In addition, after the polymerization reaction, γ-CD allows pNIPAAm macromolecular chains to easily slide through. Indeed, it is known that smaller cavity size CDs are not able to do that. [210] This is very important, since it may significantly affect the mechanical behavior of the resulting system. Besides, the γ-CD used in this work was monoacrylated, in order to act as a NIPAAm comonomer, being it eventually covalently linked to pNIPAAm chains. The resulting PPR system is constituted of macromolecular chains bearing CDs as pendant groups; at the same time, these chains are non-covalently crosslinked and characterized by non-covalent sliding crosslinking.

As a first evidence, we noticed that the resulting hydrogels swell without dissolving in water. Since AγCD is monoacrylated, it cannot act as a covalent crosslinker. However, the observed behavior of the hydrogels containing AγCD suggested us that a sort of crosslinking should actually be present, which may be attributed to the PPR formation (Figure 3.6).

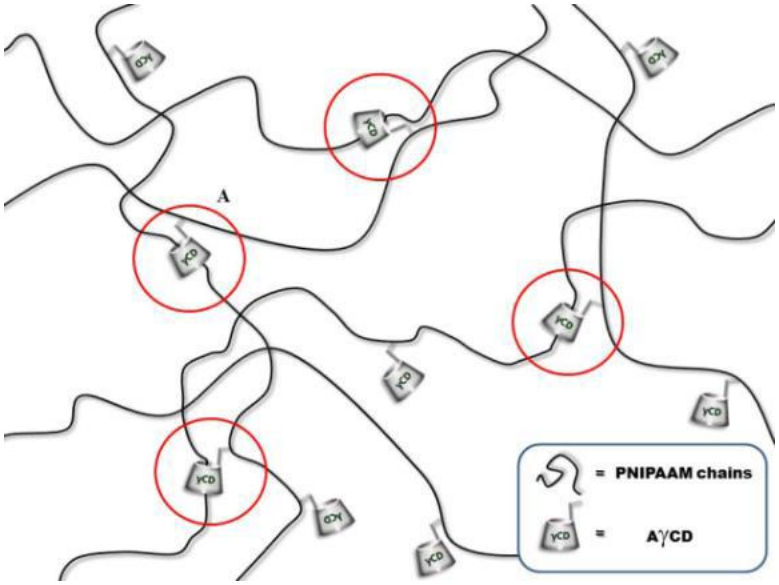

Figure 3.6: Schematic illustration of sliding crosslinking exerted by AγCD.

On the basis of what reported in literature about elastomers, which typically contain ca. 1 mol% of crosslinker, [211-213] we chose similar amounts for AγCD in order to ensure a close degree of crosslinking, but resulting from non-covalent, sliding characteristics instead of covalent bonds. Thus, the concentration of AγCD was kept between 0.5 and 2 mol%, while that of initiator [I], was always between 0.25 and 1.0 mol%.

From a qualitative point of view, two opposite situations were considered:

- when [I] and [AγCD] are, respectively, 0.25 and 2 mol%, the highest number of AγCD units linked to the macromolecular chains is present;
- conversely, when [I] and [AγCD] are 1 and 0.5 % mol, respectively, the lowest number of AγCD units is linked to the polymeric chains.

The reaction temperature was also a parameter that was taken into proper account. In particular, the polymerizations were carried out in water at 4 °C in order to avoid solvent evaporation and bubble formation and to obtain hydrogels that are already in their swollen state (the LCST of PNIPAAm is at about 32 °C). [214]

The composition and the T_g, LCST and modulus values (E) of the samples are listed in Table 3.2.

Table 3.2 Composition, T_g, LCST and modulus values of the samples synthesized in the present work.

Sample code	AγCD (mol%)	APS (mol%)	T_g (°C)	LCST (°C)	E (kPa)
A0.5	0.5	0.25	138	34	16.8
A1	1.0	0.25	152	35	21.8
A2	2.0	0.25	149	37	25.5
B0.5	0.5	0.5	148	35	11.9
B1	1.0	0.5	148	35	18.5
B2	2.0	0.5	153	37	21.3
C0.5	0.5	1.0	145	35	17.0
C1	1.0	1.0	152	35	16.0
C2	2.0	1.0	152	38	17.0

	γ-CD (mol%)				
DγCD	1.0	1.0	-	-	-
	MBAm (mol%)				
DMBAM	1.0	1.0	124	32	-

After synthesis, samples belonging to the A, B and C series looked as colorless semi-solids, like the covalently cross-linked sample (DMBAM). Once put in water, they just swell without dissolving. On the contrary, the sample DγCD, containing the unmodified γ-cyclodextrin only, looked physically different from the others: it was a colorless viscous liquid, completely soluble in water. This finding confirms that AγCD actually acts as a crosslinker.

DSC analyses performed on just-synthesized samples did not show any residual polymerization heat (exothermal), thus confirming that monomer quantitatively converted into polymer.

In order to better characterize the thermal properties of hydrogels, DSC analyses were performed also on washed and subsequently dried samples. A heat/cool/heat cycle was performed on each sample. (Table 3.2) A wide endothermic transition at about 160 °C appeared during the first heating for all samples, probably due to the release of water molecules from the cavity of AγCD. This transition was not recorded in the second heating ramp.

Furthermore, from the second heating, it was possible to evaluate the T_g values of polymers. (Table 3.2) It was found that, as the AγCD amount increased, T_g values remarkably increased. Indeed, by comparing samples having the same amount of initiator, but a different amount of AγCD (ranging between 0.5 and 2 mol%), the T_g values raised from 138 to 153 °C, respectively. In addition, by comparing the DMBAM sample with those containing AγCD, it was found that the first one exhibits significantly lower T_g (124 °C). This finding can be easily explained by considering the decrease of free volume and the consequent reduction of macromolecular chain mobility exerted by cyclodextrins, which are rigid compounds able to exert strong polar interactions, through the formation of supramolecular aggregates. [215, 216] The amount of initiator did not influence the T_g; in fact, by keeping constant the AγCD concentration and ranging the amount of APS from 0.25 to 1 mol%, the T_g values were almost unchanged.

Sample A0.5 showed a different behavior: in fact, its glass transition occurred at a temperature that is lower than that of all samples containing AγCD (i.e. 138 °C). This finding can be easily explained by considering the qualitative approach mentioned above: sample A0.5 contains the lowest amount of both AγCD and APS; thus, it is characterized by the longest macromolecular chains and the lowest number of linked AγCD. As a consequence, its chain mobility is larger than that of the others. Anyhow, this value is higher than those of the "conventionally" crosslinked sample (DMBAm, 124 °C); this fact is probably due to the strong interactions between cyclodextrin and hydrogel.

The influence of CD on the swelling properties of PNIPAAm hydrogels was also evaluated: all the synthesized hydrogels were found to significantly swell in water; furthermore, the presence of AγCD influenced their SR% as a function of temperature (Figure 3.7).

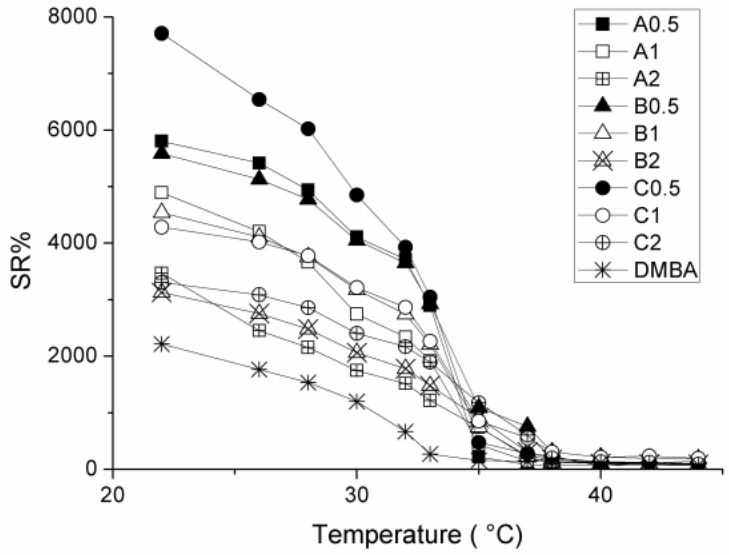

Figure 3.7: SR% as a function of temperature for synthesized samples. Series: A) squares; B) triangles; C) circles. Amount of AγCD: 0.5 mol% (solid); 1.0 mol% (empty marker); 2.0 mol% (starred).

The values of the samples belonging to the A series are represented by squares, the samples belonging to C series by triangles and samples belonging to C series by circles. The amount of AγCD is indicated in the interior of the symbol: solid for 0.5 mol%, empty for 1 mol% and starred for 2 mol%. In particular, as can be seen in Figure 3.7, the swelling ratio increases by decreasing cyclodextrin concentration, according to the following ranking: (A, B, C) 0.5> (A, B, C) 1> (A, B, C) 2.

In detail, at 22 °C, SR% goes from 7800 % for sample C0.5, to 3100 % for B2, hence demonstrating the large influence of AγCD on the swelling properties of PNIPAAm hydrogels. In addition, SR% value of DMBAM at 22 °C is ca. 2200%, a significantly lower value than that of cyclodextrin-containing samples. This agrees with the covalent nature of the crosslinker, which does not allow the chains to freely slide and swell. Furthermore, this is also a confirmation that the other samples are characterized by sliding crosslinking. By contrast, the effect of the amount of initiator was almost negligible.

AγCD influences also the thermoresponsive behavior of hydrogels. In fact, the "conventionally" crosslinked PNIPAAm (DMBAM) shows the usual LCST at about 32 °C, [214] while hydrogels containing AγCD exhibit a higher value of lower critical solution temperature (Table 3.2). LCST values increase from 35 °C, for all the samples containing 0.5 mol% of cyclodextrin (regardless of the amount of APS), to 38 °C for those samples containing 2 mol% of AγCD. We consider this result of large interest for the possible practical applications of PNIPAAm also in the biomedical field, as the range of LCST variation can be tuned by including also the physiological body temperature. Moreover, this goal was reached by using non-toxic, largely available and cheap additives as CDs are.

The mechanical properties of slide-ring gels are quite different from those of conventional physical and chemical gels. Indeed, as reported in literature, [217] the physical ones show a J-shaped stress-strain curve with large hysteresis, while the chemical gels show an S-shaped stress-strain curve. [218] The large hysteresis in the physical gel is caused by recombination among non-covalent crosslinks in a polymer network on deformation.

Actually, the polymeric hydrogels studied in this work exhibited a force/deformation curve characterized by a "J" shape without hysteresis (or very limited hysteresis phenomena; Figure 3.8), for A1, B1 and C1 samples.

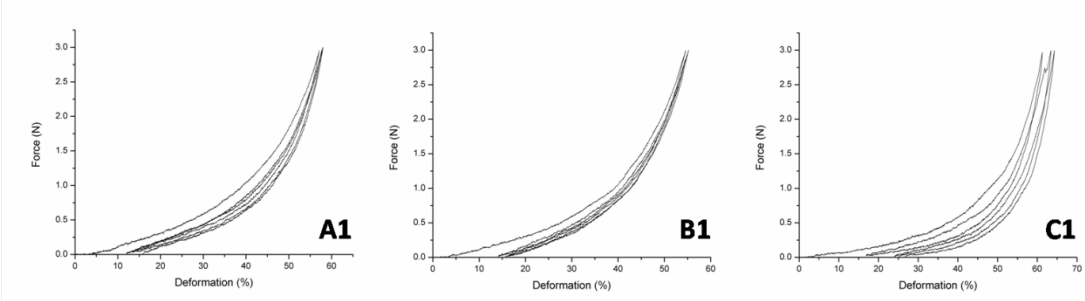

Figure 3.8: Several cycles compression curves for A1, B1 and C1 samples with "J" shape.

This finding supports the hypothesis that cyclodextrin acts as a sliding, non-covalent crosslinking agent. [218] It was not possible to perform this characterization on sample DMBAM because of its high brittleness. Then, pNIPAAm/AγCD hydrogels were subjected to compression tests: as presented in Table 3.2, the compression modulus E increases with increasing the cyclodextrin content. This agrees with the observed T_g increase. Furthermore, the presence of higher APS amounts in the hydrogel formulation turns out to lower the stiffness of the samples. This result confirms that, as the amount of initiator increases, the macromolecular chains are shorter: therefore, the probability that AγCD units are linked to the polymeric chains decreases. For the same reason reported above, the E modulus value of sample DMBAM could not be recorded.

3.3 Synthesis and characterization of oxypropylated cork and preparation and characterization of PLA films

3.3.1 Oxypropylated cork with CDs

α-cyclodextrin, β-cyclodextrin and γ-cyclodextrin were introduced in different quantities into the oxypropylated cork products, using an autoclave, in order to verify their influence in the properties of the final material. In table 3.3 are listed the samples synthesized in this work:

Table 3.3 Composition of the sample in series A, B, C, D and E.

Sample	Cork (g)	PO (mL)	α-CD (g)	β-CD (g)	γ-CD (g)
A1	1.5	14.1			
B1	1.5	14.1	1.32		
B2	1.5	14.1		1.32	
B3	1.5	14.1			1.32
C1	1.2	14.1	0.3		
C2	1.2	14.1		0.3	

C3	1.2	14.1			0.3
D1		14.1	1.32		
D2		14.1		1.32	
D3		14.1			1.32
E1		14.1			

The acronym A1 indicates the product obtained for reaction of cork and propylene oxide with the use of KOH as a catalyst. In the B and C series, cyclodextrins were also used. In the B series, the amount of CD added was 88 wt% with respect to the weight of the cork; in the C series, the amount of cyclodextrin was equal to 20 wt%, with respect to the weight of the cork. The two series have a large difference in the amount of CDs because the synthesis aims to the obtainment of data with a visible great variations with respect to the cork modification procedure through the reaction with propylene oxide, as indicated in paragraph 1.3.2. For completeness, two other types of samples have been synthesized: in the D series the samples consist in CD and PO without the presence of cork, and the E1 sample is made exclusively of polypropylene oxide. (Table 3.3)

From each synthesis two types of products were obtained: a fraction soluble in hexane at 70 °C and an insoluble one. The insoluble fraction most probably is the oxypropylation product of cork, according to the literature, and appears as a viscous solid having a brown color; instead, the part soluble in hexane (at 70 °C) is the homopolymer, polypropylene oxide, which after the evaporation of the solvent, appears as a viscous, transparent liquid with a yellow color.

Solubility tests were performed on series A, B, C and E to highlight their behavior in solvents with different polarity and characteristics. For this reason, water, methanol, acetone, tetrahydrofuran and hexane (at room temperature) have been taken into consideration. Table 3.4 shows the results obtained.

Table 3.4 Solubility of the samples of series A, B, C and E.

Sample	**H_2O**	**MeOH**	**Acetone**	**THF**	**Hexane**
A1 insoluble fraction	+	++	+++	++	-
A1 soluble fraction	-	++	++	++	-

B1 insoluble fraction	++	++	++	++	-
B1 soluble fraction	++	++	++	++	-
B2 insoluble fraction	++	++	++	++	-
B2 soluble fraction	++	++	++	++	-
B3 insoluble fraction	++	++	++	++	-
B3 soluble fraction	++	++	++	++	-
C1 insoluble fraction	++	++	++	++	-
C1 soluble fraction	++	++	++	++	-
C2 insoluble fraction	++	++	++	++	-
C2 soluble fraction	++	++	++	++	-
C3 insoluble fraction	++	++	++	++	-
C3 soluble fraction	++	++	++	++	-
E1	++	++	++	++	++

Legend: + = slightly soluble; ++ = soluble; +++ = very soluble; - = insoluble

As can be seen in table 3.4, almost all the samples are soluble in water, methanol, acetone and THF. However, this solubility is limited because the samples show this behavior only when subjected to sonication. Upon its removal, the only sample soluble in all the solvents tested is E1, polypropylene oxide, while all the other samples were completely insoluble in hexane. Another important fact is the improvement of solubility of the B and C series in water: this is probably due to the presence of CDs that thanks the presence, in their structure, of numerous hydroxyl groups, improve the solubility of the final products.

Other types of characterization, e.g. light scattering, ^{1}H NMR, GPC (Gel permeation chromatography) and Mass Spectroscopy, were not successful because in all cases problems of solubility of the samples were found.

The DSC analyses were performed on the samples of series A, B, C, D and E to verify whether the introduction of cyclodextrin influenced the glass transition temperature (T_g). Table 3.5 shows the updated values.

Table 3.5: T_g values of the A, B, C, D and E series of soluble and insoluble fractions.

Sample code	Insoluble fraction	Soluble fraction
A1	-62	-72
B1	-33	-70
B2	**-34**	**-72**
B3	-46	-71
C1	-53	-69
C2	-49	-68
C3	-54	-68
D1	-48	-67
D2	-63	-69
D3	-64	-68
E1	-	-76

From table 3.5, it can be seen that sample A1, (starting sample for the synthesis of the other series), shows a T_g of -62 °C for the insoluble part, while the soluble one shows a T_g of -72 °C, which coincides with that of neat poly(propylene oxide).

The insoluble fraction of both B and C series show a significant change in T_g values after the introduction of cyclodextrins. In B1 and C1, α-CD was introduced in different percentages

and the samples showed T_g of -33 and -53 °C, respectively. Comparing these temperatures with the A1 sample, an increase in the glass transition temperature can be noticed with the increase of the percentage of cyclodextrin, as in the sample B1, which showed an increase of 29 °C. (Figure 3.9)

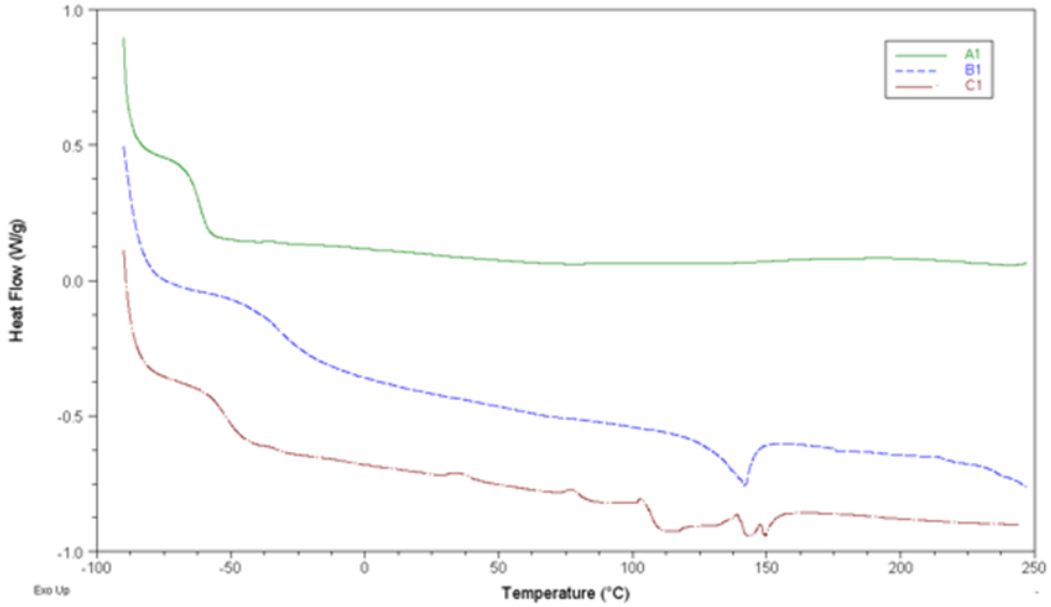

Figure 3.9: Thermograms of the samples A1, B1 and C1.

Similarly, the insoluble fraction of samples B2 and C2 containing β-CD showed analogous modification effects to those soluble in the same series: sample B2 showed a T_g of -34 °C while the sample C2, having a lower percentage of CD, showed a T_g of -49 °C. Also, in this case the increase of T_g is evident (related to the sample A1), in fact the sample B2, which has a higher percentage of CD, the increase of T_g is of 28 °C. (Figure 3.10)

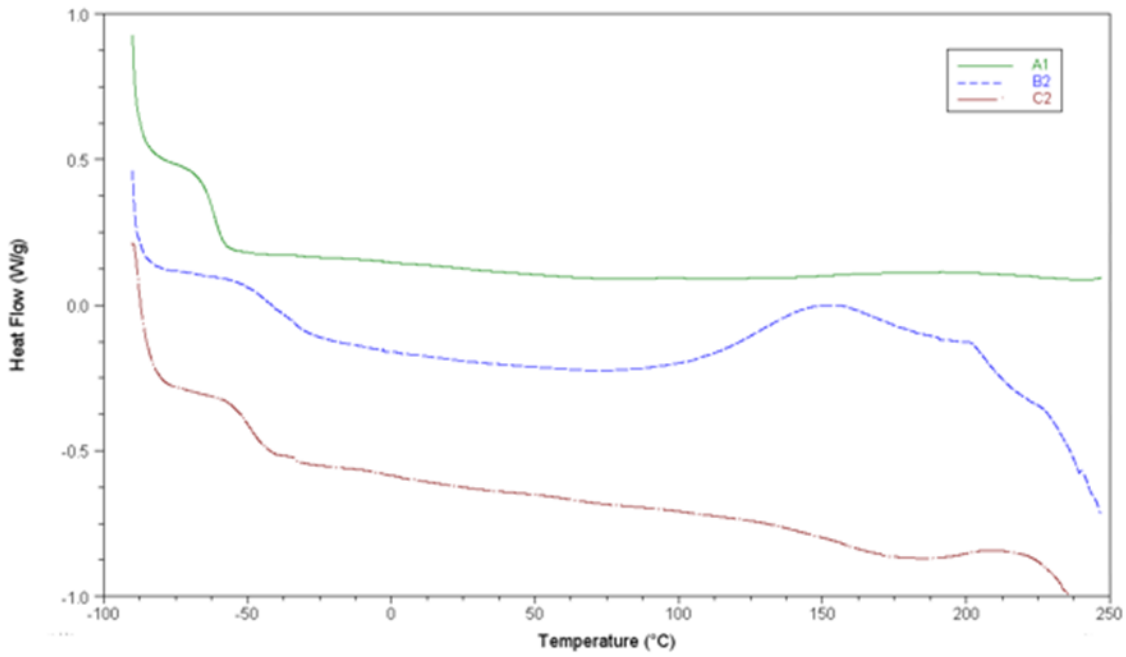

Figure 3.10: Thermograms of the samples A1, B2 and C2.

From the comparison between the series B and C and the sample A1 it can be deduced that the cyclodextrins, α-, β- and γ-, have a reinforcing effect, from the point of view of T_g, with respect to the sample that contains only oxypropylated cork, thus leading to modification of the final properties of the products obtained.

The sample E1, polypropylene oxide, is useful for comparing the values of the soluble fractions of the other synthesized series. The T_g values of these fractions of the A, B, C and D series range between -72 and -67 °C, a narrow range that allows to hypothesize that all the soluble fractions during the extraction phase are homopolymer of propylene oxide, obtained during the synthesis phase and which has not been integrated into the cork structure.

From the IR analyses, performed on the insoluble fraction of the sample A1 and those of the series B in the solid state, it has not been possible to deduce explanations on the structure of the compounds because from the IR spectra, represented in figures 3.11 and 3.12 respectively for sample A1 and B2, it is not possible to grasp any obvious difference.

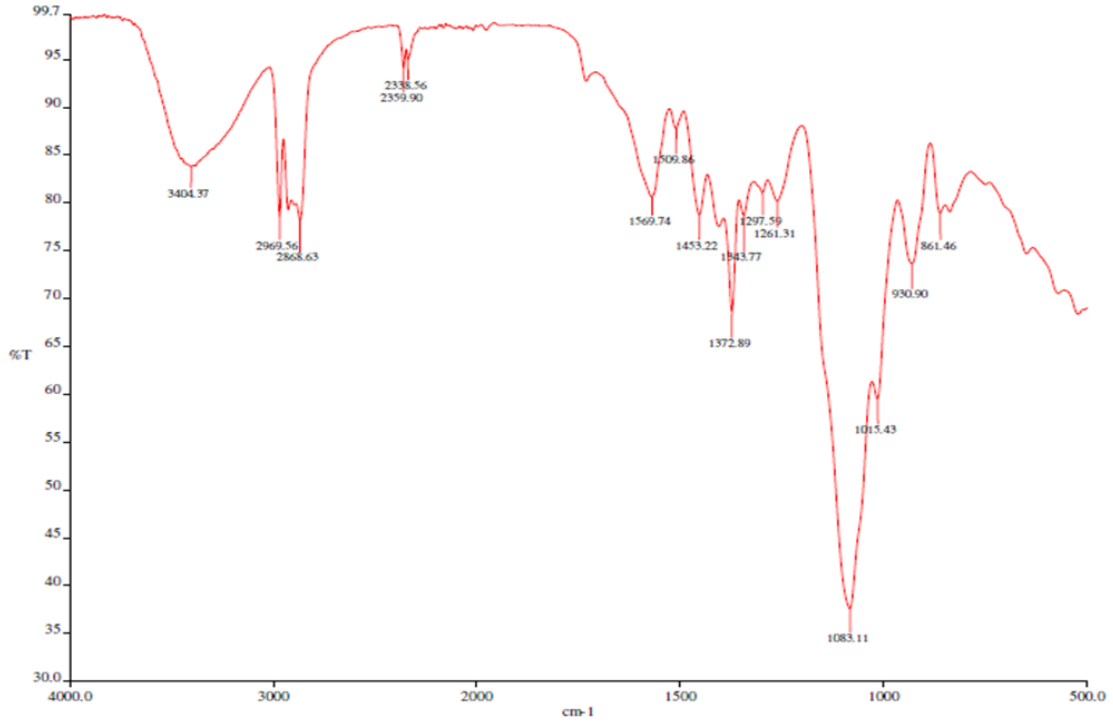

Figure 3.11: IR spectra of insoluble fraction of the sample A1.

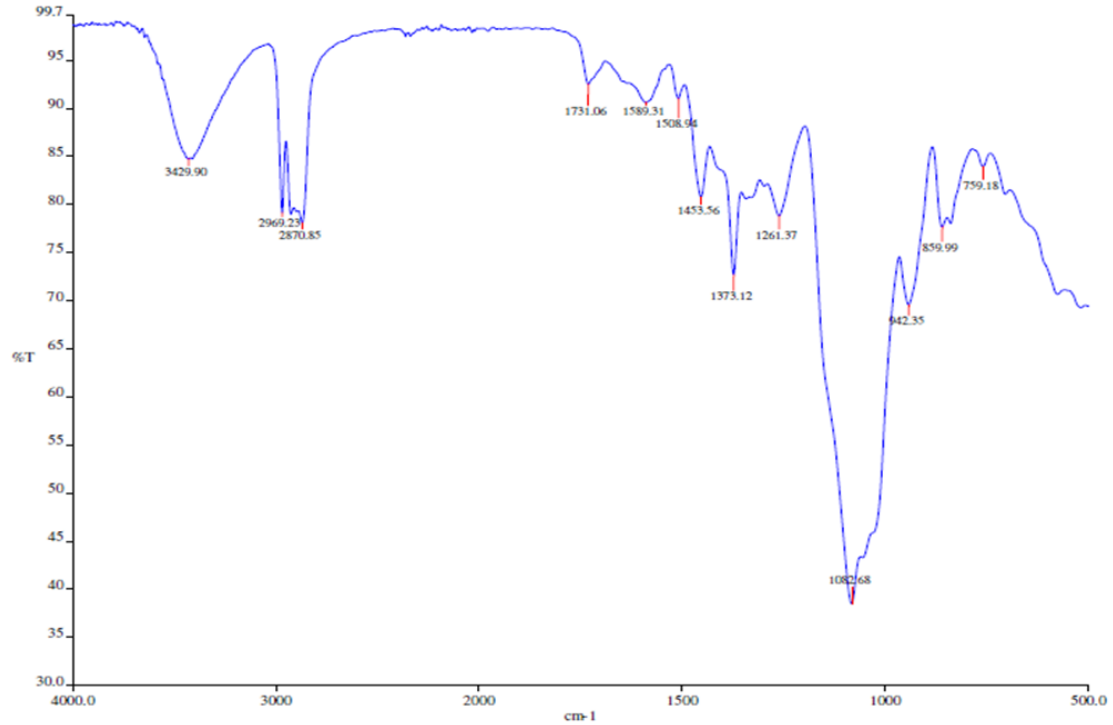

Figure 3.12: IR spectra of insoluble fraction of the sample B2.

In fact, in both cases there are the peak at 3400 cm^{-1}, attributable to the OH group stretching, the peaks at~2900 and~2800 cm^{-1} due to the stretching of the CH bonds, the signal at 1453 cm^{-1} due to the banding of the CH_2, the peak at~1373 cm^{-1} due to the deformation on the plane of the C-OH bonds and finally also the band present at~1083 cm^{-1} attributable to the stretching of the C-OH bonds.

3.3.2 Preparation and characterization of PLA films with CD-based oxypropylated cork

The F series samples are all polymeric films composed of poly(lactic acid) and variable percentages of products A1 and B2 (Table 3.6), introduced with the aim of verifying the possible modification of the properties of the PLA.

Table 3.6: Compositions, Young's moduli (E) and T_g of synthesized films.

Sample	**PLA (wt%)**	**A1 (wt%)**	**B2 (wt%)**	**E (MPa)**	**T_g (°C)**
F1	100			2785	60
F2	90	10		1933	54
F3	70	30		665	50
F4	90		10	877	51
F5	70		30	545	48
Oxypropylated cork	-	-	-		-62
PPO	-	-	-		-76

As can be seen from the table 3.6, the samples tested to modify the properties of the PLA are the insoluble fraction of the A1 sample, in percentage of 10 and 30 % respectively, and the insoluble fraction of the sample B2, containing oxypropylated cork and β-cyclodextrin, also these at 10 and 30 %, respectively.

All films obtained with the integration of cork-based products have shown an evident change in color: the F1 sample (i.e., neat PLA) is transparent and almost colorless, while the remaining samples of the series have a brownish color even if they are transparent as well.

For the characterization of the samples, the analysis was carried out with the scanning electron microscope which allows information on the morphology of the products, on the uniformity of the composition or any anomalies in the structure.

Figure 3.13 shows the SEM image of sample F2 (a) and sample F4 (b).

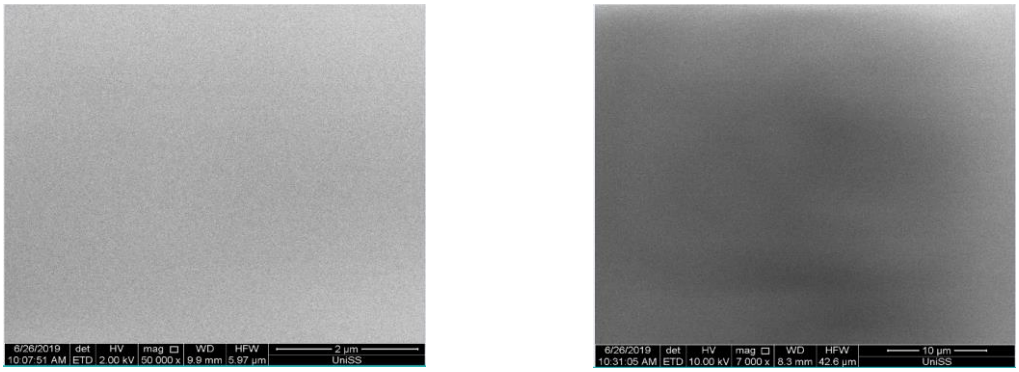

a) b)

Figure 3.13: SEM imagine of sample a) F2 b) F4.

No significant difference between the two images can be seen. In fact, both samples show a totally uniform morphology with no change in the distribution. This is probably due to the fact that the entire composition of the samples is based on carbon, thus making hard to distinguish the components of the products. The SEM image of the sample F2 was taken at 2 kV but, also working at 10 kV, as in the image of sample F4, the results obtained are the same and the slight changes in the color of the image b) in Figure 3.13 are caused by the high voltage at which the analysis was performed.

DSC analyses were performed on the F series films in order to determine the influence of CD-based oxypropylated cork on the glass transition temperatures of PLA. In table 3.6 the results obtained are shown. As it can been seen in table 3.6, the sample F1 (pure PLA) has shown a T_g value of 60 °C. As expected, the introduction of oxypropylated cork, (A1, having a T_g of -62 ° C) have resulted in a decrease in the T_g of the polymeric film. In particular, it was noticed a lowering of 6 and 10 °C for samples F2 and F3, with the introduction of an amount of oxypropylated cork (A1) equal to 10 and 30 wt%, respectively. For samples F4 and F5 the behavior is the same: as the amount of CD added increases, the T_g of the polymer film decreases. In fact, it can be seen from table 3.6 that for sample F4 (which contains 10wt% of B2**)** the T_g is equal to 51 °C, while for sample F5 (30 wt% of B2) the T_g lowers to 48 °C.

Accordingly to the current literature, this decrease is unexpected as, generally, the introduction of CDs causes an increase in the glass transition temperature, because supramolecular interactions between the CDs occur, which lead to a decrease in chain mobility. This result is particularly interesting as it makes the use of these compounds doubly useful for application purposes, particularly in the active packaging sector. Further in-depth studies from the point of view of thermal properties will be needed to verify this possibility.

DMA analyses were performed on films in order to study the mechanical properties of PLA the influence of oxypropylated cork and CDs products. In table 3.6 the values obtained from analyses are shown.

DMA data confirm the DSC analyses since with the addition of cork derivates, a lowering of Young's modulus was obtained and so a decrease of the rigidity of materials. In particular, starting from a modulus value of 2785 MPa for pure PLA, it can be noted that E decreases with the addition of oxypropylated cork for the F2 and F3 samples (from 1933 MPa to 665 MPa, for the addition of 10 and 30 wt% of oxypropylated cork, respectively). Samples containing β-CD and oxypropylated cork also confirm the DSC analysis. Moreover, it can be said that the presence of the CD allows to have a greater decrease of module (and therefore of rigidity) compared to samples containing only oxypropylated cork. This variation is more evident in the sample containing the greater quantity of CD (sample F5), which shows a decrease from 2785 to 545 MPa.

These data confirm again what previously assumed, that is that the cyclodextrins integrated in the samples containing cork and propylene oxide can be exploited not only in active packaging but also only as plasticizers for PLA.

3.4 Synthesis of β-cyclodextrin-based oligomers of lactic acid and preparation of PLA films with β-CD-OLA as plasticizers

3.4.1 Synthesis and characterization of β-cyclodextrin-based oligomers of lactic acid

This part of the work was carried out during the internship period abroad, at the Department of Nutrition, Chemistry and Bromatology of the University of Alicante (Spain). During this period the synthesis of lactic acid oligomers was developed in the presence of β-CD, as a

chain initiator in order to introduce the CD as end group. The synthesis was carried out by using microwaves as energy source. Various parameters were studied, including microwave power, temperature, time and LA/CD molar ratios and catalyst. For comparison, a synthesis reaction was carried out with the conventional method. Table 3.7 lists the samples prepared:

Table 3.7: Compositions, studied parameters of synthetized samples.

	Code sample	**molar ratio LA/CD**	**$SnOct_2$ (mol%)**	**Max power (W)**	**Temperature (°C)**	**time (min)**
Power study	M-1	~8	0.1	**200**	120	3
	M-2	~8	0.1	**150**	120	4
	M-3	~8	0.1	**100**	120	10
	M-4	~8	0.1	**50**	100	43
Molar ratio LA/CD	M-5	**~8**	0.1	100	100	10
	M-6	**~40**	0.1	100	100	10
	M-7	**~80**	0,1	100	100	10
	M-8	**~400**	0,1	100	100	10
Catalyst study	M-9	~40	**0**	80	80	35
	M-10	~40	**0,5**	80	80	35
	M-11	~40	**1**	80	80	40
Conventional method	M-12	~8	0.1	-	80	6h

FT-IR analyses were performed on all the synthesized samples and all the samples showed the same peaks. Figure 3.14 shows the overlap of the infrared spectra for at least one sample of each series; in particular, the sample M-2, M-7, M-10 and M-12 are reported. The infrared spectra of the β-CD and lactide reagents are also displayed. As can be seen, beyond the CD-related peaks, the peak at ~1750 cm^{-1}, due to the absorption of the C=O of the aliphatic ester

present in both the samples and in the monomer (lactic acid), is present. At variance, the peak at 930 cm^{-1}, due to the COC ring of the lactide, is absent.

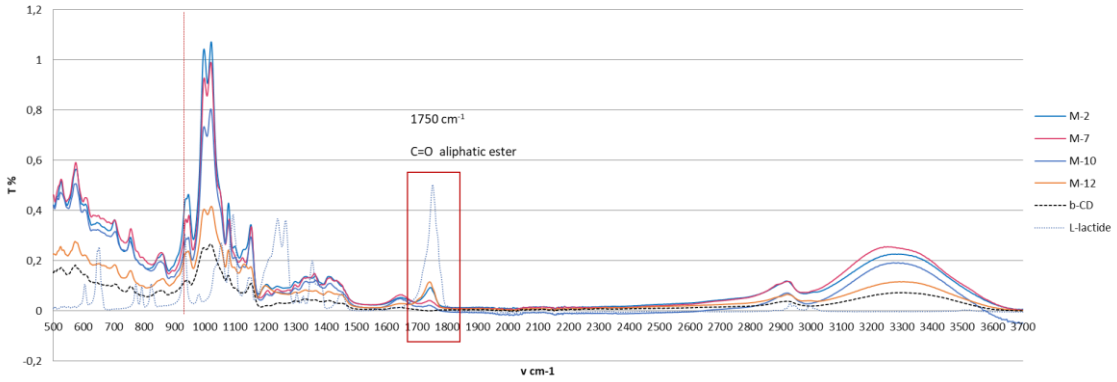

Figure 3.14: FT-IR spectra of M-2, M-7, M-10 and M-12 samples.

Confirmation of the success of the reaction was given by NMR. NMR analyses were performed on all samples including pure β-cyclodextrin. Table 3.8 compares the δ-shift values for pure β-cyclodextrin and for lactic acid and β-cyclodextrin oligomers (molecular mass~1630 g/mol) in D_2O.

Table 3.8: Chemical shift (δ) of β-cd and OLA-β-CD.

β-CD		**OLA-β-CD (D_2O) (MW:~1630 g/mol)**	
5.05	d, 7H, C(1)H	5.06	
3.94	t, 7H, C(3)H	4.94	m,12.41H, -COCH-(CH_3O)-; C'1H
3.86	m, 14H, C(5)(6)H	4.33	m, 4.65H, -COCH(CH_3)OH; C'6H
3.63	m, 7H, C(2)H	3.78-3.52	m, 40.45H, C2'H,3'H,4'H,5'H,6'H
3.56	t, /H, C(4)H	1.47-1.26	m, 20.87H, -CH_3

In figure 3.15 the ^{1}H-NMR spectra of M2 sample is shown. In this case, the peaks are not intense because of the proton-deuterium exchange due to the use of deuterated water as a the solvent.

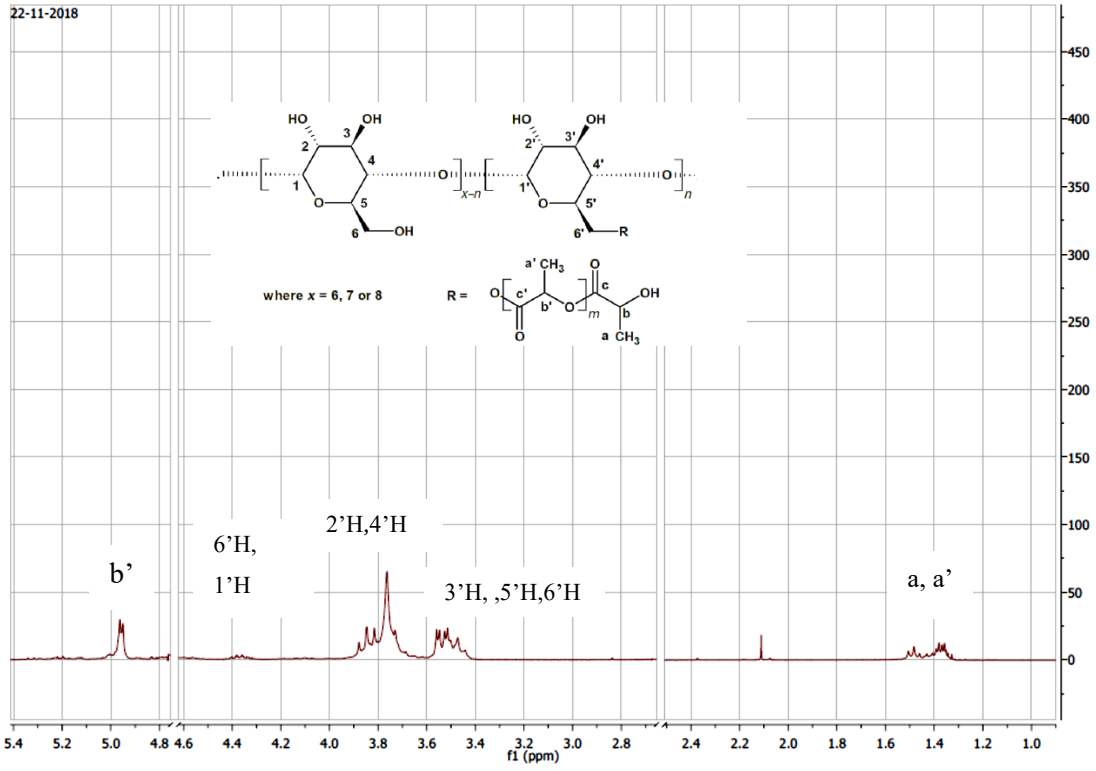

Figure 3.15: ^{1}H-NMR spectra of M-2 sample.

SEM analyses were performed initially on the samples of the "power study" (M-1, M-2, M-3, M-4 in Table 3.7) and on the sample synthesized with the conventional method (M-12), to see the morphological differences on the CD surface, after esterification reaction. As can be seen in figure 3.16, the morphological differences are evident passing from pure CD to the various samples synthesized by microwave.

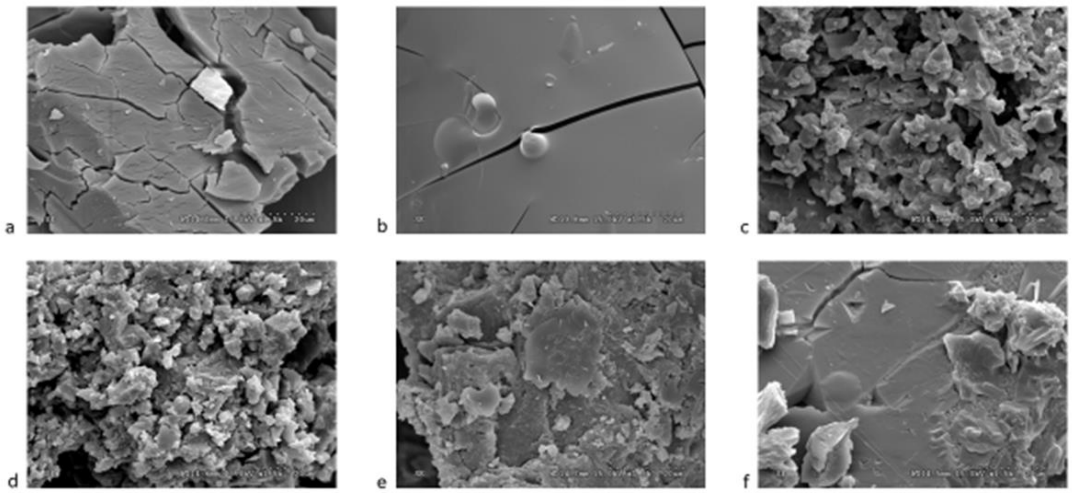

Figure 3.16: SEM images (x3k) of a) β-CD, b) M-12, c) M-1, d) M-2, e) M-3, f) M-4

DSC analyses (not reported) of the oligomers did not show the presence of any glass transition temperature, thus probably suggesting that the molecular weight of the poly(lactic acid) chain is too low.

The ESI-MS spectra were recorded on samples at β-CD-OLA in concentration of 1ppm. For convenience, an ESI-MS spectrum of M-2 sample is shown in figure 3.17. As can be seen, there are two sets of peaks: the first set is attributed to the species β-CD-OLA with charge Z = 2, which form the adduct with potassium [β-CD-OLA +K]. While the second set is attributed to the species β-CD-OLA with charge Z = 1, which form the adduct with sodium [β-CD-OLA+Na]. Moreover, it is seen that in this sample (but on average also in the others) the monomeric units of lactic acid, bound to the β-CD, are 6 as a maximum.

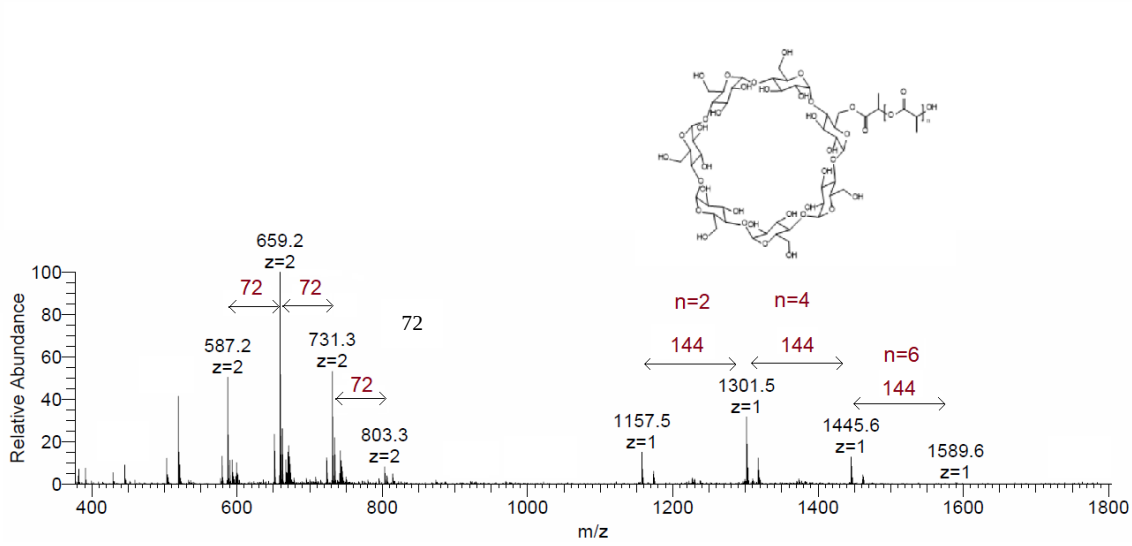

Figure 3.17: ESI-MS spectrum of M-2.

3.4.2 Preparation and characterization of PLA films with β-CD-OLA

PLA films were prepared by casting solution method. Table 3.9 summarizes the films synthesized with the compositions in wt% of β-CD-OLA, the Young's modulus and the glass transition temperature (T_g). As can be seen from the table, the module decreases with the increase of β-CD-OLA. Compared to the pure PLA, the module goes from a value of 2800

MPa (for F1), to one of 800 MPa (F5). However, a lowering of the module is obtained even in the presence of the β-CD only.

As regards DSC data, it can be noted that T_g is not influenced by the presence of β-CD-OLA for which the desired plasticizing effect is not obtained.

Table 3.9 Composition, Young's modulus and T_g of the synthetized films.

Sample	**PLA (g)**	**β-CD-OLA (wt%) ***	**E (MPa)**	**T_g (°C)**
F1	1	0	2683	56
F2	1	5	1220	55
F3	1	10	1268	56
F4	1	15	1035	56
F5	1	20	815	56
		β-CD		
F6	1	15	760	56

3.5 Semi-Interpenetrating Polymer Networks Based on Crosslinked Poly(N-Isopropyl Acrylamide) and methylcellulose prepared by Frontal Polymerization

In this work, semi-interpenetrating gels of pNIPAAm and MC were successfully synthesized by using FP. To obtain samples that do not contain bubbles, DMSO and TETDPPDS were used as polymerization solvent and radical initiator, respectively.

Namely, DMSO was utilized because of its high boiling point (189 °C), which is higher than that reached by the polymerization fronts (see T_{max} in Table 3.10).

Table 3.10 FP parameters and T_g of the samples synthesized.

Sample code	MBAm[a] (mol%)	T_{max} (°C)	V_f (cm/min)	T_g (°C)
FP1	0.0	116	0.6	89
FP2	0.1	110	0.7	107
FP3	0.5	97	0.5	107
FP4	1.0	107	0.5	110
FP5	2.0	110	0.6	116

[a] MBAm concentration referred to NIPAAm.

As a matter of fact, low boiling solvents are generally avoided in FP runs in that they may give rise to bubble-containing materials. In addition, since the boiling process is endothermic, it could cause excessive heat dissipation, hence resulting in a non-self-sustaining front. On the other hand, TETDPPDS was chosen since it decomposes without forming gaseous compounds; besides, it shows high reactivity when ignited,[200] but large stability at low temperature (thus ensuring long pot-lives), which are desirable features in all FP experiments. [207, 219]

T_{max} and V_f are the main parameters to be considered in FP experiments. As can be seen in Table 3.10, these parameters are not significantly affected by the amount of crosslinker. In fact, V_f values remain almost constant at ca. 0.6 ± 0.1 cm/min, while T_{max} is always around 106 ± 10 °C. This is due to the quite low amount of crosslinker used in all runs.

Figures 3.17 and 3.18 show the typical FTIR-ATR spectra of NIPAAm, MC and their copolymer, respectively. The spectrum of NIPAAm (Figure 3.17) clearly shows the stretching band at 1655 cm^{-1} of N-H group of carbonyl amide and the CH stretching band of isopropyl at 1367 cm^{-1}. MC shows an intense signal at 3447 cm^{-1} (stretching vibration of hydroxyl, Figure 3.18), as well as the stretching of the ether bond at 1054 cm^{-1}. The PNIPAAm-MC spectrum (Figure 3.19) shows the presence of all the above-mentioned bands: this finding clearly substantiates that the prepared gels embed MC molecular chains.

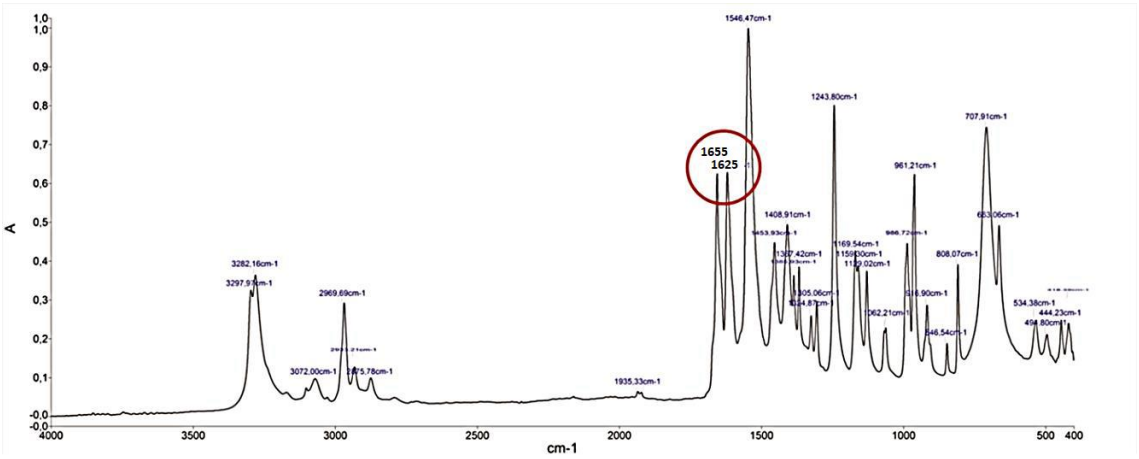

Figure 3.17: FTIR-ATR spectrum of NIPAAm

Besides, in similar systems, the occurrence of the grafting reaction has been already reported in the scientific literature and demonstrated just on the basis of the concurrent presence of the signals related to the two components in the resulting FTIR spectra. [220] However, this cannot justify the formation of PNIPAAm-*g*-MC 3D networks.

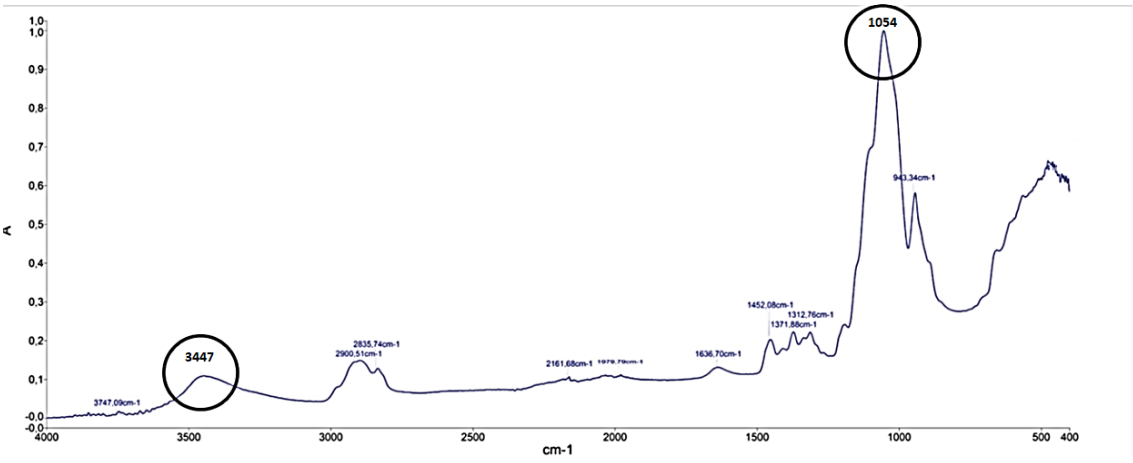

Figure 3.18: FTIR-ATR spectrum of MC.

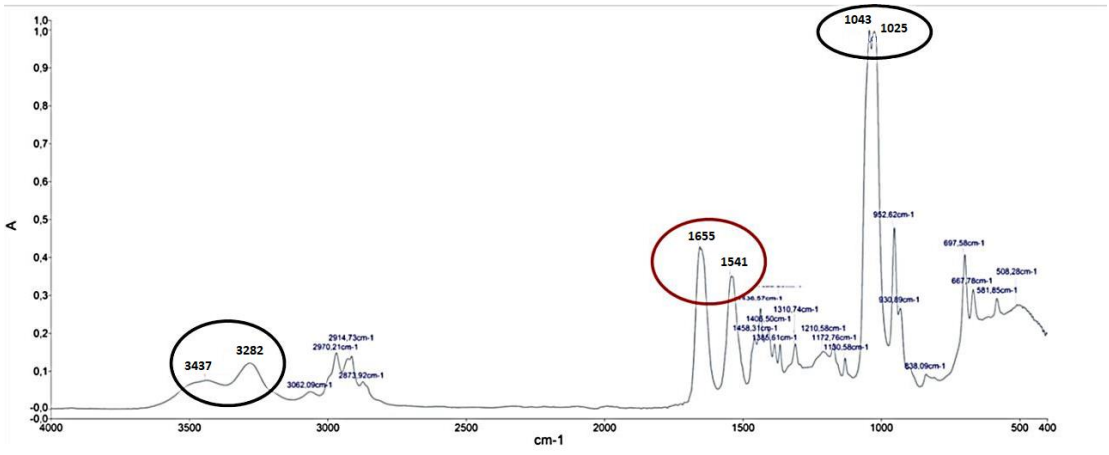

Figure 3.19: FTIR-ATR spectrum of PNIPAAm-MC.

DSC analyses were performed on all washed and dried samples, in order to evaluate the glass transition temperatures. Table 3.10 collects the T_g values as a function of the mole percentages of MBAm. As expected, T_g increases with increasing the crosslinker content: in particular, T_g values range from 89 °C for the linear gel, to 120 °C for the sample containing 2 mol% of crosslinker. It is noteworthy that, unlike the negligible effect on T_{max} and V_f, a very small variation in the amount of crosslinker from 0 to 0.1 mol% causes a very high increase in the T_g value, from 89 °C (linear gel, FP1) to 107 °C (FP2). This behavior can be ascribed to the mobility decrease of the polymer segments as a consequence of the formation of more crosslinking points.

To evaluate the mechanical properties of MC-NIPAAm gels, the E values and the tangent modulus at different strain percentages were measured. Both these parameters were evaluated, since, under unrestricted compression, hydrogels usually display a non-linear stress–strain response. [221, 222] In particular, the E value is usually very low but the modulus as a function of strain follows an exponential law, thus increasing rapidly. Tangent modulus is defined as the slope of the tangent to the stress–strain curve at a definite point.

Table 3.11 collects the tangent moduli for the gels containing DMSO: the latter show that the Young‘s moduli increase with increasing MBAm. In particular, at 50 % strain (E50), the sample with the highest concentration of MBAm (FP5) exhibits the highest tangent modulus. It is noteworthy that all the tested gels did not break and fully recovered their pristine shape after the removal of the applied stress.

Table 3.11 Young and tangent modulus of the gels swollen in DMSO.

Sample code	MBAm[a] (mol%)	E_0 (kPa)	E_{25} (kPa)	E_{50} (kPa)
FP1	0.0	1.8	6.4	30.2
FP2	0.1	3.1	9.0	52.3
FP3	0.5	4.6	30.3	124.0
FP4	1.0	6.4	55.4	190.3
FP5	2.0	7.9	78.7	280.3

[a] MBAm concentration referred to NIPAAm. [b]n: crosslinking density.

The mechanical behavior of the hydrogel samples is shown in Table 3.12; furthermore, the stress-strain curves are shown in Figure 3.20. Similarly to the gels swollen in DMSO, Young's moduli rise with the amount of MBAm; however, as compared to the DMSO-containing counterparts, all hydrogels show lower values of modulus and break at the end of the tests.

In Table 3.12, the crosslinking densities determined by eq. 1 are also listed. As expected, their trend follows that of Young's modulus and ranges from 0.027 to 1.156 mol m^{-3}.

Table 3.12. Young and tangent moduli of the gels swollen in H_2O, and their crosslinking density.

Sample code	MBAm[a] (mol%)	E_0 (kPa)	E_{25} (kPa)	E_{50} (kPa)	n[b] (mol m^{-3})
FP1	0.0	1.8	6.4	30.2	0.027
FP2	0.1	3.1	9.0	52.3	0.067
FP3	0.5	4.6	30.3	124.0	0.148
FP4	1.0	6.4	55.4	190.3	1.156
FP5	2.0	7.9	78.7	280.3	0.900

[b]n: crosslinking density.

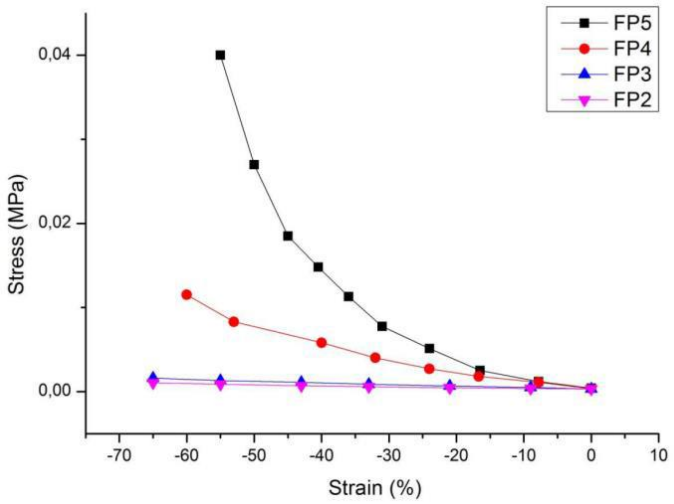

Figure 3.20: Stress-strain curves for the hydrogels.

Figure 3.21 shows the swelling behavior of all the hydrogels with different amounts of MBAm, as a function of temperature. In particular, the LCST of PNIPAAm-MC hydrogels was evaluated in the range of temperatures from 4 to 45 °C. Usually, the LCST of the PNIPAAm is at 32-33 °C;[223] conversely, in the present work the LCST of the PNIPAAm-MC hydrogels is below 30 °C, because of the presence of MC. W. Liu et al. have investigated the gelation of PNIPAAm-MC samples as a function of MC content, around body temperature: they demonstrated that LCST decreases at low MC contents, whereas it raises up when MC content increases. [220]

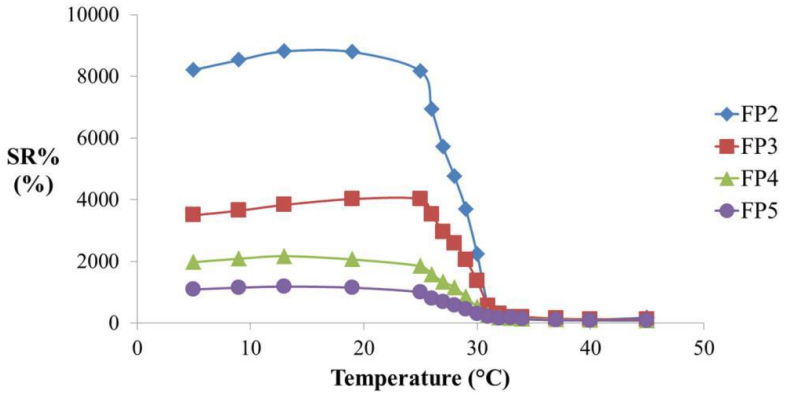

Figure 3.21: SR% as a function of temperature.

As expected, the SR% of the gels, below LCST, increases with decreasing the amount of crosslinker. In addition, for all the samples investigated, the highest SR% value is found at about 15 °C. The SR% value of the linear PNIPAAm-MC hydrogel is around 42000 %. Hydrogels, for which MBAm amount is in between 0.1 and 2 mol%, exhibit SR% values of approximately 9000 and 1200 %, for the lowest and highest crosslinked one, respectively.

Figure 3.22 shows the effect of the crosslinker on the SR% values. Interestingly, these parameters have been found to be inversely proportional at 20 °C, thus confirming that the swelling degree becomes lower as the crosslinking density increases.

The remarkable decrease by two orders of magnitude of the SR% values from room temperature to body temperature (SR% 25°C≈ 37200; SR% 37°C≈ 240 for the linear PNIPAAm-MC hydrogels), suggests the suitability of the PNIPAAm-MC hydrogels as drug delivery systems.

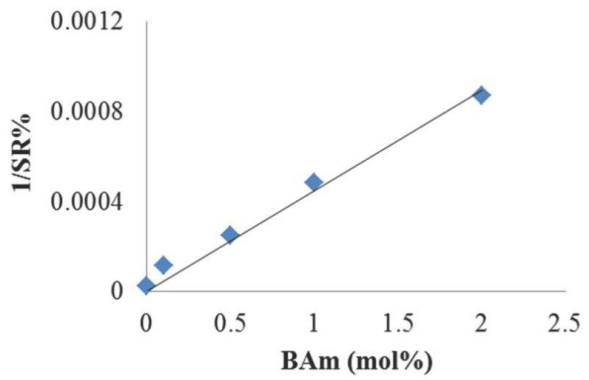

Figure 3.22: Relationship between SR% crosslinker concentration at 20 °C.

3.6 Semi-interpenetrating Polymer Networks of Methyl Cellulose and Polyacrylamide Prepared by Frontal Polymerization

Tables 3.13 and 3.14 list the samples prepared in the present work. In particular, two series of hydrogels were synthesized for each reaction solvent, namely water and glycerol (W and G series, respectively).

Table 3.13: Composition, glass transition temperature, Young‘s modulus and tangent modulus of the samples synthesized in the presence of water. (Sample code WX-Y-Z identifies solvent, AAm/MC weight ratio, MBAm mol% and a progressive identification number, respectively).

	Sample code	MBAm	T_g	E	Et_{30}
		(mol%)	(°C)	(kPa)	(kPa)*
W9 series	W9-0.1-1	0.1	156	2	100
	W9-0.5-2	0.5	145	10	200
	W9-1.0-3	1.0	156	40	300
	W9-2.0-4	2.0	134	30	300
(AAm:MC= 9:1 w/w)					
W20 series	W20-0.1-1	0.1	165	3	20
	W20-0.5-2	0.5	174	5	60
	W20-1.0-3	1.0	150	20	200
	W20-2.0-4	2.0	182	10	70
(AAm:MC= 20:1 w/w)					

Table 3.14: Composition, glass transition temperature, Young‘s modulus and tangent modulus of the samples synthesized in the presence of glycerol. (Sample code GX-Y-Z identifies solvent, AAm/MC weight ratio, MBAM mol% and a progressive identification number, respectively).

	Sample code	MBAm	T_g	E	Et_{30}
G9 series		(mol%)	(°C)	(kPa)	(kPa)*
	G9-0.1-1	0.1	-	-	-
	G9-0.5-2	0.5	154	30	20
	G9-1.0-3	1.0	151	40	100
	G9-2.0-4	2.0	166	90	600
(AAm:MC= 9:1 w/w)					
G20 series	G20-0.1-1	0.1	-	-	-

	G20-0.5-2	0.5	150	4	30
	G20-1.0-3	1.0	160	50	200
	G20-2.0-4	2.0	165	90	600
	(AAm:MC= 20:1 w/w)				

The first ones (W9 and G9) group the samples characterized by an AAm/MC weight ratio equal to 9, while the second ones (W20 and G20) gather those samples in which the above ratio is equal to 20. As an example, WX-Y-Z code identifies the sample synthesized in the presence of water, for which X is the AAm/MC weight ratio, Y is the MBAm mol% and Z is a progressive identification number; similarly, GX-Y-Z code identifies the samples synthesized in the presence of glycerol.

Moreover, while the molar amount of AmPS was kept constant (0.3 mol%), that of the crosslinking agent (MBAm) was varied along each series, from 0.1 to 2.0 mol%.

In Figures 3.23 and 3.24, V_f and T_{max} data are reported for W9 and G9 series respectively, as a function of the variation of MBAm content. In particular, by considering V_f values, Figures 3.23 a) and 3.24 a) show that all samples (W and G series) follow the same general trend: V_f increases going from 0.1 to 0.5 mol% of MBAm, decreases at 1.0 mol%, and increases again for higher amounts of crosslinker. This trend is also shown by the T_{max} values (Figures 3.23 b) and 3.24 b)). While the general increase of T_{max} and V_f as a function of MBAm concentration was expected on the basis of the larger amount of reactive groups present in the reaction mixture, no explanation can be given for the non-monotonic trend exhibited by all series. It should also be noticed that the G series samples show both T_{max} and V_f values greater than those of the W counterparts. This is mainly due to water evaporation occurring during front propagation, which results in heat loss and, consequently, in a decrease of both maximum temperature and, in turn, front velocity. However, it is noteworthy that FP could be performed also in this low boiling medium.

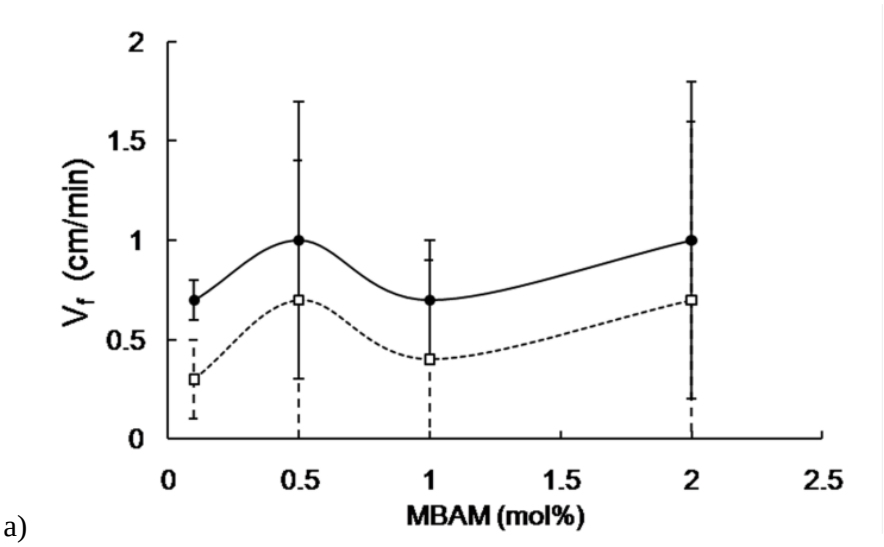

a)

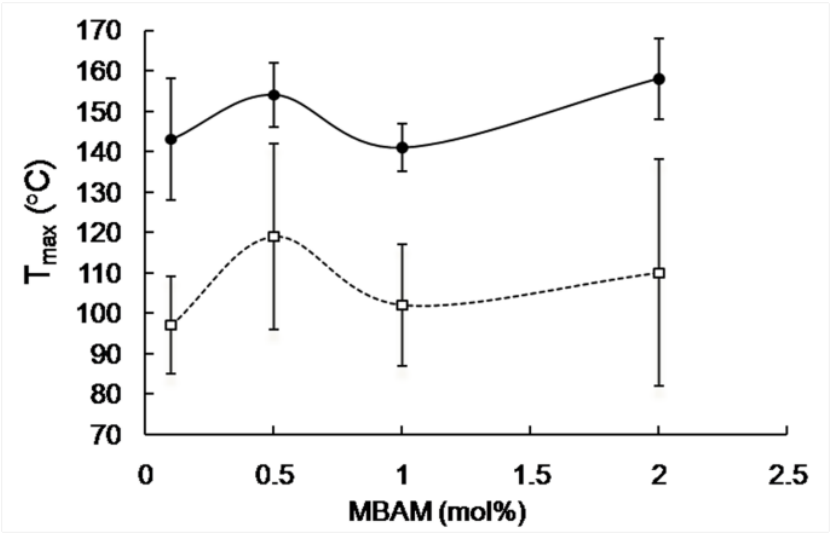

b)

Figure 3.23: V_f (a) and T_{max} (b) as a function of the amount of MBAM for W9 (□) and G9 (●) series.

Furthermore, by comparing W and G data, it should be noticed that the samples with AAm:MC ratio equal to 20:1 (i.e. W20-G20 series) are characterized by V_f and T_{max} values higher with respect to those containing lower AAm amounts (namely, W9-G9 series). This finding can be ascribed to the larger amount of inert material (MC) present in the W20-G20 samples, which facilitates the heat dispersion.

a)

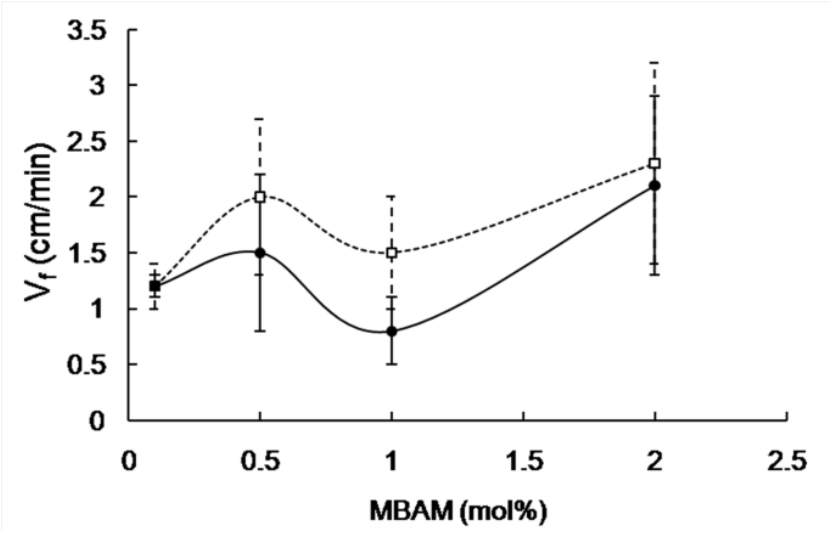

b)

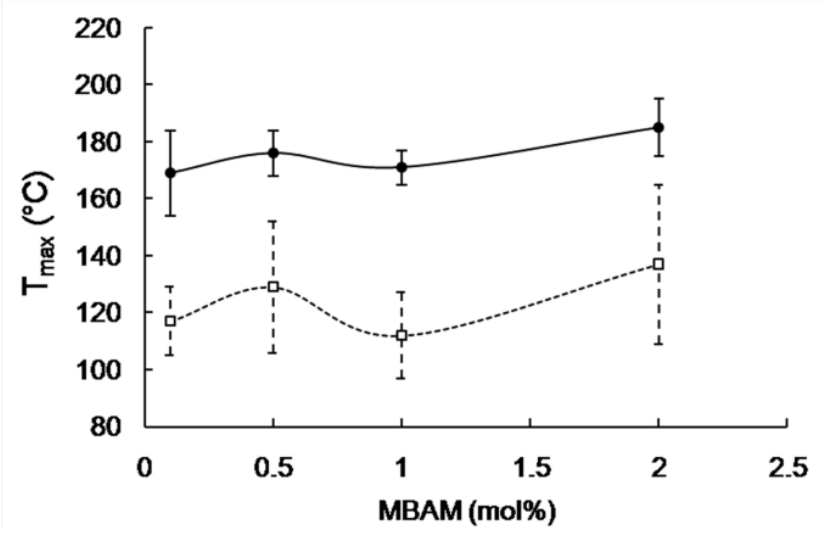

Figure 3.24: V_f (a) and T_{max} (b) as a function of the amount of MBAM for W20 (□) and G20 (●) series.

DSC analyses were performed on all washed and dried samples in order to determine the glass transition temperatures.

The samples synthesized in glycerol show a different behavior as compared with those obtained in water. In particular, G9 samples exhibit a monotonic increase of T_g from 154 to 166 °C for MBAm concentrations in between 0.5 and 2.0 mol% (Table 3.14). Analogously, G20 materials are characterized by increasing T_g values as the amount of crosslinker increases, ranging from 150 to 165 °C as the MBAm amount goes from 0.5 to 2.0 mol%. This finding can be explained by taking into account the reduced chain mobility occurring as the crosslinking degree becomes larger.

Conversely, by considering the corresponding samples obtained in water, such a behavior is not confirmed, it being characterized by an alternating trend (Table 3.13).

However, this result might be ascribed to the poorer control of the reaction conditions when water was used as polymerization medium. This, in turn, is probably a consequence of the boiling-related effects observed during FP runs.

As already mentioned, after the synthesis, each sample was cut into three parts for the different characterizations. First, the swelling behavior of hydrogels obtained after washing and swelling in water was investigated. As can be seen in Figure 3.25, in both water and glycerol SR% increases with decreasing the amount of MBAm. This is an expected behavior due to the decrease in crosslinking and is particularly evident for MBAm amounts below 1.0 mol%. In fact, only slight variations are found beyond this concentration, even by comparing the syntheses performed in water with those made in glycerol. At variance, for MBAm amounts below 1.0 mol%, SR% rapidly increases from ca. 1000 up to values comprised between ca. 2500 and 5000.

It should also be noticed that samples prepared in water swell differently from those prepared in glycerol. This can be explained again by considering that water boils at the temperature reached by the propagating front, thus generating large pores.

a)

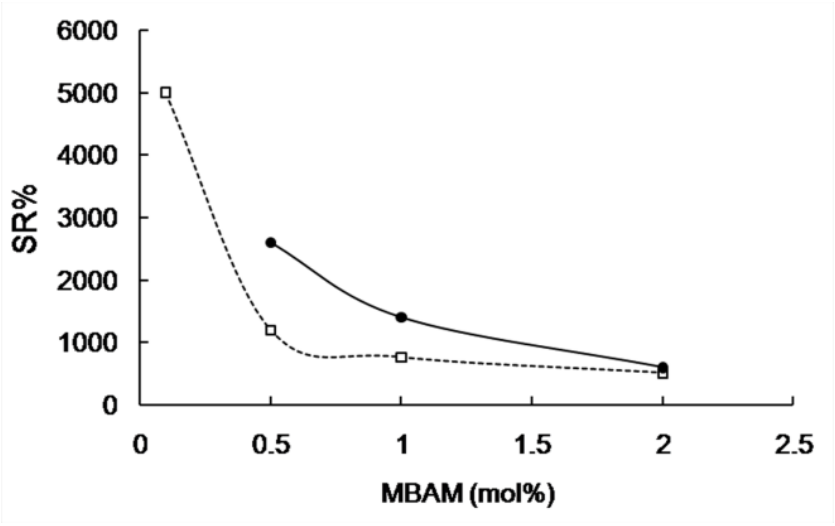

b)

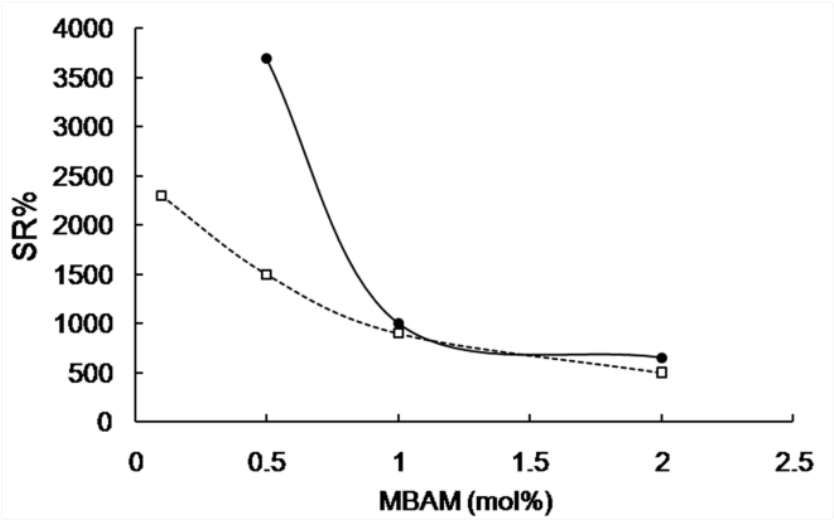

Figure 3.25: SR% as a function of the amount of MBAm for W9-G9 series (a), and W20-G20 series (b). (□= W series, ●= G series)

To evaluate the mechanical properties of gels, the Young's modulus (E) and the tangent modulus at 30% of strain (E_{t30}) were evaluated (Tables 3.13 and 3.14). Both these parameters were determined, since, under unconfined compression, hydrogels typically show a non-linear stress–strain response. [221] In particular, despite its very low value, the modulus as a function of strain follows an exponential increase law, thus increasing rapidly. Tangent modulus is defined as the slope of the tangent to the stress–strain curve at a specific point. In this work, 30% of strain was taken as reference value for all samples.

From an overall point of view, as shown in Tables 3.13 and 3.14, all tested samples increase both their E and E_{t30} values as the amount of crosslinker increases. Moreover, as expected, large differences are found by comparing the E with the corresponding, and more significant, E_{t30} values. Namely, E_{t30} regularly increases along the W9 series from 100 and 300 kPa as the amount of MBAm increases. At variance, an initial increase followed by a decrease of E_{t30} values is observed for the W20 series. As stated above, this non-monotonic trend can be explained by assuming that gels made in water are characterized by many inhomogeneities resulting from the boiling of water during the FP occurrence.

On the other hand, modulus trends in glycerol series are more consistent and turn out to increase with increasing the amount of crosslinker. In particular, E_{t30} goes from 20 (G9 series) or 30 (G20 series) to 600 kPa as the amount of MBAm increases, thus indicating a strong effect due to the crosslinking degree. This latter value, which is higher than the largest found

in both W9 and W20 series, may also account for the aforementioned larger homogeneity of these samples as compared with those obtained in water.

Aiming at further evaluating the mechanical behavior of the materials under investigation, tensile tests were performed on both water and glycerol series, notwithstanding that it was not possible to test the samples, synthesized either in water or glycerol, with the highest amount of MBAm (i.e. 2 mol%), which turned out to break during clamping. In fact, these samples, irrespective of the swelling solvent, are very brittle and difficult to handle, hence they cannot undergo tensile tests. The obtained results are collected in Table 3.15, in terms of elastic modulus and elongation at break.

Concerning the samples synthesized in the presence of water, the elastic modulus increases with increasing the crosslinker content; at the same time, the elongation at break decreases significantly, hence indicating a remarkable effect of an increased number of crosslinks. A similar behavior is observed for all the samples synthesized in the presence of glycerol: the only difference refers to the elastic modulus values, which are slightly higher with respect to the corresponding samples synthesized in the presence of water. Finally, it is worthy to note that the elastic modulus values determined in tensile tests are somehow comparable with those deriving from dynamic mechanical compression tests (collected in Tables 3.13 and 3.14), despite of the presence of defects (voids and bubbles) in the synthesized samples, which may affect the two mechanical tests in a different way.

Table 3.15: Composition, elastic modulus and elongation at break for the samples synthesized in the presence of water and glycerol. (Sample code WX-Y-Z o GX-Y-Z identifies solvent, AAm/MC weight ratio, MBAM mol% and a progressive identification number, respectively).

	Sample code	**MBAM (mol %)**	***E*** **(kPa)**	**Elongation at break (%)**
W9 series	W9-0.1-1	0.1	2.2	838
	W9-0.5-2	0.5	7.0	123
	W9-1.0-3	1.0	11.6	34
	W9-2.0-4	2.0	-	-
	(AAm:MC = 9:1 w/w)			
W20 series	W20-0.1-1	0.1	2.9	928

	W20-0.5-2	0.5	8.8	300
	W20-1.0-3	1.0	33.5	115
	W20-2.0-4	2.0	-	-
	(AAm:MC = 20:1 w/w)			
G9 series	G9-0.1-1	0.1	3.6	750
	G9-0.5-2	0.5	9.4	144
	G9-1.0-3	1.0	16.0	25
	G9-2.0-4	2.0	-	-
	(AAm:MC = 9:1 w/w)			
G20 series	G20-0.1-1	0.1	4.1	775
	G20-0.5-2	0.5	9.5	135
	G20-1.0-3	1.0	20.2	46
	G20-2.0-4	2.0	-	-
	(AAm:MC = 20:1 w/w)			

201. Caria, G., et al., *Poly (N, N-dimethylacrylamide) hydrogels obtained by frontal polymerization.* Journal of Polymer Science Part A: Polymer Chemistry, 2009. **47**(5): p. 1422-1428.
202. Lu, G.D., Q.Z. Yan, and C.C. Ge, *Preparation of porous polyacrylamide hydrogels by frontal polymerization.* Polymer International, 2007. **56**(8): p. 1016-1020.
203. Nuvoli, D., et al., *Synthesis and characterization of poly (2-hydroxyethylacrylate)/β-cyclodextrin hydrogels obtained by frontal polymerization.* Carbohydrate Polymers, 2016. **150**: p. 166-171.
204. Alzari, V., et al., *Stimuli-responsive polymer hydrogels containing partially exfoliated graphite.* Journal of Polymer Science Part A: Polymer Chemistry, 2010. **48**(23): p. 5375-5381.
205. Alzari, V., et al., *Graphene-containing thermoresponsive nanocomposite hydrogels of poly (N-isopropylacrylamide) prepared by frontal polymerization.* Journal of Materials Chemistry, 2011. **21**(24): p. 8727-8733.
206. Feng, Q., et al., *Frontal polymerization synthesis and drug delivery behavior of thermo-responsive poly (N-isopropylacrylamide) hydrogel.* Colloid and Polymer Science, 2010. **288**(8): p. 915-921.
207. Sanna, R., et al., *Synthesis and characterization of graphene-containing thermoresponsive nanocomposite hydrogels of poly (N-vinylcaprolactam) prepared by frontal polymerization.* Journal of Polymer Science Part A: Polymer Chemistry, 2012. **50**(19): p. 4110-4118.
208. Marques, H.M.C., *A review on cyclodextrin encapsulation of essential oils and volatiles.* Flavour and fragrance journal, 2010. **25**(5): p. 313-326.
209. Coleman, A.W., et al., *Aggregation of cyclodextrins: An explanation of the abnormal solubility ofβ-cyclodextrin.* Journal of inclusion phenomena and molecular recognition in chemistry, 1992. **13**(2): p. 139-143.
210. Wang, J., et al., *Formation of a Polypseudorotaxane via Self-Assembly of γ-Cyclodextrin with Poly (N-isopropylacrylamide).* Macromolecular rapid communications, 2012. **33**(13): p. 1143-1148.
211. Alemán, J., et al., *Definitions of terms relating to the structure and processing of sols, gels, networks, and inorganic-organic hybrid materials (IUPAC Recommendations 2007).* Pure and Applied Chemistry, 2007. **79**(10): p. 1801-1829.
212. Flory, P.J. and J. Rehner Jr, *Statistical mechanics of cross-linked polymer networks I. Rubberlike elasticity.* The journal of chemical physics, 1943. **11**(11): p. 512-520.
213. Mooney, M., *A theory of large elastic deformation.* Journal of applied physics, 1940. **11**(9): p. 582-592.

214. Fujishige, S., K. Kubota, and I. Ando, *Phase transition of aqueous solutions of poly (N-isopropylacrylamide) and poly (N-isopropylmethacrylamide).* The Journal of Physical Chemistry, 1989. **93**(8): p. 3311-3313.

215. Jansook, P., M.D. Moya-Ortega, and T. Loftsson, *Effect of self-aggregation of γ-cyclodextrin on drug solubilization.* Journal of Inclusion Phenomena and Macrocyclic Chemistry, 2010. **68**(1-2): p. 229-236.

216. Valero, M., J. Tejedor, and L.J. Rodríguez, *Encapsulation of nabumetone by means of-drug:(β-cyclodextrin) 2: polyvinylpyrrolidone ternary complex formation.* Journal of luminescence, 2007. **126**(2): p. 297-302.

217. Takata, T., N. Kihara, and Y. Furusho, *Polyrotaxanes and polycatenanes: recent advances in syntheses and applications of polymers comprising of interlocked structures*, in *Polymer Synthesis*2004, Springer. p. 1-75.

218. Ito, K., *Novel cross-linking concept of polymer network: synthesis, structure, and properties of slide-ring gels with freely movable junctions.* Polymer Journal, 2007. **39**(6): p. 489.

219. Nuvoli, D., et al., *Preparation and characterization of polymeric nanocomposites containing exfoliated tungstenite at high concentrations.* Composites Science and Technology, 2014. **96**: p. 97-102.

220. Liu, W., et al., *A rapid temperature-responsive sol–gel reversible poly (N-isopropylacrylamide)-g-methylcellulose copolymer hydrogel.* Biomaterials, 2004. **25**(15): p. 3005-3012.

221. Joshi, A., et al., *Functional compressive mechanics of a PVA/PVP nucleus pulposus replacement.* Biomaterials, 2006. **27**(2): p. 176-184.

222. Russo, S., et al., *High-molecular-weight aromatic polyamides by direct polycondensation.* Macromolecules, 1993. **26**(18): p. 4984-4985.

223. Schild, H.G., *Poly (N-isopropylacrylamide): experiment, theory and application.* Progress in Polymer Science, 1992. **17**(2): p. 163-249.

-CHAPTER IV-

Conclusions

4.1 Synthesis of β-Cyclodextrin-based supramolecular poly(N-isopropylacrylamide) hydrogels

As a conclusion, one of the main FP limits has been represented by the need of relatively large molar amounts of covalent crosslinkers that may prevent fingering occurrence. This drawback has decreased the potential of FP as a convenient alternative technique for the synthesis of macromolecular materials. In this work, we have shown that the use of supramolecular crosslinking agents may be extremely useful on this respect.

Namely, for the first time, frontal polymerization was successfully applied to the synthesis of PNIPAAm-grafted-AβCD supramolecular crosslinked hydrogels. We have found that the presence of AβCD on supramolecular and covalent crosslinked samples did not influence Tmax but resulted in a slight increase of Vf. Analogously, AβCD did not significantly affect the glass transition temperatures (always at ca. 135-142 °C) of supramolecular samples. At variance, a Tg increase of 12 °C was observed along the series of samples containing also the covalent crosslinker when βCD amount raised from 0.1 to 2.0 mol%. This is due to the decrease of chain mobility resulting from the increased number of crosslinking points.

The most interesting effect was observed on the swelling behavior of hydrogels. Indeed, all samples were thermoresponsive, they being characterized by a lower critical solution temperature at ca. 28-30 °C. However, their extent of swelling was very different. In particular, samples containing also the covalent crosslinker swell much less than those that are totally supramolecularly crosslinked, which exhibited swelling degrees typical of superabsorbent hydrogels. This clearly demonstrate that supramolecular crosslinking may be a great added value in frontal polymerization in that it allows obtaining stable fronts, prevents fingering formation and permits large swelling even in absence of ionic monomers.

Moreover, this goal has been reached by using CDs, which are largely available, much lower toxic and cheaper than NIPAAm.

4.2 Synthesis of Sliding Crosslinked Thermoresponsive materials made of Poly(N-Isopropylacrylamide) and Acrylamide-γ-Cyclodextrin.

In this work, novel polypseudorotaxanes based on poly(N-isopropylacrylamide) and acryloyl-γ-cyclodextrin were successfully synthesized. AγCD acted as a pendant group and, at the same time, allowed macromolecular PNIPAAm chains to flow through its empty cavity, giving rise to a sliding crosslinking system with peculiar features. The amount of AγCD in the hydrogels was varied from 0.5 to 2 mol% in order to study the influence of cyclodextrins on hydrogel properties, such as swelling behaviour, LCTS values and mechanical properties. In addition, the amount of initiator was varied from 0.25 to 1 mol%, in order to investigate its effect on the macromolecular chains length and on the probably that AγCD units can link to the polymeric chains. All the results were compared with covalent crosslinked samples (DMBAM). All hydrogels were found to swell without dissolving in water; furthermore, since AγCD is monoacrylated and it cannot act as a covalent crosslinker, this behaviour suggests that a polypseudorotaxan structure is formed.

AγCD influenced the thermoresponsive behavior of PNIPAAm hydrogels, by modifying their LCST value that increased with increasing AγCD amount, from 32 °C (DMBAM sample) to 38 °C (C2 sample). This result that approaches the LCST value of classical PNIPAAm to body temperature widens the practical applications of PNIPAAm in the biomedical field. It is also noteworthy that this goal was reached by using CDs, which are largely available, non-toxic and cheap materials.

Furthermore, AγCD influenced also the swelling behavior of the resulting hydrogels; in fact, in particular, at temperatures below the LCST, the swelling of polymers increased with decreasing AγCD content. Besides, the presence of AγCD influenced the thermal and mechanical properties of hydrogels. In detail, the Tg values of samples increased with increasing AγCD content, owing to the decrease of free volume and the consequent reduction of macromolecular chain mobility exerted by the cyclodextrins. This result was in agreement with the observed increase of the compression modulus E of the hydrogels. Finally, the synthesized hydrogels showed a force/deformation curve characterized by a "J" shape without or with a very limited hysteresis. This finding strongly supports the hypothesis that cyclodextrin acts as a sliding, non-covalent crosslinking agent.

4.3 Synthesis and characterization of oxypropylated cork and preparation and characterization of PLA films

In this work, cork-based products and propylene oxide polymers were synthesized and characterized; subsequently, these materials were reacted with the three cyclodextrins α, β and γ to introduce them into the structure.

Being a preliminary work, to understand the influence of CDs on the final material, two quantities of CDs were chosen: the first was equal to 88 wt% with respect to the weight of the cork powder while the second was equal to 20 wt% (always compared to the initial weight of the powder cork). In this way, obvious variations were obtained with respect to the synthesis of the starting materials.

DSC analyses showed that the introduction of CDs resulted in an increase in the glass transition temperature of non-soluble fractions, most evident in samples containing 88 wt% of α-CD and β-CD that showed an increase of about 30 °C. The T_g of the soluble fractions, on the other hand, did not show such evident temperature variations, which assumed that they were composed of polypropylene oxide obtained during the synthesis step.

With the use of IR spectroscopy, it was not possible to highlight differences in structure between the samples of oxypropylated cork and those containing cyclodextrins, as the overlapping of the various peaks did not allow to discriminate between the two sample types.

With the techniques of Light Scattering, Mass Spectrometry, GPC (gel permeation chromatography) and NMR it has not been possible to obtain reliable and evaluable data due to solubility problems of the samples obtained in the solvents typically used to perform the characterizations, such as acetone , methanol, THF, chloroform, etc.

Considering, in general, the behavior and the differences between the synthesized series it was possible to notice that in the samples containing CDs the solubility worsened. This data has allowed to hypothesize that CDs can be integrated into the structure by creating a supramolecular mobile cross-linking with cork and PO and can therefore, thanks to their cavity, move along the polypropylene oxide chains or that the CDs can be covalently linked through the reaction with one, two, three or more OH going to form three different structures.

The oxypropylated cork products and those containing the highest amount of β-CD were tested as reinforcing materials for the PLA films and through the SEM images it was possible to notice that the distribution of these materials in the PLA was completely uniform.

This preliminary work will be further investigated to determine, more accurately, the positions of the cyclodextrins within the structures. Furthermore, further tests will have to be performed to evaluate the influence of the synthesized samples on the PLA properties.

4.4 Synthesis of β-cyclodextrin-based oligomers of lactic acid and preparation of PLA films with β-CD-OLA as plasticizers

In this part of work, β-CD- based oligomers of lactic acid were synthesized. The reaction was conducted by microwave system and various parameters such as microwave power, temperature, time and LA/CD molar ratios and catalyst were studied.

All samples were characterized by different techniques such as FT-IR, NMR, SEM, DSC e ESI-MS.

The FT-IR analyses have confirmed the success of the esterification reaction between the cyclodextrin and the lactide (the opening of the ring and attachment to the cyclodextrin) as the FT-IR spectra showed the characteristic peak (1750 cm-1) of lactic acid while the characteristic peak of lactide (930 cm-1) was absent.

The SEM analyses have showed the morphological variation of the cyclodextrin following the reaction, while the DSC analyzes have showed that, as far as the esterification reaction occurs, the polymerization of the lactide does not go ahead (absence of the glass transition temperature (T_g) of the oligomer) for which it is assumed that oligomers with a very low molecular weight were obtained.

No obvious differences were found following the variation of the investigated parameters, among the various synthesized samples, and this may be due to the fact that the propagation reaction in lactide polymerization depends more on the type of chemical initiator (in this case the CDs) than from the reaction parameters. This part of the work will be expanded in the most appropriate manner.

Regarding the analysis of PLA films with synthesized oligomers:

DSC analyses show that the addition of these oligomers does not affect on the T_g of the material, this means that the plasticizing effect of the synthesized oligomers is naught, most likely due to the shortness of the oligomeric chain of lactic acid. While from the dynamo-mechanical analyses a decrease in the Young's modulus was found, but this decrease does not clearly reflect the decrease in material rigidity.

4.5 Semi-Interpenetrating Polymer Networks Based on Crosslinked Poly(N-Isopropyl Acrylamide) and methylcellulose prepared by Frontal Polymerization

In this work, frontal polymerization was exploited for obtaining semi-interpenetrating polymer networks of poly(N-isopropyl acrylamide) and methylcellulose. To this aim, the effect of the crosslinking density provided by the crosslinker and by the interactions taking place between poly(N-isopropyl acrylamide) and methylcellulose on the overall thermal, dynamic-mechanical and swelling behavior of the synthesized systems swollen either in dimethyl sulfoxide or water was thoroughly investigated. Despite a negligible effect of the crosslinker content on the frontal polymerization parameters (namely, Tmax and Vf), it significantly affected Young‘s moduli of the polymer networks, irrespective of the type of swelling medium. Besides, all the hydrogels showed lower values of moduli with respect to their counterparts swollen in dimethyl sulfoxide and broke at the end of the dynamic-mechanical tests.

Specifically concerning the swelling behavior of the hydrogels, their LCST was found below 30 °C, because of the presence of methyl cellulose. Furthermore, the highest swelling ratio value was determined at about 15 °C for all the samples investigated. Finally, the remarkable lowering (i.e. by two order of magnitude) of the swelling ratio values from room temperature to body temperature suggested the suitability of the synthesized hydrogels as tailored drug delivery systems.

4.6 Semi-interpenetrating Polymer Networks of Methyl Cellulose and Polyacrylamide Prepared by Frontal Polymerization

For the first time, frontal polymerization was successfully applied to the synthesis of MC-PAAm gels. The FP parameters, glass transition temperature, swelling and mechanical properties as a function of molar amount of MBAm and AmPS have been investigated. As regards FP parameters, the results indicated that the increase of molar concentration of MBAM caused a linear increase of T_{max} values for all set of samples with an exception of the all samples containing 1.0 mol% of MBAm. The samples synthesized in glycerol have shown T_{max} values greater of ca. 45 °C than the samples synthesized in water, and this is due to the characteristics of solvent: water evaporates at the front temperature with a consequent loss of heat. The study on glass transition temperature showed a linear increase of the T_g values for the samples synthesized in glycerol, indeed the T_g values of samples synthesized in water increase and decrease in casual mode: this is due to the uncontrolled conditions of synthesis of the hydrogels in water. For swelling measurement, the results indicated that the increase of MBAm concentrations caused a pronounced decrease in swelling degree values for both W and G series. Finally, the increase of MBAm concentrations caused an increase in mechanical properties, as assessed by tensile and dynamic-mechanical tests: these effects are more evident for the samples synthesized in glycerol. This is a consequence of the increase of rigidity of the hydrogel networks that influences the ability of the hydrogel to absorb large quantities of water. The obtained results indicate that PAAm-MC gels are excellent candidates for several applications, such as matrices for cell transplantation, controlled release (agrochemicals and drugs), tissue repair and regeneration as changing the amounts of AAm, MBAm and AmPS makes it possible to modulate the characteristics of hydrogels.

- Acknowledgments-

Mariella Rassu gratefully acknowledges Sardinian Regional Government for the financial support of her PhD scholarship (P.O.R. Sardegna F.S.E.- Operational Programme of the Autonomous Region of Sardinia, European Social Fund 2014-2020 - Axis III Education and training, Thematic goal 10, Investment Priority 10ii), Specific goal 10.5.